Observer's Handbook for Cycle 9 Home

Observer's Handbook for Cycle 9

Exported on 10/07/2022

Table of Contents

Search

Changelog

To export the handbook as a PDF, click on the three dots in the upper right, then choose "Export with Scroll PDF Exporter". In the Template drop-down menu, choose "Handbook Template", and then click "Export".

The following log includes the dates of publication and lists sections containing major updates for all current and past versions of the handbook. The current version is listed at the top in **bold** font.

v9.1.0 April 15, 2020 Opened for Cycle 9 updates

v8.1.0 June 1, 2019 Observer's Handbook for Cycle 8 released.

New versions of the Observer's Handbook from Cycle 6 onward will follow the schedule of releases as demonstrated for Cycle 8 below:

Observer's Handbook Versions

Version	Coincides with
8.1.0	Call for Proposals
8.1.1	Update to Call for Proposals
8.2.0	Phase II begins
8.2.x	Phase II Concludes

Versions have the format (Observing Cycle).(Phase).(Revision). Intermediate revisions may be released until the conclusion of Phase II.

ii. Preface

To export the handbook as a PDF, click on the three dots in the upper right, then choose "Export with Scroll PDF Exporter". In the Template drop-down menu, choose "Handbook Template", and then click "Export".

The SOFIA Observer's Handbook for Cycle 9 (hereafter referred to as the Observer's Handbook), provides detailed information about SOFIA operations and the instruments that will be available for observations during Cycle 9. This document is the primary technical reference for astronomers who wish to submit a proposal in response to the SOFIA Cycle 9& Calls for Proposals (CfPs). The CfP documents and the Observer's Handbook (along with the documents and websites explicitly referred to within) contain information sufficient for planning viable SOFIA observations. Additional reference documentation is available on the Proposal Documents webpage. When writing publications, the Information for Authors webpage provides instructions for acknowledgements and citations; additional references may be found on the SOFIA Publications webpage.

This version of the handbook is applicable for Cycle 9 only. The Observer's Handbook will be updated as necessary and the list of changes will be included at the beginning of the document. Critical updates will also be published on the main Cycle 9 webpage. Any information that supersedes what is given in this document will be explicitly indicated.

Cycle 9 features two Calls for Proposals: one Call for regular programs, and a separate Call for the SOFIA Legacy Program (SLP).

For regular proposals, approximately 400 hours of observations will be available with EXES, FIFI-LS, FORCAST, FPI+, GREAT, and HAWC+. Cycle 9 offers new standard modes: the new honeycomb OTF mapping mode for GREAT, the new total power mode on FIFI-LS. In addition, the new FIFI-LS on-the-fly mapping mode and the 63 microns (Band B) for HAWC+ are offered as shared risk.

The SOFIA Legacy Program (SLP) enables programs targeting a rich archival dataset of significant scientific value to the astronomical community for future analysis. The resulting data are released without an exclusive use period. During Cycle 9, SOFIA will accept 1-4 proposals with each allocated up to ~200 hours of observing time (~ 100 hours of observations per cycle).

Tutorials are available for common data analysis objectives using SOFIA processed data, written for a graduate student audience. Slides from the webinar and associated video tutorials for the 2019 Proposal Tool webinar are available here. In addition, data analysis tools are available for in-depth exploration of FIFI-LS and GREAT data cubes.

SOFIA is a joint project of NASA and the Deutsches Zentrum für Luft und Raumfahrt (DLR). The SOFIA Science Center (SSC), responsible for overseeing the scientific aspects of the mission, is located at the NASA Ames Research Center in Moffett Field, CA. Flight operations are conducted out of the NASA Armstrong Flight Research Center (AFRC) in Palmdale, CA. The Science Mission Operations are jointly managed by the Universities Space Research Association (USRA) for NASA and by the Deutsches SOFIA Institut (DSI), in Stuttgart, for DLR. Aircraft operations are managed by NASA AFRC.

1. Introduction

To export the handbook as a PDF, click on the three dots in the upper right, then choose "Export with Scroll PDF Exporter". In the Template drop-down menu, choose "Handbook Template", and then click "Export".

1.1 SOFIA and Its Instruments

The Stratospheric Observatory for Infrared Astronomy (SOFIA) is a telescope with an effective diameter of 2.5 meters, carried aboard a Boeing 747-SP aircraft. It is the successor to the smaller Kuiper Airborne Observatory, which was operated by NASA from 1974 to 1996. The observing altitudes for SOFIA are between 37,000 and 45,000 feet, above 99% of the water vapor in the Earth's atmosphere. The telescope was designed to allow imaging and spectroscopic observations from 0.3 to 1600 μm, with specific capabilities dependent on an evolving science instrument suite, making it one of the premier facilities for astronomical observations at infrared and sub-millimeter wavelengths. The present instrument suite provides coverage from 0.3–612 μm with additional capabilities currently in development.

The telescope for SOFIA was supplied by the DLR as the major part of the German contribution to the observatory. It is a bent Cassegrain with 2.7 m parabolic primary mirror (2.5 m effective aperture) and a 0.35 m diameter hyperbolic chopping secondary mirror. The telescope is mounted in an open cavity in the aft section of the aircraft and views the sky through a port-side door. The telescope is articulated by magnetic torque motors around a spherical bearing through which the Nasmyth beam passes. The unvignetted elevation range of the telescope is 20°–60°. The cross-elevation travel is only ± 3° and, therefore, most of the azimuthal telescope movement required for tracking is provided by steering the airplane. Thus, the flight plan is determined by the list of targets to be observed during each flight.

The telescope feeds two f/19.6 Nasmyth foci, an IR focus for the science instruments and a visible light focus for guiding, using a dichroic and an aluminum flat. The secondary mirror is designed to chop at amplitudes of up to ± 5 arcmin at a frequency ≤ 10 Hz and up to ± 10 arcmin at a rate of ≤ 2 Hz. The visible beam is fed into the Focal Plane Imager (FPI+), which is an optical focal plane guiding camera. Independent of FPI+ are two other optical imaging and guiding cameras, the Wide Field Imager (WFI) and the Fine Field Imager (FFI), both of which are installed on the front ring of the telescope.

Six instruments, covering a wide range of wavelengths and resolving powers as shown in Figure 1.1-1, are available for use on SOFIA. Two of the instruments are Facility-class Science Instruments (FSIs), which will be maintained and operated by the Science Mission Operations (SMO) staff.

FIFI-LS: Far Infrared Field-Imaging Line Spectrometer
An integral-field far-infrared spectrometer

FORCAST: Faint Object InfraRed Camera for the SOFIA Telescope
A focal plane CCD imager-IR camera (including its grism modes) (FSI)

FPI+: Focal Plane Imager
A focal plane CCD imager

HAWC+: High-resolution Airborne Wideband Camera + Polarimeter
A far-IR camera and polarimeter (FSI)

Two instruments are Principal Investigator-class Science Instruments (PSIs), which will be maintained and operated by the Instrument Principal Investigator (PI) teams.

EXES: Echelon-Cross-Echelle Spectrograph
A mid-infrared high-resolution spectrograph (PSI)

GREAT: German Receiver for Astronomy at Terahertz Frequencies
A heterodyne spectrometer, including the seven-beam receiver array upGREAT (PSI)

Figure 1.1-1.

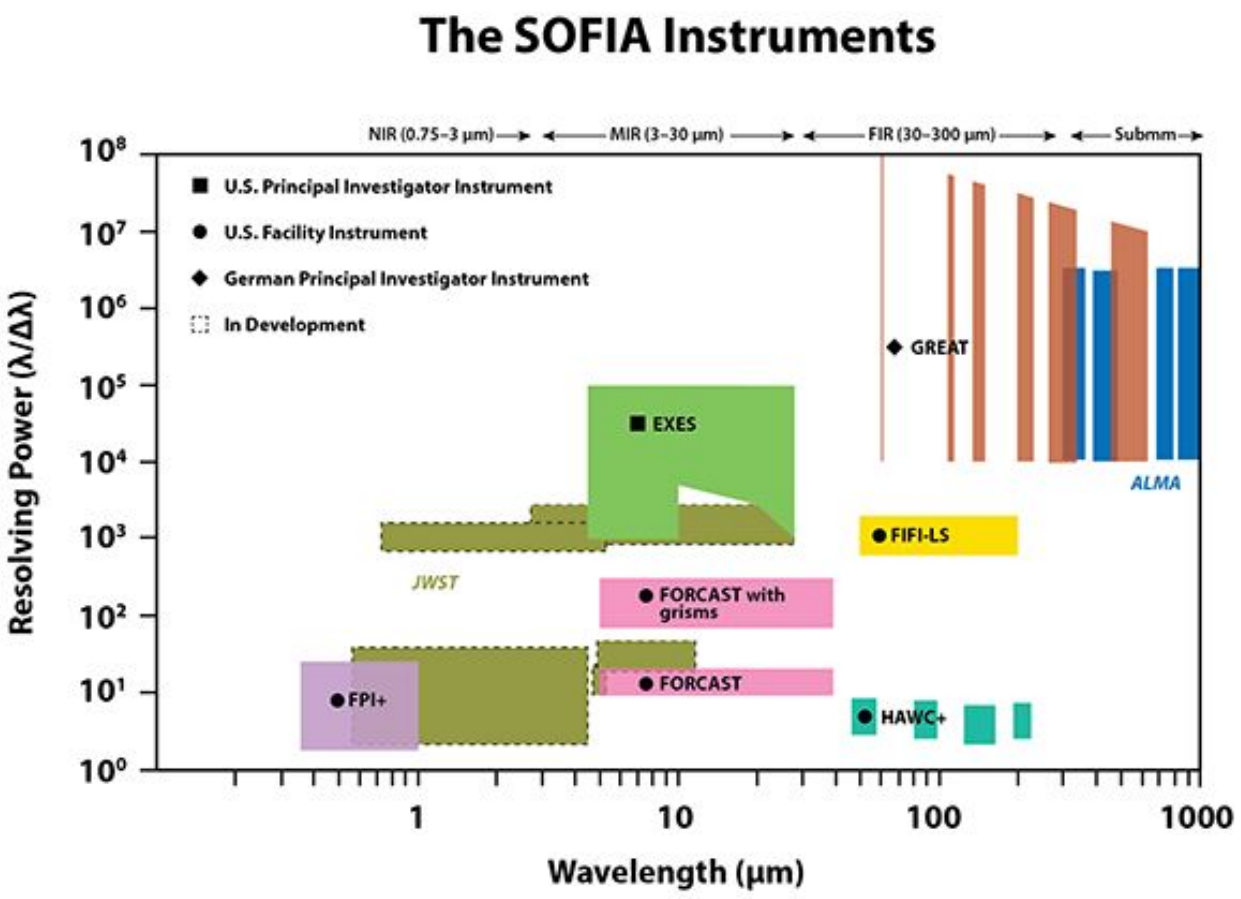

The instrument capabilities, the available modes, and the resulting performance specifications of the telescope are described in later sections. For the purpose of this document, *configuration* refers to the setup of the telescope and instrument whereas *mode* refers to observational techniques employed during operations. Common combinations of configurations and modes are represented as selectable options within the Unified SOFIA Proposal and observation Tool (USPOT) via individual Astronomical Observation Templates (AOTs). Please note that this naming convention may not necessarily be employed uniformly in external resources for the instruments, i.e. in websites or documentation not managed by the SOFIA team.

Most of the observing time on SOFIA is open to the international astronomical community via Guest Observer (GO) proposal calls, which are issued on a yearly basis. The current proposal call is for Cycle 9 observations, solicited by USRA on behalf of NASA. The observations will take place from July 1, 2021 to September 30, 2022. Most of the observations depart from Palmdale, CA. Two Long Southern Hemisphere deployments are planned to take place in the northern summers of 2021 and 2022, carrying GREAT and HAWC+. In addition, a short deployment in March 2021 with FIFI-LS will be carried out.

1.2 Observing on an Aircraft

The duration of each SOFIA flight is expected to be between 9–10 hours, 7–8 hours of which will be available for observing at altitudes of 37,000–45,000 feet. FPI+ is always available. Among the other instruments, only one will be installed on the telescope at any time. The SMO director will determine the total number of flights dedicated to each instrument, after consideration of the number of TAC (Time Allocation Committee) approved proposals for each.

Proposals should request observing time in units of hours. Once a proposal has been approved, the first stage is complete and the proposer is then expected to carry out the detailed planning of their observations in consultation with a support scientist or, for PI instruments, with the instrument team. This second stage of observation planning is known as Phase II. Proposers of successful proposals will be informed who their SMO support scientists are and how to contact them.

On each SOFIA flight, there will be one or more seats available for Guest Observers (GOs) or designated Co-Investigators (CoIs) of the proposals scheduled for that flight. Since there are a limited number of seats available on each flight, the choice of proposers given the opportunity to fly on SOFIA will be made by the SMO director according to a number of considerations, including the complexity of the observations to be performed, the duration of science observations for each program on the flight, and the proposal rank.

The observations will be carried out either by members of the instrument team along with SOFIA personnel, or solely by SOFIA personnel. The proposers on board SOFIA will participate in the observing, and monitor the data as it is received, but will have limited decision making abilities. For example, the proposer will be allowed to make real-time changes to exposure times for different filters or channels. However, changing targets or any modifications that alter the durations of flight-legs will not be allowed.

Those GOs or CoIs chosen to fly aboard SOFIA will be required to complete a flight participation form, a medical release form, and documentation related to badging. In addition, they will be required to participate in an Egress Training course prior to being allowed on board the aircraft. Full details will be provided to proposers of approved proposals during the Phase II process.

Return to Table of Contents

1.2.1 Scheduling and Flight Planning

Scheduling and flight planning will be handled by the SMO staff and is not the responsibility of the proposer. However, an understanding of the flight planning process and the restrictions inherent to airborne astronomy may be useful in preparing a successful proposal.

The most distinctive aspect of SOFIA flight planning is the interdependency of the targets observed in a flight. Because the azimuthal pointing is controlled primarily by the aircraft heading and because, in normal operations, the take-off and landing air fields are the same, efficient flight plans must generally balance eastbound with westbound flight legs and southbound with northbound legs. This also means that for any flight only a limited fraction of the observing can be performed in a given region of the sky. An example of a flight plan flown during Basic Science in May 2011 is shown in Figure 1.2-1 below. More examples of flight plans can be found on the webpages for earlier cycles.

Figure 1.2-1.

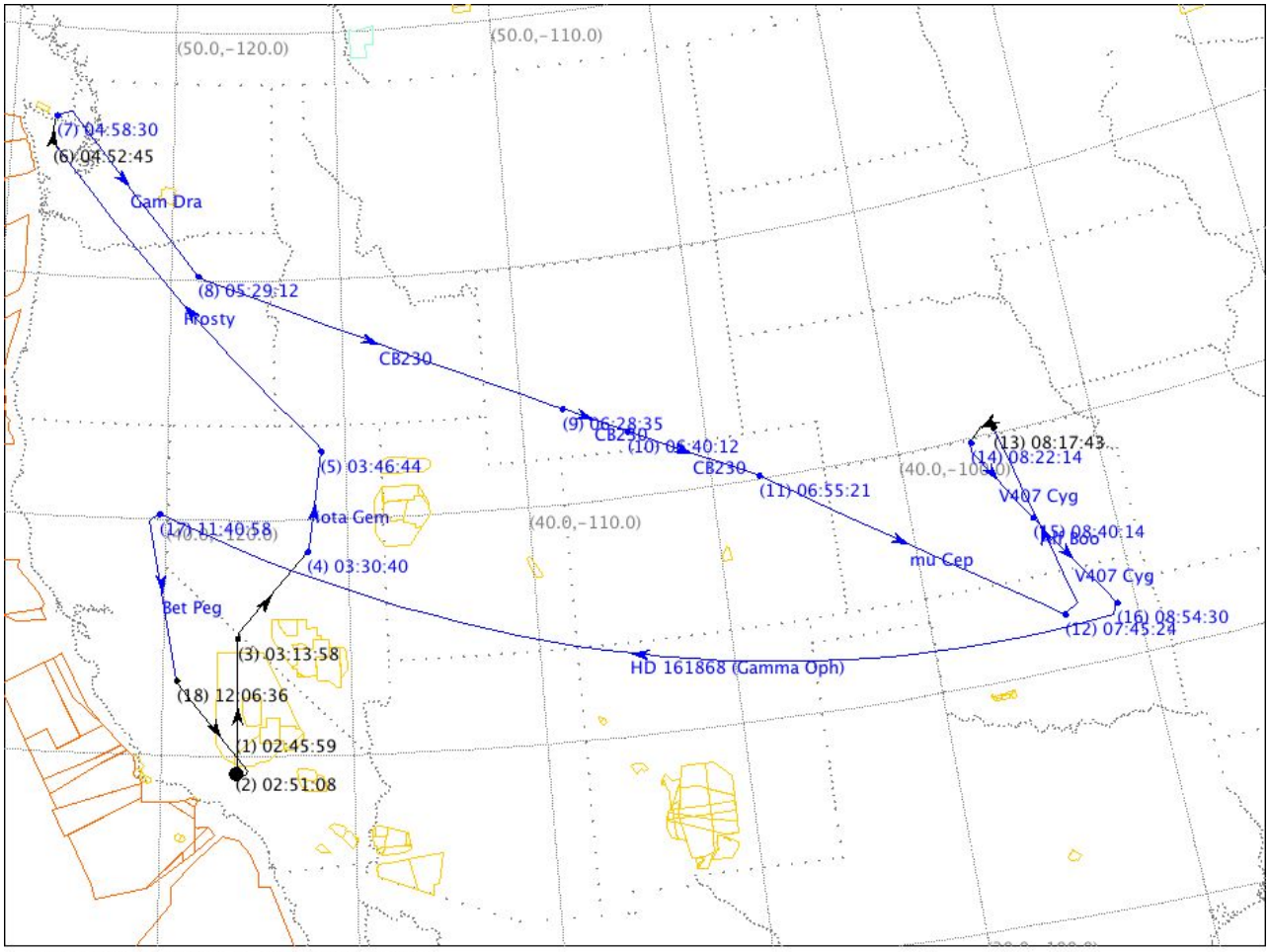

Flight Plan Name: File: BS1_01_Wx12_Fallon.fp
Flight ID: 2011/05/06
Est. Takeoff Time: 2011-May-06 02:45 UTC
Est. Landing Time: 2011-May-06 12:29 UTC
Flight Duration: 09:44
Weather Forecast : 0000 Mon May 16 2011 - 1200 Wed May 18 2011 UTC
Saved: 2011-May-16 22:37 UTC User: kbower

For the proposer this leads to several considerations:

- The sky availability for SOFIA observations is constrained by several factors, including the need to return to the home base at the end of a flight and the avoidance of restricted airspace. Due to these constraints, the southernmost declination available on flights departing and landing in Palmdale is -36˚. Note that, depending on the sensitivity of a given observation to atmospheric opacities, the limiting Declination may be significantly more stringent in practice. A strong scientific case must be made for observations with rigid time constraints or strict cadences in order to justify the restrictions they will impose on flight planning.
- Because the sky distribution of targets typically proposed for SOFIA observations (centered on the Galactic plane and certain regions of star formation, including Orion) is highly inhomogeneous, targets in areas that complement these high-target-density regions will allow more efficient flight planning and will likely have a higher chance – for a given scientific rating – to be scheduled. Consequently, it may be advantageous for those who can choose between targets from a large source pool for their SOFIA proposals and for those who plan to submit survey proposals to emphasize sources from complementary regions.
- For example, objects that complement the potentially popular Orion molecular clouds include circumpolar targets or targets north of about 40° with a right ascension in a roughly 6 to 8 hour wide window centered about 6 hours before or after the right ascension of Orion.

- The maximum length of flight legs will be determined by the need for efficient flight plans as well as the typical requirement that SOFIA take-off and land in Palmdale, California. In most cases, the longest possible observing leg on a given target is ~ 4 hours. Therefore, observations of targets requiring long integrations may have to be done over multiple flights and flight legs.
- Proposals may be submitted for observations for which the flight does not originate or end in Palmdale, CA, for example, in order to conduct observations under time constraints that require a specific flight path or that require a single flight leg in excess of ~ 4 hours. Such proposals would be equivalent to a deployment and due to resource requirements and the impact that this would have on flight planning, the scientific justification must be strong. The final decision on whether to allow programs with such a high impact on scheduling and flight planning will be made at the Director's discretion.

Proposers are encouraged to review the Flight Planning presentation delivered by Dr. Randolf Klein at the SOFIA User's Workshop in November, 2011. The full list of presentations can be found on the SOFIA web site. In addition, a much more detailed discussion of target scheduling and flight planning can be found in the Observation Scheduling and Flight Planning White Paper.

Return to Table of Contents

1.2.2 Acquisition and Guiding

SOFIA has three optical cameras for acquisition, guiding, and tracking. The Wide Field Imager (WFI) and Fine Field Imager (FFI) are mounted on the telescope head ring. The upgraded Focal Plane Imager (FPI+) images the focal plane of the telescope via a dichroic and a tertiary mirror. All three imagers use 1024x1024 pixel, frame-transfer CCD cameras.

The WFI has a 6°x6° field of view, and is expected to achieve a centroid precision of ~8'' for stars brighter than R = 9. The field of view of the FFI is 70 x 70 arcmin^2. It is expected to achieve a centroid precision of ~1 arcsec for R = 11 or brighter stars. The FPI+ has an ~8 arcmin diameter field of view and is expected to provide a centroid precision of 0.05 arcsec for R = 16 (no chopping) and R = 14 (chopping) or brighter stars.

Most observers do not need to select guide stars as they will be chosen by the SMO staff. However proposers should be aware that the guiding cannot be done on IR sources unless they are optically bright.

Return to Table of Contents

1.2.3 Observing Moving Targets

Once SOFIA achieves its nominal operating capabilities, it will be able to observe solar system targets by (i) guiding on the object itself, (ii) offset guiding from field stars, or (iii) predictive tracking based on accurate ephemerides.

Successful guiding on a moving target requires it to be bright at visible wavelengths, where the guider cameras operate. We are typically able to guide on solar system targets with R ≤ 10 and that have a non-sidereal angular speed of 1 arcsed/s or less. The minimum acceptable solar elongation for a target is limited by the lower elevation limit of the telescope and the rule that no observations can be acquired before sunset or after sunrise. The minimum solar elongation is roughly 24 degrees.

Identification of solar system targets will be done manually by the Telescope Operator by inspecting images obtained with FPI+. The ephemerides of the proposed target must be accurate enough to allow for unambiguous identification. While the required accuracy could vary somewhat based on the complexity of the background star field, it should in general be better than about 30/arcsec.

Return to Table of Contents

1.2.4 Line-of-Sight (LOS) Rewinds

The SOFIA telescope mounting is similar to that of a typical altitude-azimuth telescope. One such similarity is that while tracking a target, the image rotates within the field of view. However, the SOFIA telescope is also similar to an on-orbit gyro-stabilized telescope, with a third control axis along the line of sight (LOS). So the sky image in the focal plane does not change orientation until the telescope approaches an LOS limit. Then the telescope must be slewed about the LOS axis to at least mid-range, or more typically to near the opposite limit. Each of these "LOS rewinds" interrupts observing for ~10 to 15 seconds and may have to occur several times during an observing leg. The range of LOS rotation is limited to only ± ~3°, and the frequency of LOS rewinds depends on the rate of field rotation. This in turn depends on the target's current azimuth and elevation, and weakly on the aircraft latitude. This is similar to the field rotation that occurs at ground-based altazimuth telescopes, but the rate differs due to the aircraft ground speed. Each target's azimuth and elevation are unknown until the observation is scheduled into a flight plan, and therefore the field rotation angles and rotation rate are not available until then. The overall character of the airborne field rotation rate in the observable sky above the aircraft is shown in Figure 1.2-2. The corresponding maximum time between LOS rewinds is shown in Figure 1.2-3.

Figure 1.2-2.

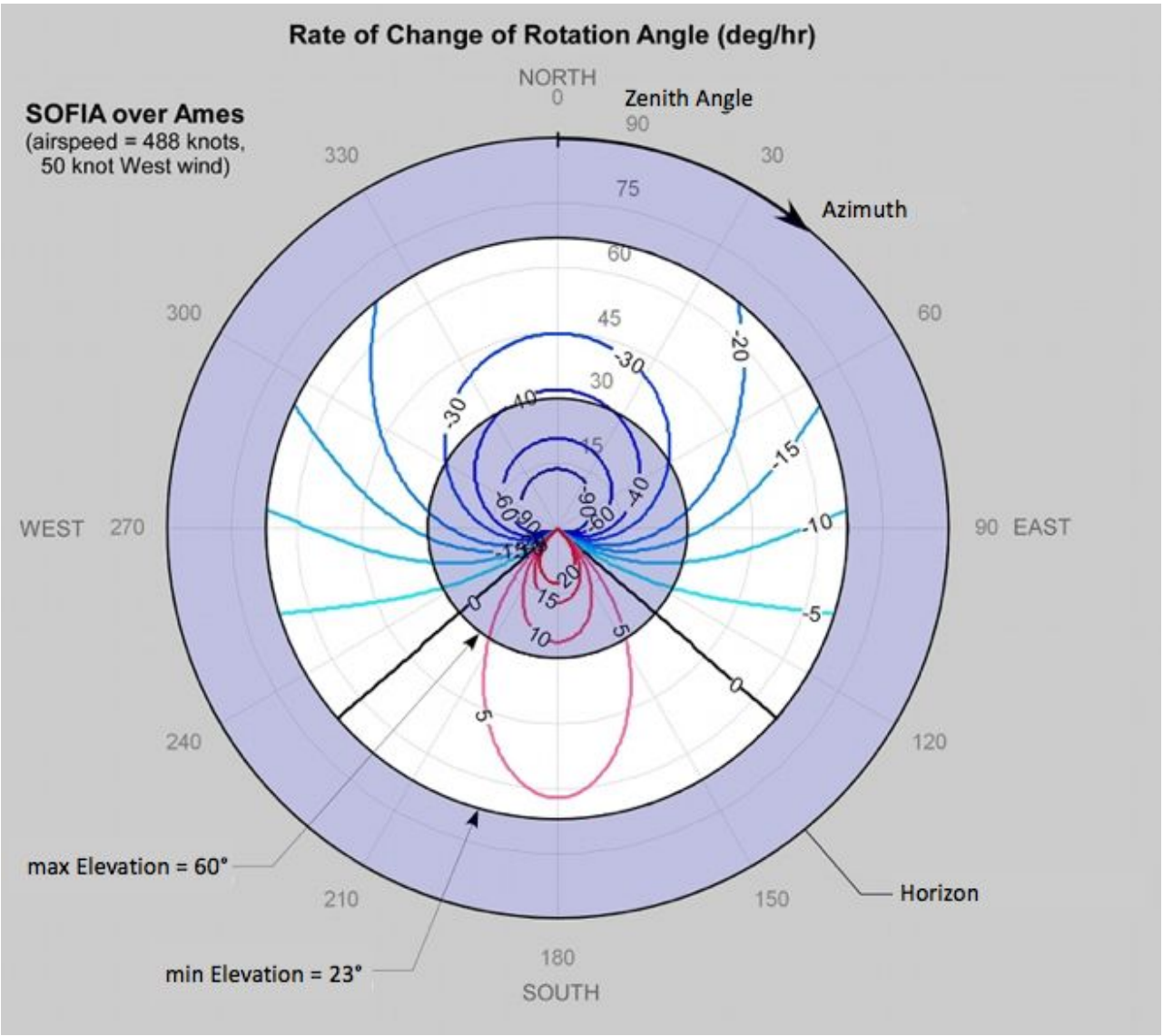

Figure 1.2-3.

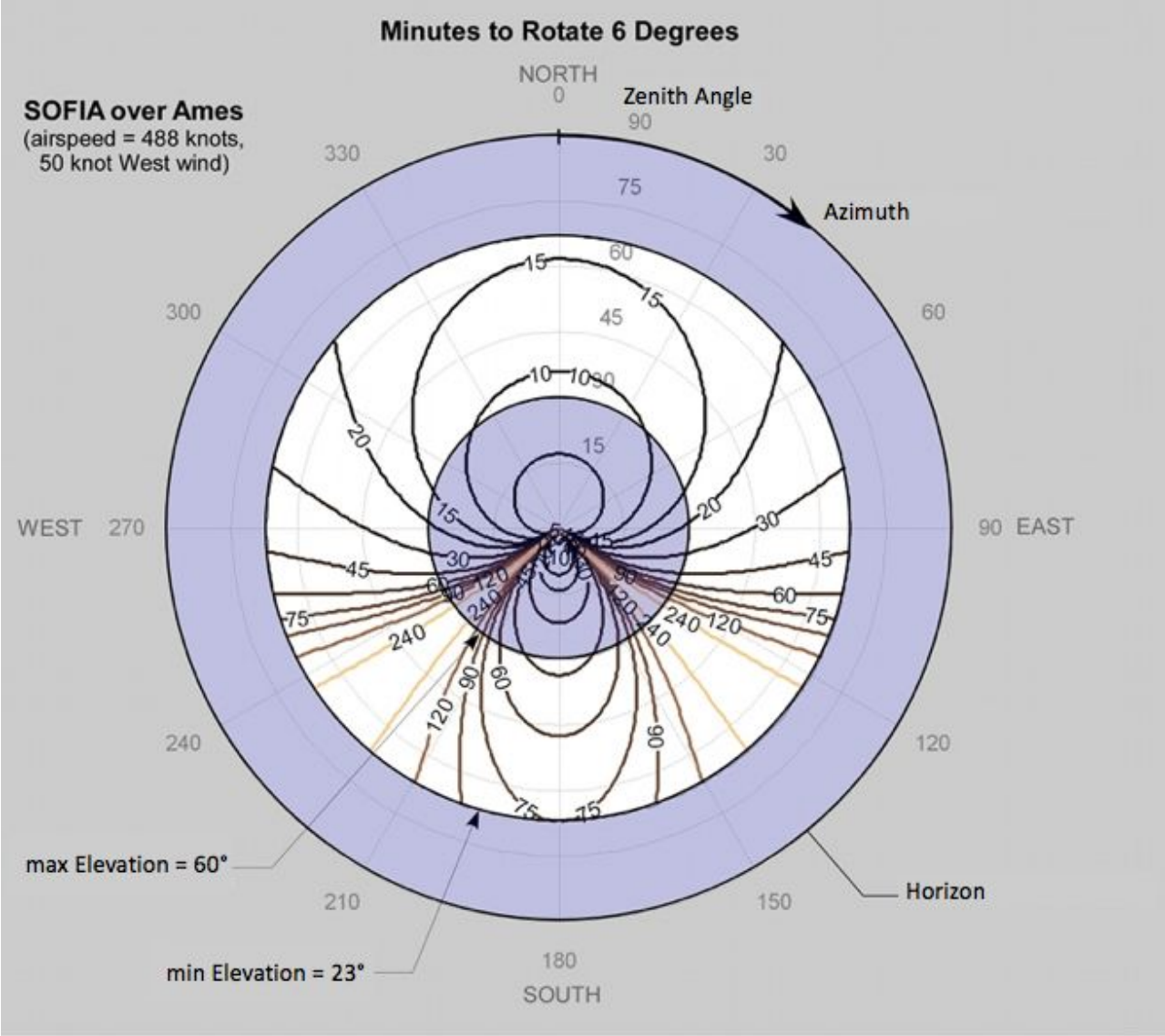

For the majority of SOFIA flights that originate in Palmdale, Figures 1.2-2 or 1.2-3 can be used to anticipate what may occur in this regard. Targets at high northern declinations require eastward headings, and may require quite frequent LOS rewinds. Targets near the celestial equator are likely to have very little or no field rotation and may not need any LOS rewind, even during a long observing leg.

For example, during the summer months the W3 star forming region rises in the northeast while it is in the observable elevation range (20° to 60°). On Figure 1.2-2, this indicates field rotation rates of about -25° to -35° per hour, or roughly 6 degrees every 15 minutes as indicated on Figure 1.2-3.

When using Figures 1.2-2 and 1.2-3 to estimate the rotation of field, it is important to bear in mind some associated caveats. In practice the time between LOS rewinds is often a little shorter due to the need for some margin near the limits, especially if there is any turbulence. The plotted rates were calculated for latitude North 37° and the rates are weakly dependent on latitude. Even on local flights from Palmdale, SOFIA may make observations in the latitude range North 20° to North 55°.

Special care must be taken when designing spectroscopic observations of extended regions. Proposers should bear in mind that the orientation of the slit on their targets will change with each LOS rewind. For point sources this should not cause problems—but for extended sources this means that after each rewind the slit will be sampling a slightly different region of the source. In addition, there is no way to choose the orientation of the slit on the target.

However, once the likely range of rotation angle values is known, the orientation of a spectrograph slit (e.g. in EXES) on a region can be anticipated.

Two of the Science Instruments, FIFI-LS and GREAT, use a K-mirror to rotate the telescope FIR image before it arrives at the detectors. This is slaved to the onboard real-time rotation angle, so that during an observing leg the observed orientation of the FIR image is held constant.

Return to Table of Contents

1.3 Performing Background Limited Observations

Because the sky is so bright in the infrared (IR) relative to astronomical sources, the way in which observations are made in the IR is considerably different from the (more familiar) way they are made in the optical. Any raw image or spectrum of a region in the IR is overwhelmed by this sky background emission. The situation is similar to trying to observe in the optical during the day. The bright daylight sky swamps the detector and makes it impossible to see astronomical sources in the raw images.

SOFIA operates at altitudes above 99% of the water vapor in the atmosphere. The average atmospheric transmission across the SOFIA bandpasses is about 80% at these altitudes. There are however a number of strong absorption features which, even at these altitudes, can make the atmosphere opaque. Broad band filters, such as those on FORCAST, account for the presence of such features. However, when using high-resolution tunable instruments such as EXES, FIFI-LS, and GREAT, it is necessary to examine the atmospheric transmission at the wavelengths of interest in detail. This may be done using the more general web interface to the ATRAN program that was developed and provided to the SOFIA program by Steve Lord, or through the more instrument specific SOFIA Instrument Time Calculator (SITE). A plot of the atmospheric transmission seen by SOFIA in comparison to that achieved at Mauna Kea is shown in Figure 1.3-1 below.

Figure 1.3-1.

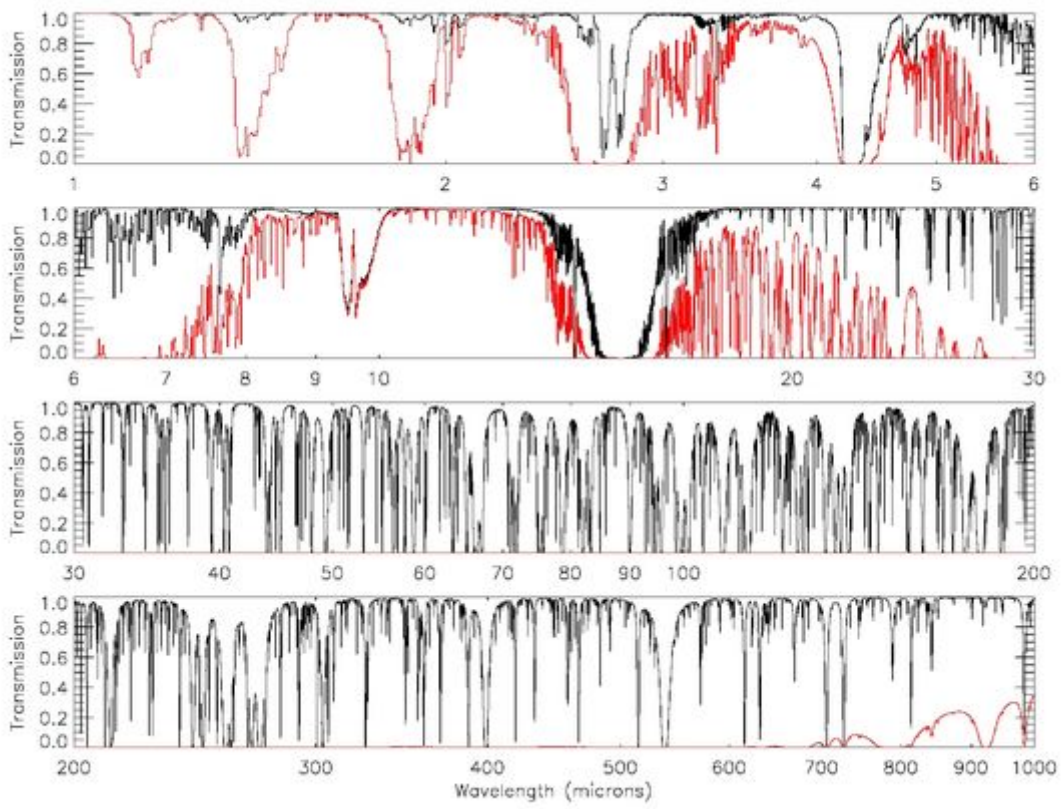

1 Figure 1.3-1. This is a plot showing the atmospheric transmission for SOFIA (black) at an altitude of 41K feet and 7.3 µm of precipitable water vapor compared to Mauna Kea (red) at an altitude of 13.8K feet and 3.4 mm water vapor over the range of 1 – 1000 µm. The transmission was calculated using the ATRAN code with a telescope zenith angle of 45°. and the data were smoothed to a resolution of R=2000.

In addition to its dependence on wavelength due to the presence of absorption features, the atmospheric transmission varies with latitude and with time of year, primarily due to differences in the amount of water vapor. It also exhibits variations on smaller time scales due to changes in the location of the tropopause. Full discussions of these issues may be found in Haas & Phister 1998 (PASP, 110, 339) and Horn & Becklin 2001 (PASP, 113, 997).

The variations in atmospheric water vapor could have a significant impact on some observations, particularly when using EXES, FIFI-LS, and GREAT or grism modes with FORCAST. For example, GREAT observations of a line situated on the shoulder of an atmospheric water feature could be strongly affected by water vapor variability. SITE allows the user to specify the water vapor overburden and adjusts the time estimates appropriately. The water vapor monitor has been installed and is currently undergoing testing, but may not be fully functional during Cycle 9.

Return to Table of Contents

1.3.1 Chopping and Nodding

In order to remove the background from the IR image and detect the faint astronomical sources, observations of another region (free of sources) are made and the two images are subtracted. However, the IR is highly variable, both spatially and—more importantly—temporally. It would take far too long (on the order of seconds) to reposition a large telescope to observe this sky background region: by the time the telescope had moved and settled at the new location, the sky background level would have changed so much that the subtraction of the two images would be useless. In order to avoid this problem, the secondary mirror (which is considerably smaller than the primary mirror) of the telescope is tilted, rather than moving the entire telescope. This allows observers to look

at two different sky positions very quickly (on the order of a few to 10 times per second) by tilting the secondary. Tilting the secondary between two positions is known as **chopping**.

Unfortunately, moving the secondary mirror causes the telescope to be slightly misaligned, which introduces optical distortions in the images—notably, the optical aberration known as coma and additional background emission from the telescope that is considerably smaller than the sky emission but present nonetheless. The additional telescopic background mentioned can be removed by moving the entire telescope to a new position and then chopping the secondary again between two positions. (Subtracting the two chop images at this new telescope position will remove the sky emission but leave the additional telescopic background due to the misalignment; subtracting the result from the chop-subtracted image at the first telescope position will then remove the background.)

Since the process of moving to a new position is needed to remove the additional background from the telescope, not the sky, it can be done on a much longer timescale. (The variation in the telescopic backgrounds occurs on timescales on the order of tens of sec to minutes, much slower than that the variation in the sky emission.) This movement of the entire telescope, on a much longer timescale than chopping, is known as **nodding**. The two nod positions are usually referred to as nod A and nod B. The distance between the two nod positions is known as the **nod throw**.

The chop-subtracted images at nod position B are then subtracted from the chop-subtracted images at nod position A. The result will be an image of the region, without the sky background emission or the additional emission resulting from tilting the secondary during the chopping process. The sequence of chopping in one telescope position, nodding, and chopping again in a second position is known as a **chop/nod cycle**.

Again, because the IR sky is so bright, deep images of a region cannot be obtained (as they are in the optical) by simply observing the region for a long time with the detector collecting photons (integrating) continuously. As stated above, the observations require chopping and nodding at fairly frequent intervals. Hence deep observations are made by effectively stacking a series of chop/nod images. Furthermore, IR detectors are not perfect, and often have bad pixels or flaws. In order to avoid these defects on the arrays, and prevent them from marring the final images, observers employ a technique known as dithering. **Dithering** entails moving the position of the telescope slightly with respect to the center of the region observed each time a new chop/nod cycle is begun, or after several chop/nod cycles. When the images are processed, the observed region will appear in a slightly different place on the detector. This means that the bad pixels do not appear in the same place relative to the observed region. The individual images can then be registered and averaged or medianed, a process that will eliminate (in theory) the bad pixels from the final image.

Many of the instruments onboard SOFIA implement chopping and/or nodding techniques in order to minimize the contribution of background noise in observations; Table 1.3-1 provides the nomenclature between some of the SOFIA instruments with similar chopping and nodding techniques. Depending on the instrument and the required exposure time and resolution for the object being observed, other methods of optimization may be more beneficial to the observation (Section 1.3.2).

Table 1.3-1: Inter-Instrumentation Mode Translations

Technique	EXES	FIFI-LS	FORCAST	GREAT[3]	HAWC+
Symmetric Chopping[1]		Symmetric Chop	NMC	Beam Switching	NMC
			NPC		
Asymmetric Chopping[1]		Bright Object			

Technique	EXES	FIFI-LS	FORCAST	GREAT[3]	HAWC+
		Asymmetric Chop	C2NC2		
			NXCAC		
Nodding Only	Nod On Slit			Total Power	
	Nod Off Slit				
Dithering Only	Map		Slitscan		
Continuous[2]					OTFMAP

[1]Modes listed under Chopping may or may not also nod and/or dither.

[2]Modes listed under Continuous are non-discrete methods of observation for eliminating background noise and are discussed in Section 1.3.2.

[3]GREAT impliments chopping and nodding techniques, but is also limited by the temperature of the receiver. See Section 7.1.2.1 for calculations.

Return to Table of Contents

1.3.1.1 Symmetric and Asymmetric Chopping Techniques

Chopping can be done either symmetrically or asymmetrically. The distance between the two chop positions is known as the **chop throw**.

Symmetric chopping implies that the secondary mirror is tilted symmetrically about the telescope optical axis (also known as the **boresight**) in the two chop positions. Variations of symmetric chopping techniques include the general C2 and C2N techniques, with variations known as NMC (Nod Match Chop) and NPC (Nod Perp Chop). Symmetric chopping modes use the standard ABBA nod cadence, as described in Section 1.3.1.1a below.

Asymmetric chopping means that the secondary is aligned with the telescope boresight in one position, but is tilted away from the boresight in the chop position. A variation of the basic asymmetric chop mode is C2NC2. Asymmetric chopping modes use an ABA nod cadence, as described in Section 1.3.1.1b.

Figure 1.3-2.

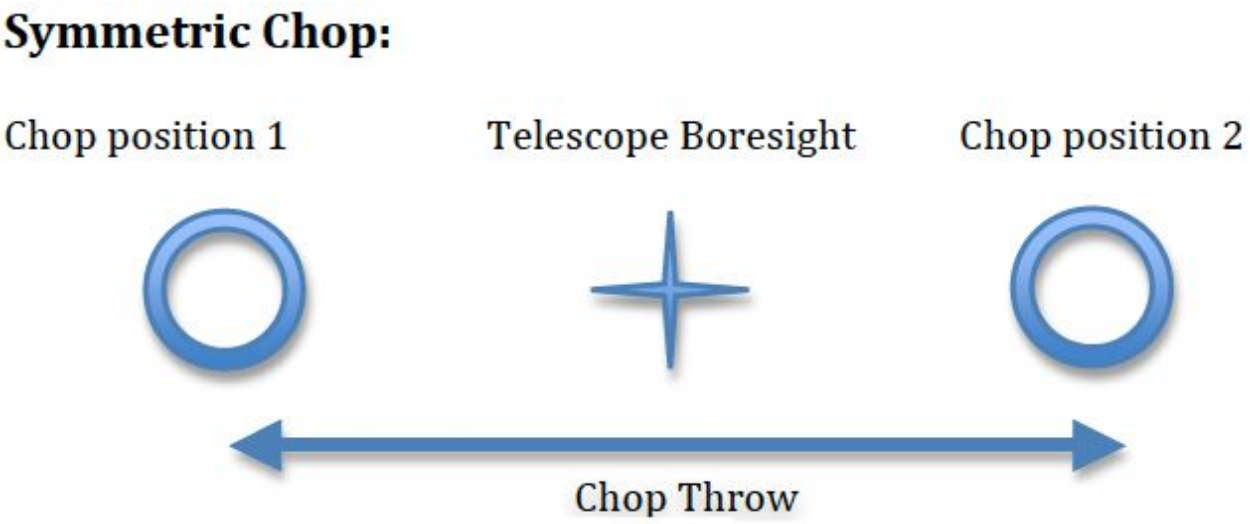

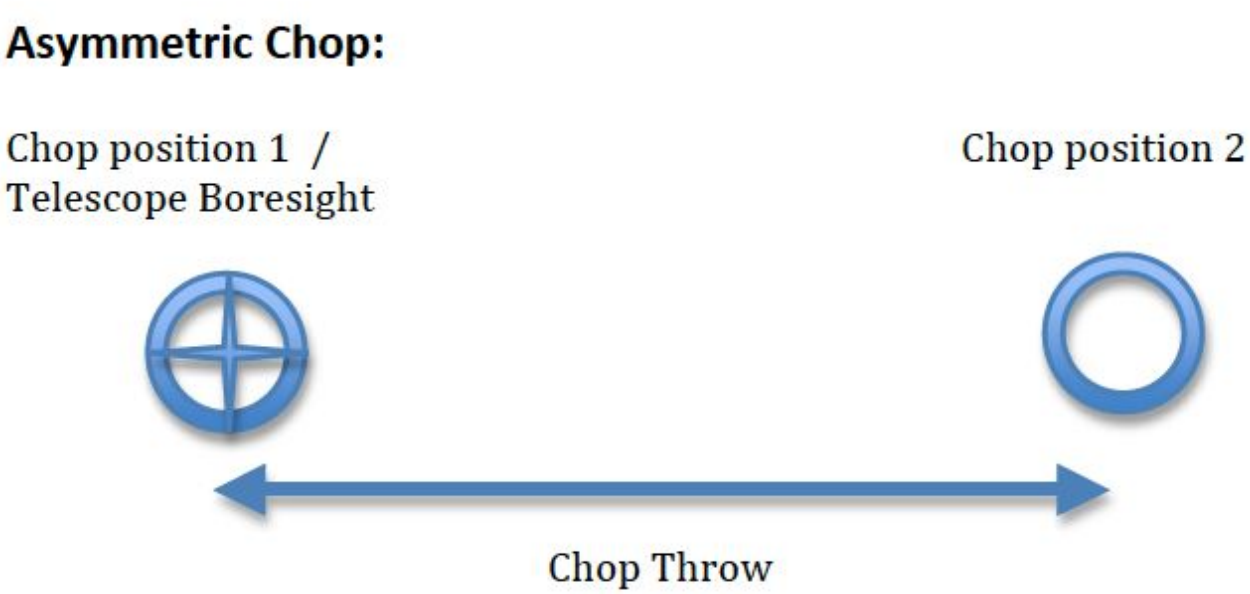

2 Figure 1.3-2.

Figure 1.3-3.

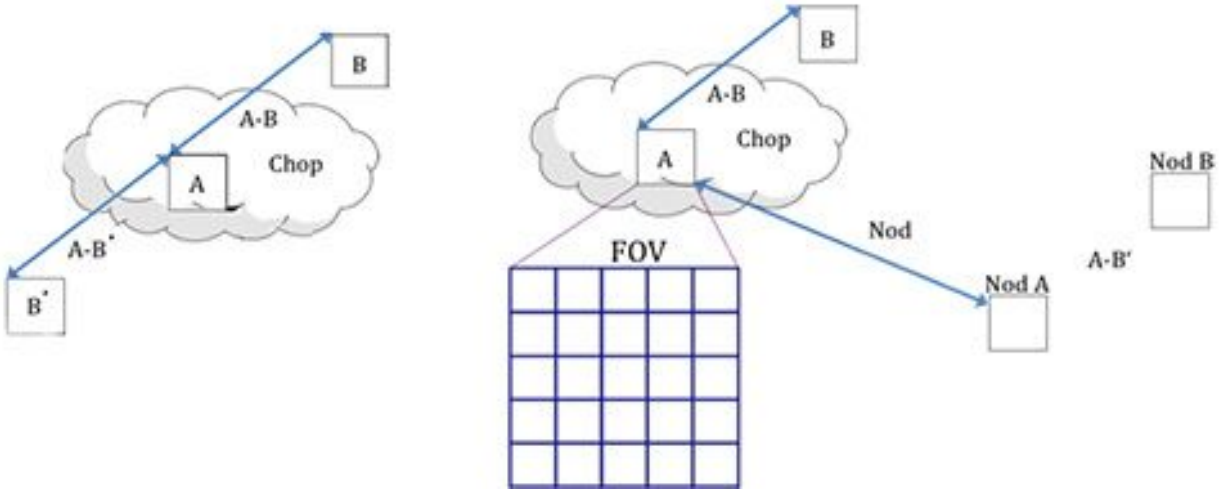

3 Figure 1.3-3. A simple AB nod cadence involves (1) an exposure at position A, (2) a move to position B, (3) an exposure at position B, and (4) a move back to position A. The ABBA nod cadence: (1) an exposure at position A, (2) a move to position B, (3) two exposures at position B, (4) move back to position A, and (5) a final exposure at position A.

Return to Table of Contents

1.3.1.1a Symmetric Chopping Variations

The shared characteristic of symmetric chopping methods is the symmetric chop about the optical axis of the telescope. NMC and NPC differ in their nodding techniques. Note from Table 1.3-1 that NMC is referred to as Asymmetric Chop for FIFI-LS, Beam Switching for GREAT, and NMC for both HAWC+ and FORCAST.

The Nod Match Chop observing pattern is defined by the two alternating positions of the telescope: Nod A and Nod B.

The telescope begins with its boresight centered at a position, Nod A. The secondary mirror then alternates (chops) between a position on the target (position Chop A) and a position equidistant from and on the opposite side of Nod A (position Chop B). The distance between Chop A and Chop B is called the chop throw. The chop angle is the direction between Chop A and Chop B from east-of-north in sky coordinates (or counterclockwise from the top of the array in array coordinates).

The telescope then shifts to center its boresight on a new position (Nod B). The distance between Nod A and Nod B is called the nod throw, and it is equivalent to the chop throw—hence the name Nod Match Chop. The nod throw is always 180 degrees from the chop angle.

The process that occurs at position Nod B is similar to that which occurred at Nod A: the telescope's secondary mirror alternates between a position centered on the target (Chop A', which is equivalent to Chop A) and a position equidistant from Nod A on the opposite side of Nod A (position Chop B).

The observations occur in a standard ABBA nod sequence. The final image generated by subtracting the images obtained for the two chop positions at nod A and those at nod B and then subtracting the results will produce three images of the star, one positive and two negative, with the positive being twice as bright as the negatives.

In the case of NPC, the nod is perpendicular to the chop. The telescope is offset by half the nod throw from the target in a direction perpendicular to the chop direction, and the secondary chops between two positions. The nod throw usually (but not necessarily) has the same magnitude as the chop but is in a direction perpendicular to the chop direction. This mode also uses the standard ABBA nod cadence. The final image is generated by subtracting the images obtained for the two chop positions at nod A and those at nod B and then subtracting the results; it will therefore have four images of the star in a rectangular pattern, with the image values alternating positive and negative. Unlike NMC, each beam in NPC has the same relative intensity.

Figure 1.3-4.

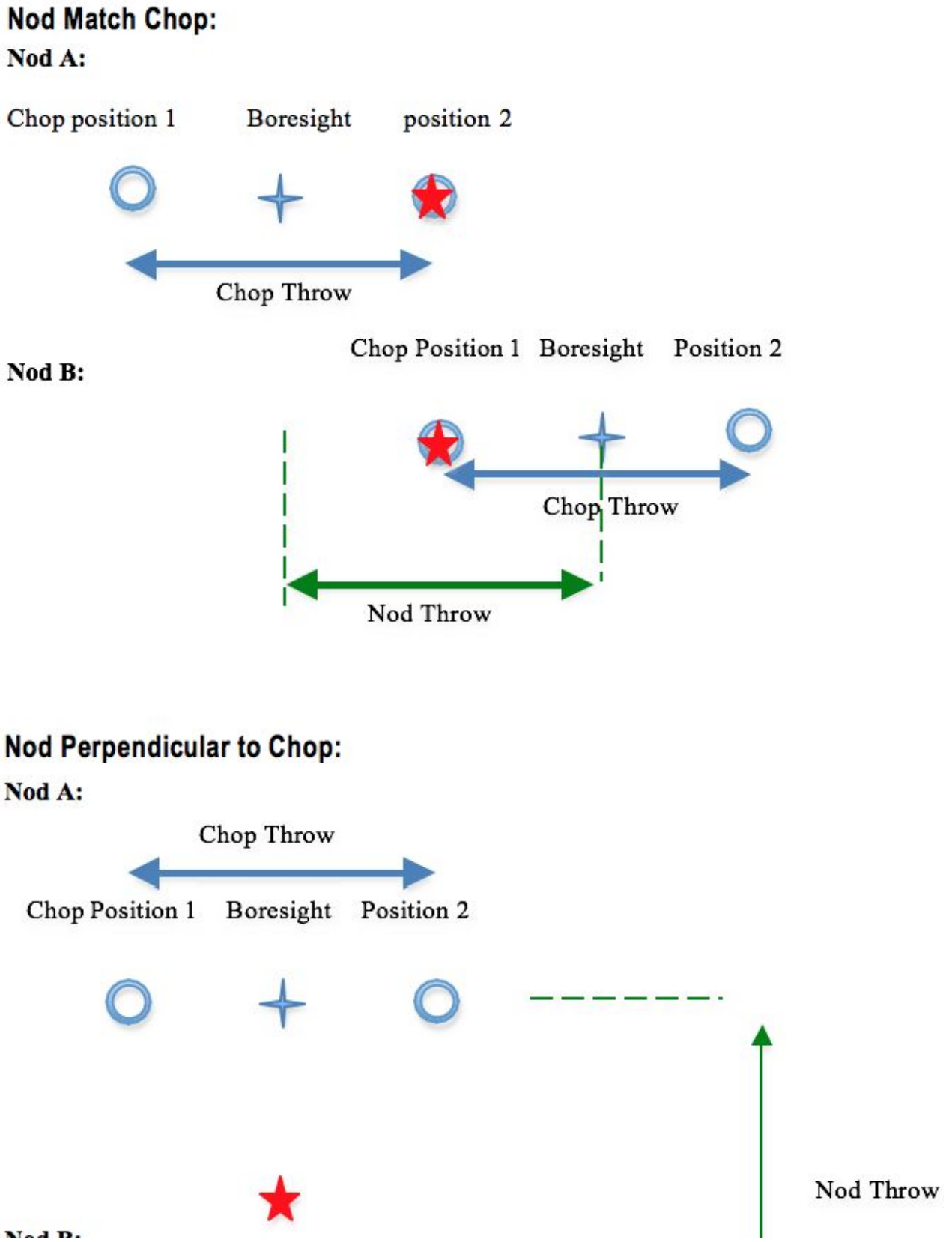
Nod Match Chop:
Nod A:
Chop position 1
Boresight
position 2
Chop Throw
Chop Position 1
Boresight
Position 2
Nod B:
Chop Throw
Nod Throw
Nod Perpendicular to Chop:
Nod A:
Chop Throw
Chop Position 1
Boresight
Position 2
Nod Throw

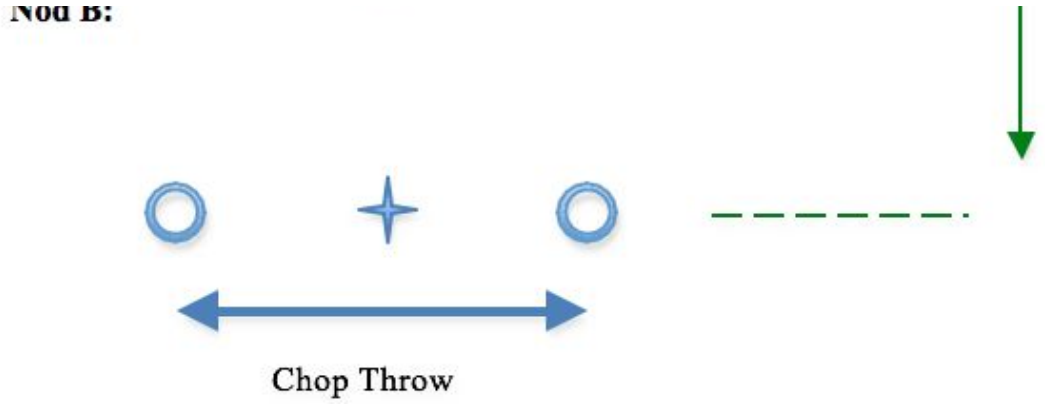

4 Figure 1.3-4. NMC vs NPC

Return to Table of Contents

1.3.1.1b Asymmetric Chopping Variations

In C2NC2 (known as Asymmetric Chop in FIFI-LS observations), the telescope is first pointed at the target (position A). In this first position, the secondary is aligned with the optical axis (or boresight) for one observation and then is tilted some amount (often 180–480 arcseconds) for the second (asymmetrically chopped) observation. This is an asymmetric C2 mode observation. The telescope is then slewed some (usually large) amount away from the target to a sky region without sources (position B), and the asymmetric chop pattern is repeated. C2NC2 observations are taken as a series of 8 (C2) files in the sequence A B A A B A A B, i.e. an ABA nod cadence with dithering to remove correlated noise. Again, the time between slews is typically 30 sec. This mode is particularly useful for large extended objects, smaller objects that are situated within crowded fields, or regions of diffuse emission with only limited sky positions suitable for background removal.

Figure 1.3-5.

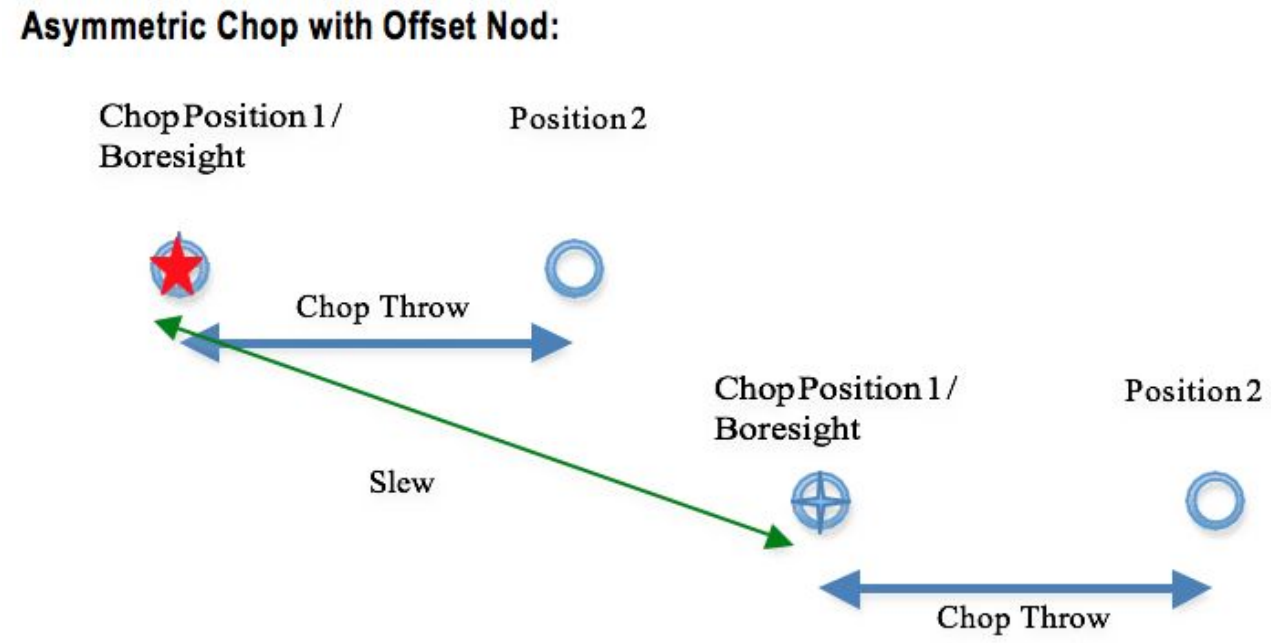

5 Figure 1.3-5.

Figure 1.3-6 demonstrates how a C2NC2 observation might be designed for a large, extended object. It is immediately apparent from the figure, that C2NC2 has an efficiency of only ~20%. This is a much lower efficiency

than either symmetric chopping variations since only a single chop position out of a full chop/nod cycle is on source. This should be taken into consideration when designing science proposals.

Figure 1.3-6.

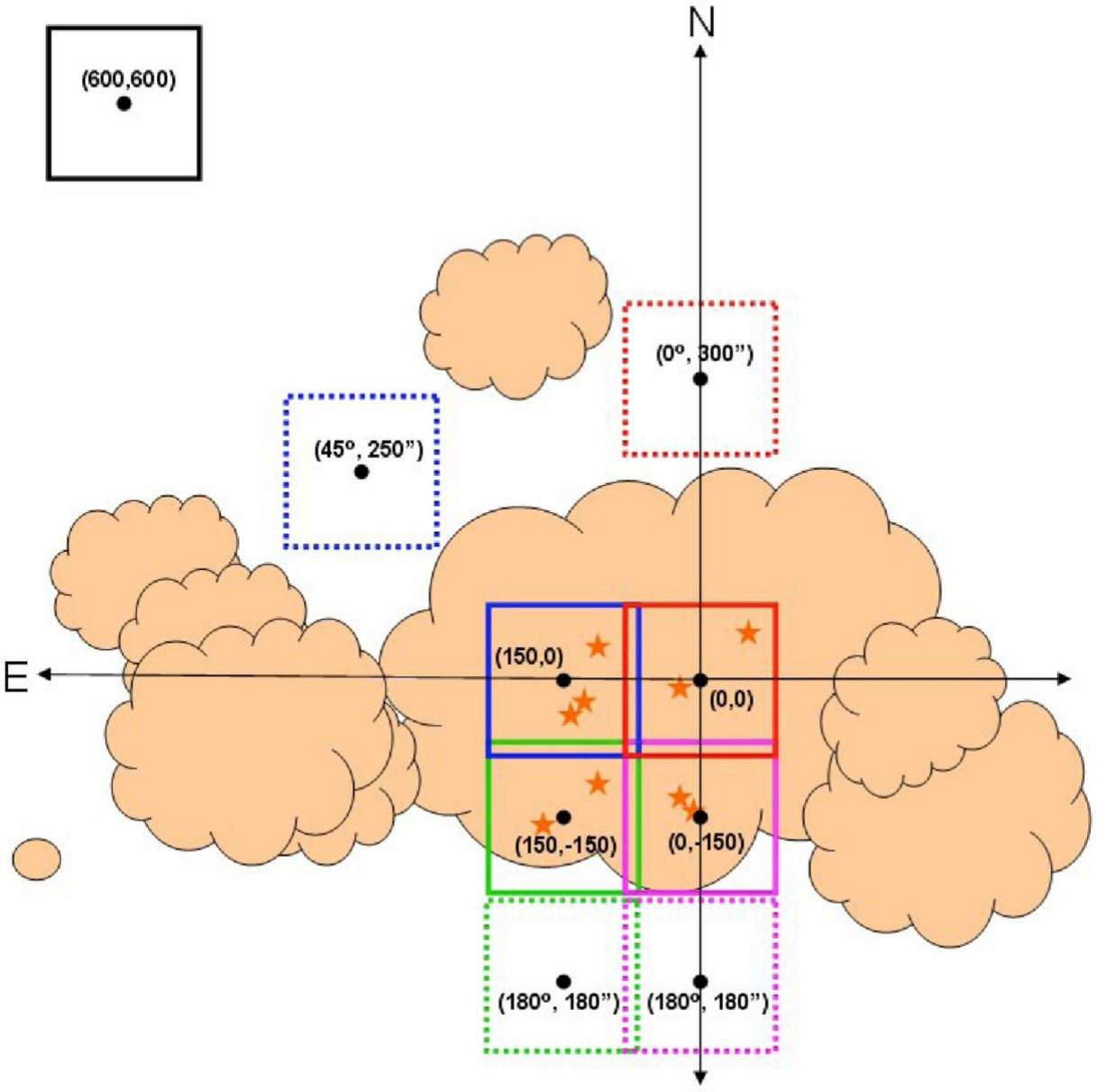

6 Figure 1.3-6. A sample C2NC2 observation design for a large, extended object. Each source position (solid line) and its associated asymmetric chop position (dashed line) have matching colors. Each source position has an independent chop configuration, the parameters for which are given in the dashed line boxes (chop angle in degrees and chop throw in arcseconds). After a full chop cycle at each position, the telescope is slewed to a location off of the source, shown in black and labeled with the coordinates (600, 600). The chop throw and angle at that position is the same as it is for the source position to which it is referenced (not shown in the figure).

The Asymmetric Chop mode of FIFI-LS typically implements an ABBA nod sequence, but is otherwise equivalent to C2NC2. NXCAC (Nod not related to Chop with Asymmetric Chop) mode is the FORCAST grism version of C2NC2.

Bright Object mode for FIFI-LS is also an asymmetric chopping mode, using observations of two map positions and one off-position per nod-cycle through an asymmetric chop. This technique is utilized to improve the efficiency of mapping bright objects, where the total observing time is dominated by telescope movements.

Return to Table of Contents

1.3.2 Alternatives to Chop-Nod Cycles

As chopping and nodding require a considerable amount of an observation's awarded time spent off-source, the amount of exposure time observing on the target is limited and subject to large observational overheads waiting for the telescope and/or secondary mirror assembly to complete chop/nod/dither movements. An alternative is to implement continuous scanning techniques. Of the instruments currently offered on SOFIA, only GREAT, HAWC+, and FPI+ offer continuous scanning methods of observation.

Nodding Only Modes

- **GREAT**
  - **Total Power** - The telescope alternates between the target and a nearby reference position that is free of emission, using ON–OFF source cycles (typically spending ≤ 30 seconds on source). This mode is used when observing an extended source or a crowded region.
- **EXES**
  - **Nod On Slit** - The telescope is nodded along the slit at distances that keep the target within the slit length. The nod throw is half the slit length. This is the most efficient EXES mode for point sources.
  - **Nod Off Slit** - The telescope is nodded such as that the object is not on the slit. This is used for extended sources or when the PSF is larger than four times the slit length.

Dithering Only Modes

- **EXES**
  - **Map** - The telescope is moved perpendicular to the slit while EXES takes spectra on a grid of telescope positions, which are always one dimensional stripes.
- **FORCAST**
  - **Slitscan** - In Slitscan mode, the slit is moved across a target in discrete steps using dithers perpendicular to the slit axis to yield a spectroscopic map of an entire area of sky.

Continuous Scans

- **HAWC+**
  - **On The Fly Mapping (OTFMAP)** - In this case, scan rates must reach (~2 Hz) x (HAWC+ beam width) in order to remove the source from the atmospheric background—implying rates of ~10–80 arcseconds per second depending on the bandpass. HAWC+ offers two scan types for OTFMAP scan patterns: Lissajous and Box. In Lissajous observations, the telescope follows a parametric curvature at a non-repeating period to eventually cover the scan amplitude. In contrast, Box scans drive the telescope in a linear fashion at a specified rate in one direction for a given length and then moved perpendicularly before scanning in the reverse direction—similar to how one would mow a very large lawn. Lissajous scans are recommended for soucres smaller than the HAWC+ FOV at a given bandpass, while Box scans are more efficient at mapping large areas several times the FOV.
  - Note: GREAT also has an On the Fly Astronomical Observation Template (AOT), but is not included in this section because GREAT observations are performed in either Total Power or Beam Switching modes.

Other Scans

- **FIFI-LS**
  - **Spectral Scan** - This mode is implemented to target spectral features much wider than the bandwidth like solid state features. The problem is a good atmospheric calibration over the whole observed wavelength range. The spectrum has to pieced together from many different exposures.

The best way to take such data and how to reduce it is still being investigated. If this observing mode is considered, please contact the instrument scientist via the SOFIA Help-Desk.

Return to Table of Contents

2. EXES

To export the handbook as a PDF, click on the three dots in the upper right, then choose "Export with Scroll PDF Exporter". In the Template drop-down menu, choose "Handbook Template", and then click "Export".

2.1 Specifications

2.1.1 Instrument Overview

The **E**chelon-**cross**-**E**chelle **S**pectrograph (EXES) operates in the 4.5–28.3 μm wavelength region, at high (R ≈ 50,000–100,000), medium (R ≈ 5000–20,000) and low (R ≈ 1000–3000) spectral resolution. The instrument uses a 1024x1024 Si:As detector array. High resolution is provided by an echelon—a coarsely-ruled, steeply-blazed aluminum reflection grating—along with an echelle grating to cross-disperse the spectrum. The echelon can be bypassed so that the echelle acts as the sole dispersive element. This results in single order spectra at medium- or low-resolution depending on the incident angle.

Return to Table of Contents

2.1.1.1 Design

EXES is a liquid helium cooled instrument. The cryostat is approximately 24 inches in diameter and 72 inches long. There are two cryogen reservoirs: one for liquid nitrogen and one for liquid helium. These are at the forward end, as mounted on SOFIA, with the entrance window on the aft end toward the telescope. There are three layers of radiation shielding within EXES: a vapor cooled shield tied only to the cryogen fill tubes, one attached to the liquid nitrogen reservoir, and the third attached to the liquid helium reservoir. All optics except for the entrance window/ lens are attached to the liquid helium level. Baffling tubes connected to the liquid nitrogen level reduce thermal emission impinging on the internal optics. Within the liquid helium level, the optics are all tied to a rigid optics box constructed out of aluminum and the detector headerboard is isolated with G10 fiberglass and is actively maintained at a uniform temperature.

Return to Table of Contents

2.1.2 Performance

EXES delivered performance appears consistent with expectations over the flight series so far. There are some variations from observation-to-observation, but we believe the values quoted here are fair estimates of what is typical. The angular resolution of EXES will match that achieved by the telescope. For the latest sensitivities, observers are recommended to consult the online Exposure Time Calculator (ETC). The ETC also provides the slit

length as a function of wavelength and instrument configuration (and therefore whether on-slit nodding is possible or not), as well as the wavelength coverage in a single setting and echelon orders that can be targeted.

The wavelength coverage ranges from 4.5–28.3 μm. There are three resolution regimes—high, medium and low—with the exact resolving power depending on wavelength, grating angle and slit width. Generally, the resolution will be higher at shorter wavelengths in each regime. The high-resolution configurations use the echelon grating and will achieve R = 50,000–100,000. If the cross disperser echelle angle is 35–65°, the configuration is called HIGH_MED and if 10–25° it is called HIGH_LOW. For these high-resolution configurations, there is non-continuous spectral coverage in high-resolution configuration for λ > 19 μm, but the central wavelength can be tuned so that lines of interest do not fall in the gaps. The Medium configuration will use high angles on the echelle grating to achieve R = 5,000–20,000, and the LOW configuration will use low angles to achieve R = 1,000–3,000.

The HIGH_MED configuration slits are 4.5–45 arcsec long, and the HIGH_LOW slits are 1–12 arcsec long. The shorter slits in HIGH_LOW allow for more orders to be packed onto the array, thus increasing the instantaneous wavelength coverage, while maintaining the high spectral resolution (see Figure 2-6 for an example). In the Medium and Low configurations the slit lengths vary from 25 to 180 arcsec depending on the number of rows to be read out.

The sensitivity of the instrument is shown in Figures 2-1 through 2-4 for the HIGH_MED, Medium, and Low configurations for both point sources and extended sources. The Noise Equivalent Flux Density for S/N of 10σ in a clock-time (Note that the other instruments in this Handbook report sensitivities based on the total time on-source, not the clock-time. The latter includes the total time on-source + applicable overheads, excluding target acquisition and instrument set-up time.) of 900 seconds is plotted as a function of wavelength. These values have been calculated for a point source assuming image quality between 2 and 4 arcsec (FWHM) and the narrowest of the available 1.4 to 3.2 arcsec slits, both of which vary with wavelength, and take into account estimated instrument efficiency. They assume an altitude of 41,000 feet, 40° elevation, and 7 μm precipitable water vapor.

Figure 2-1.

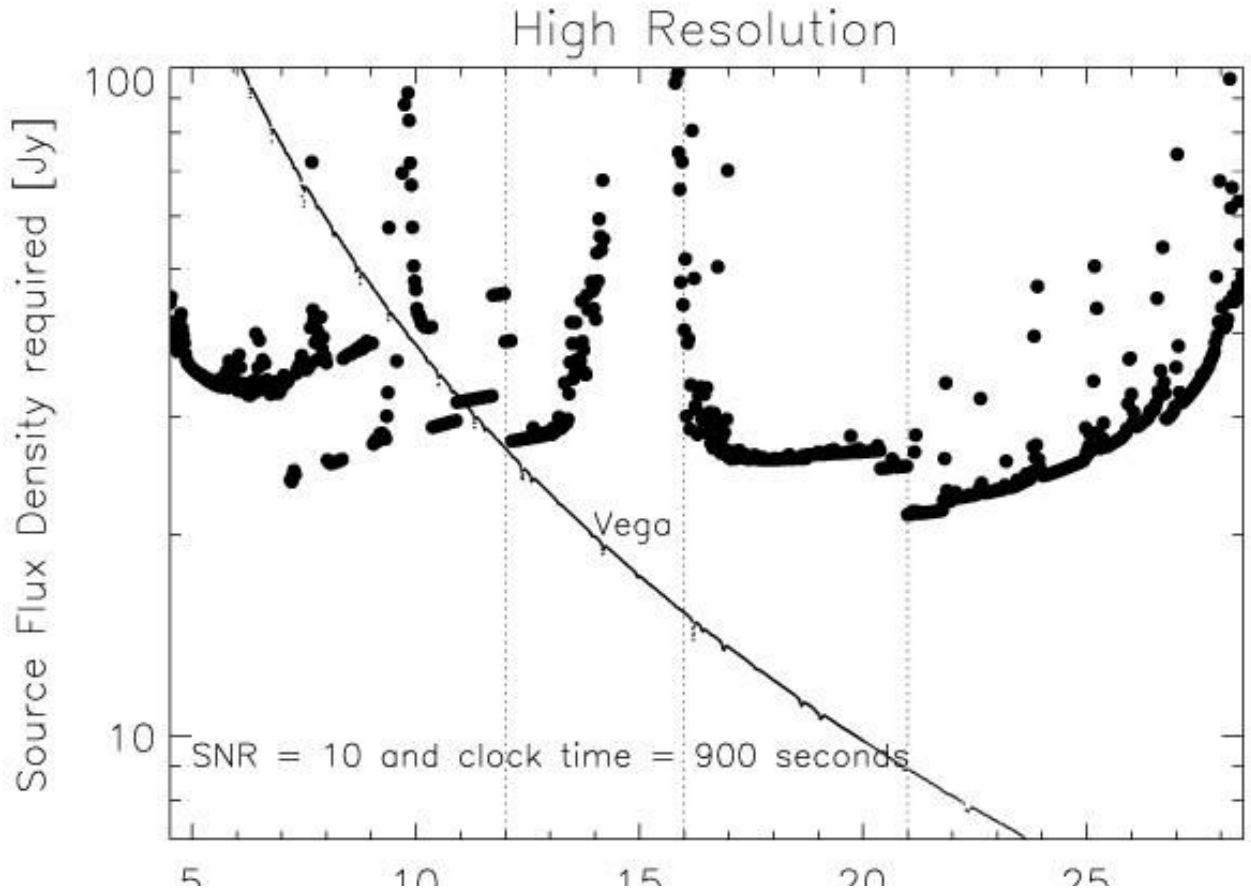

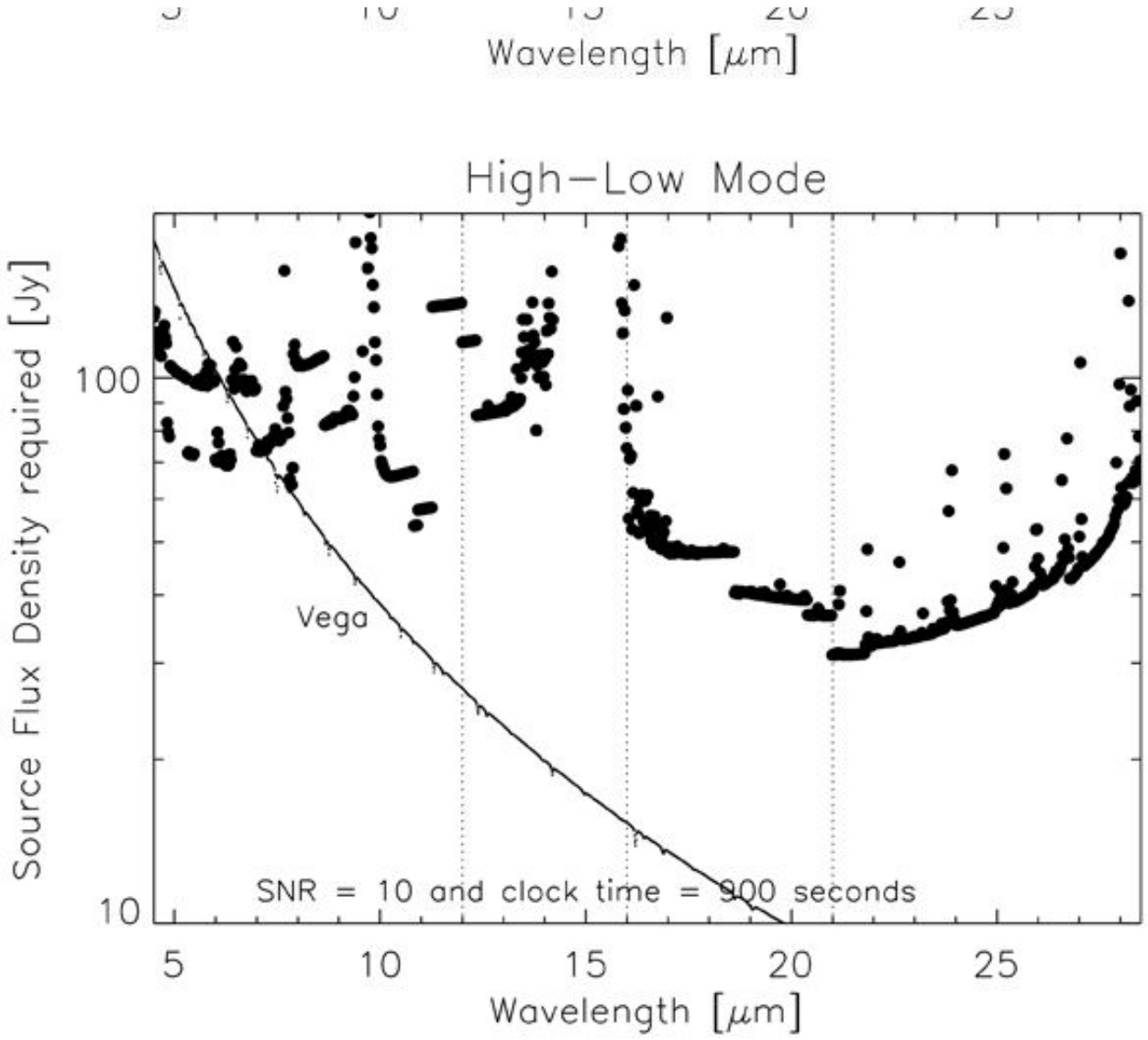

7 Figure 2-1. The minimum detectable point source flux as a function of wavelength for the EXES HIGH_MED (top) and HIGH_LOW (bottom) configurations, assuming the conditions mentioned above. It takes into account that on-slit nodding is not possible at all wavelengths. The vertical dotted lines show the boundaries between the slit widths used (1.4", 1.9", 2.4", 3.2"). For precise numbers at individual wavelengths and for the HIGH_LOW configuration please use the online .

Return to Table of Contents

2.1.2.1 Optics

The optics consist of an entrance window/lens, fore-optics, three wheels housing the slits, deckers and filters, an echelon chamber, and a cross-dispersion chamber. The entrance window/lens (2 inches diameter) forms an image of the SOFIA telescope secondary at the liquid helium cold stop within the fore-optics. The fore-optics, including the entrance window, changes the incoming f/19 beam to f/10. After coming to a focus, the beam expands through a pupil (at the cold stop) to an ellipsoidal mirror. The light is redirected off two flat mirrors to a focus at the slit plane.

As the beam comes to a focus, it passes through the slit/filter cassette. This consists of three wheels on a common axle containing (i) filters to isolate grating orders, (ii) deckers to determine the length of the slit, and (iii) slits of different widths. The filter wheel has 12 slots that will be loaded with specific filters for each cooldown cycle based on the planned observations. Broader filters for use in the Low resolution configuration are included in four of the decker wheel slots. The decker wheel has a total of 11 features, which include continuously variable length slits, fixed length slits, pinholes, and an open position. The continuously variable slit length is provided by a cutout on the decker wheel that gets larger as a function of angle. The smallest size is about 4.5 arcsec and the largest about 45 arcsec. The slit length depends on the wavelength and the instrument configuration. With that caveat, slit lengths can range from 1 to 180 arcsec on SOFIA.The slit wheel contains six slits. On SOFIA, EXES will typically use four of them (Table 2-1). There is also a wide 9.400 slit intended for flux calibration.

Table 2-1: Observing Configurations, Modes, Slits, and Spectral Resolutions

Configuration	Available Modes	Available Slit Widths[a] (arcseconds)	Resolving Power[b]
HIGH_MED	nod on slit[c], nod off slit, map	1.4	112,000
		1.9	86,000
		2.4	67,000
		3.2	50,000
HIGH_LOW	nod off slit, map	1.4	112,000
		1.9	86,000
		2.4	67,000
		3.2	50,000
Medium	nod on slit, nod off slit, map	1.4, 1.9, 2.4, 3.2	5,000-20,000[d]
Low	nod on slit, nod off slit, map	1.4, 1.9, 2.4, 3.2	1,000-3,000[d]

[a] 1.400 slit unavailable >12 µm, 1.900 slit unavailable >16 µm, 2.400 slit unavailable >21 µm

[b] Observers must check the most recent resolving powers as a function of slit width and wavelength at ETC

[c] On-slit nodding not possible at all wavelengths. Observers must check this at ETC

[d] Resolving power is a strong function of wavelength and slit width

After passing through the slit wheel, the beam hits a flip mirror mechanism, which is used to choose between instrument resolution configurations (Table 2-1) by either directing the beam into the echelon chamber (high-resolution) or into the cross-dispersion chamber (medium- and low-resolution). In the high-resolution configuration, the beam enters the echelon chamber and expands to an off-axis hyperboloid mirror that serves as

both collimator and camera mirror for the echelon grating. The dispersed light, focused by the hyperboloid, bounces off a flat into the cross-disperson chamber.

The cross-dispersion chamber is conceptually similar to the echelon chamber. The light expands from the input to an off-axis paraboloid that again serves as both collimator and camera mirror. The collimated beam is sent to the cross-dispersion grating which disperses the light in the plane of the grating. The camera mirror sends the light to our detector. When operating in single-order, long-slit spectral configurations—our Medium and Low resolution science configurations—the light never enters the high-resolution echelon chamber.

There is a wheel in front of the detector, which provides a lens for imaging the pupil through the instrument, and a dark slide for isolating the detector. The wheel would also be available for including transmissive optics to adjust the plate scale on the detector, if desired.

Return to Table of Contents

2.1.2.2 Detector

The detector is a Raytheon Vision Systems Si:As array with 1024x1024 pixels. The detector material is bonded to a SB 375 multiplexer. The array is mounted in a separate enclosure to reduce scattered light. The headerboard is thermally isolated from the rest of the optics box to permit active temperature control of the array. The photon fluxes in the Low configuration will be significantly above the level intended for the array. This prevents observations at longer wavelengths and/or with wider slits. When photon fluxes allow, only a subsection of the array will be clocked out in this configuration for a faster read-out (as well as in any imaging configuration). It is expected that a quarter to half the array will be utilized in these configurations, so the effective slit length is about 60''. There are other potential work-arounds that reduce the instrument sensitivity and may require extra overheads to prepare for and recover from low resolution observations. Proposers interested in low resolution observations should contact the instrument team to discuss their goals and possible options.

Return to Table of Contents

2.2 Planning Observations

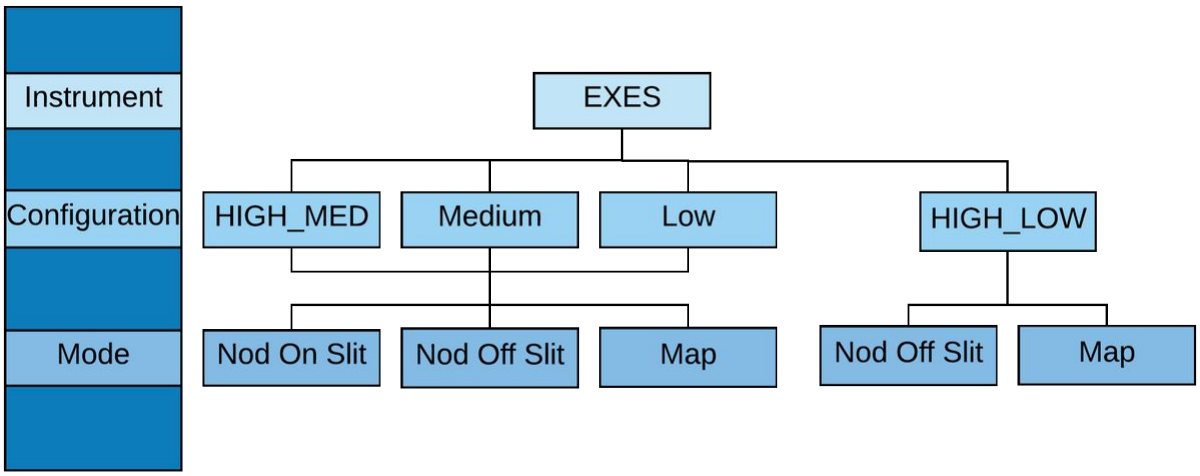

All EXES configurations and modes are released for observations. The observing modes for EXES are summarized as follows:

Nod On Slit
The telescope is nodded along the slit at distances that keep the target within the slit length. The nod throw is half the slit length. This is the most efficient EXES mode for point sources.

Nod Off Slit
The telescope is nodded such as that the object is not on the slit. This is used for extended sources or when the PSF is larger than four times the slit length.

Map
The telescope is moved perpendicular to the slit while EXES takes spectra on a grid of telescope positions, which are always one dimensional stripes.

Observers are always encouraged to contact the instrument team for the latest performance results—especially for the Low configuration, which suffers from saturation effects. There are potential work-arounds that reduce the instrument sensitivity and may require extra overheads to prepare for and recover from low resolution observations. Proposers interested in low resolution observations should contact the instrument team ready to discuss their goals and hear about possible options.

The proposer needs to supply the central wavelength, the spectroscopic configuration, the slit width, and the observing mode for each observation (Table 2-1). These parameters define the default instrument set-up. Each central wavelength specified should count as a separate observation. In addition, the proposer should estimate the clock time necessary to reach the desired S/N.

Figure 2-2.

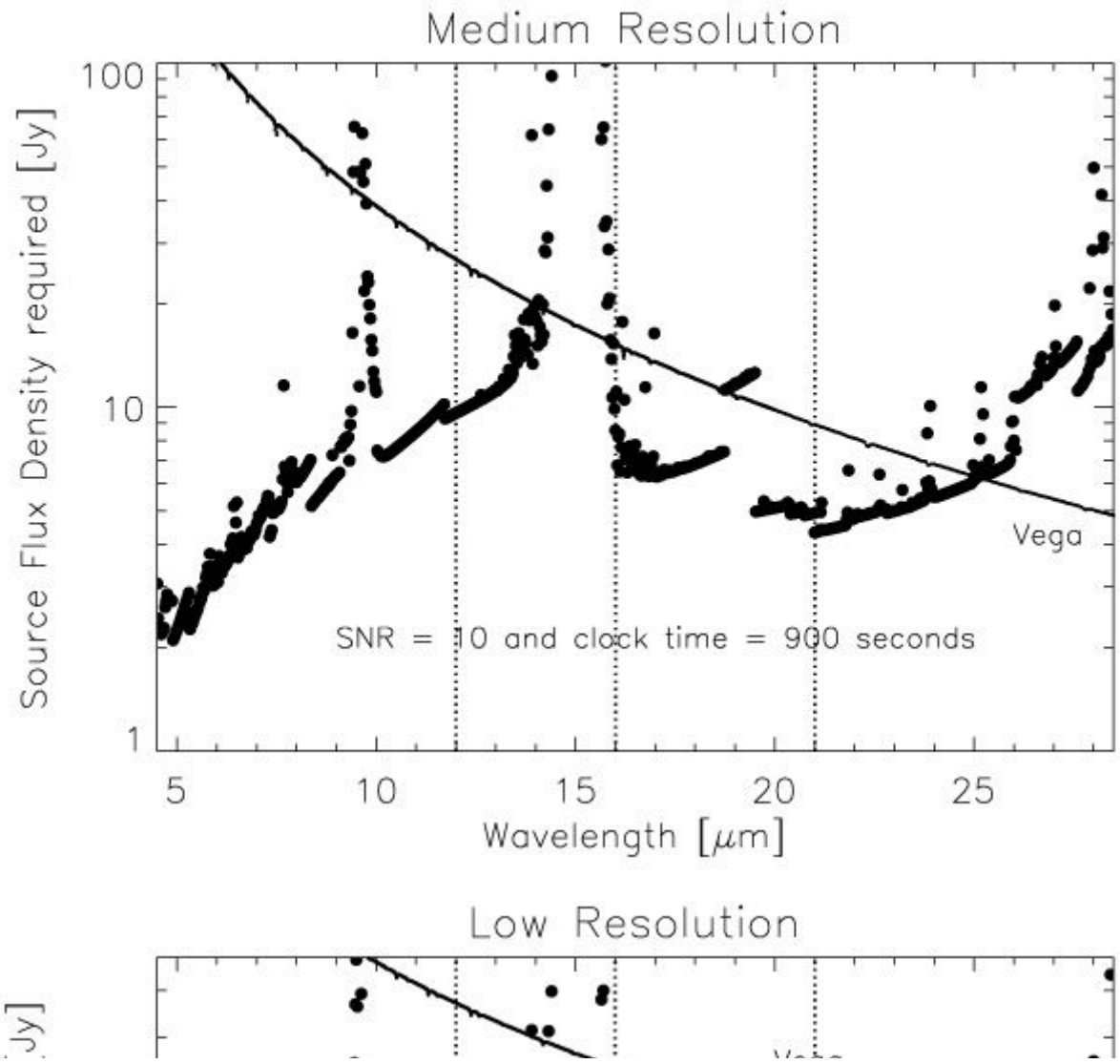

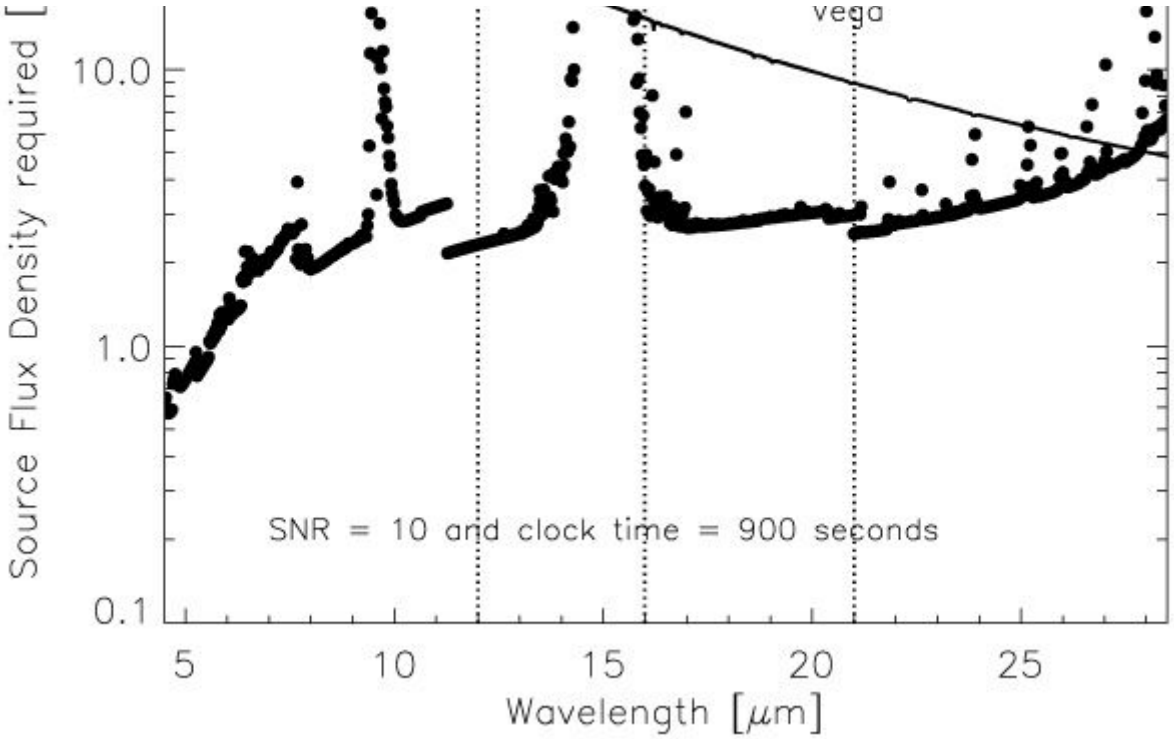

The calculation may be based on Figure 2-1 or 2-2 for point sources and on Figure 2-3 and 2-4 for extended sources, noting that the minimum detectable flux $\propto$ (S/N) / $\sqrt{(t_{exp})}$. However, it is recommended that the online ETC is checked as well for the latest updates.

Figure 2-3.

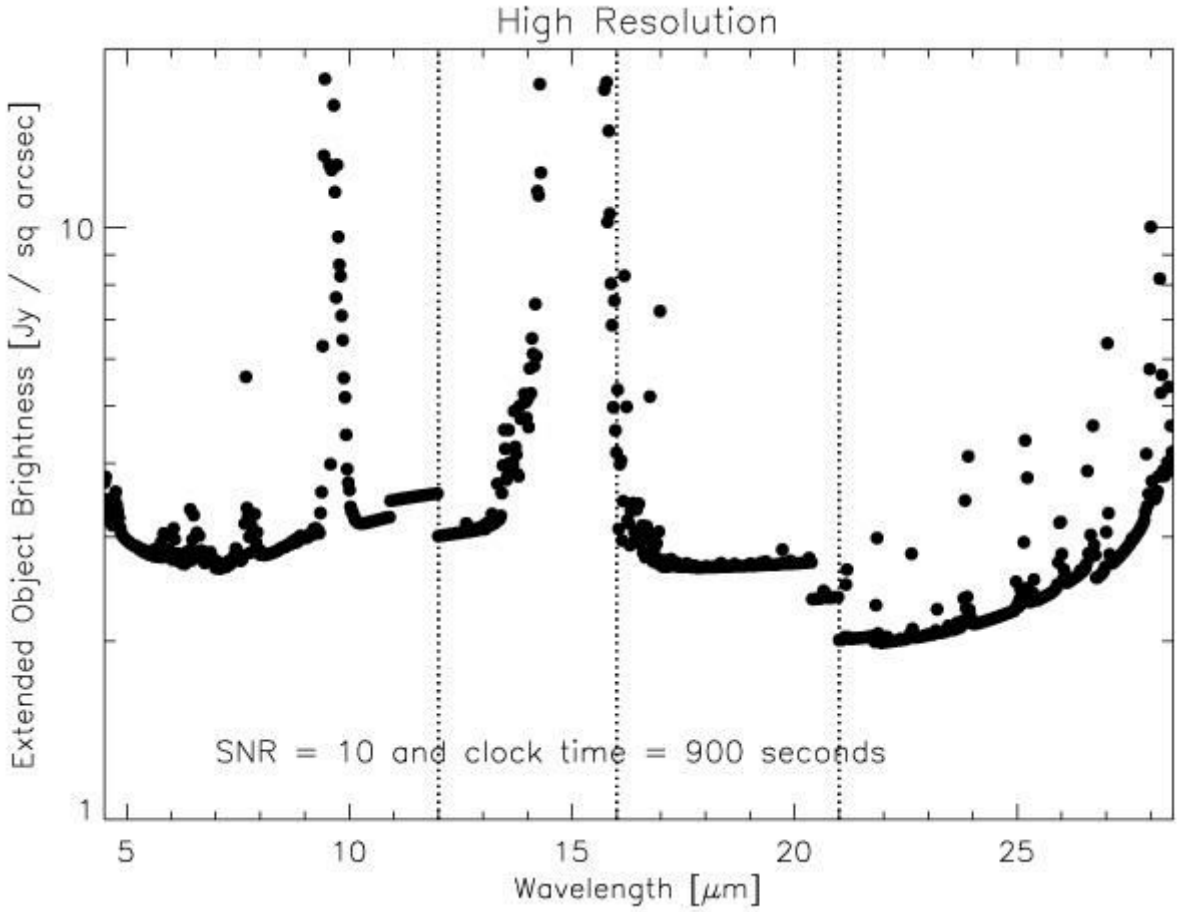

8 Figure 2-3. The minimum detectable extended source flux as a function of wavelength for the HIGH_MED and HIGH_LOW configurations (using off-slit nodding).

EXES operates in a wavelength region, parts of which are accessible from ground based telescopes. Proposers should carefully check the atmospheric transmission (using ATRAN, for example) and make sure that the observations require, or would greatly benefit from, using SOFIA. The proposer should take into account the Doppler shift of the target(s) due to their motion relative to Earth. If proposers find that the atmospheric transmission at the wavelength of interest is lower than the local median (calculated over a range ± 0.0125 μm), then more time will be required to reach the desired S/N. Higher transmission would imply shorter required times. In general, the S/N scales as *transmission*/√((1 - *transmission*) + 0.3). Note that the online ETC includes the impact of the atmosphere at precise wavelength of interest and so may differ from the figures above. The ETC provides the clock-time required to achieve the desired S/N per resolution element on a continuum object at the specific wavelength of interest and then indicates what the expected S/N should be for the entire setting.

Proposers should specify the slit width, which sets the resolving power for each configuration (Table 2-1). Note that the narrowest slit (1.4 arcsec) is only effective below 12 μm (above this wavelength no gain in resolving power is achieved, while flux is lost with respect to the wider slits). Similarly, the 1.9 arcsec slit can only be used below 16 μm, and the 2.4 arcsec slit below 21 μm.

Figure 2-4.

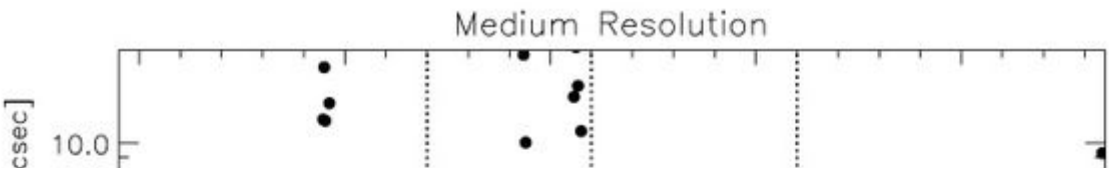

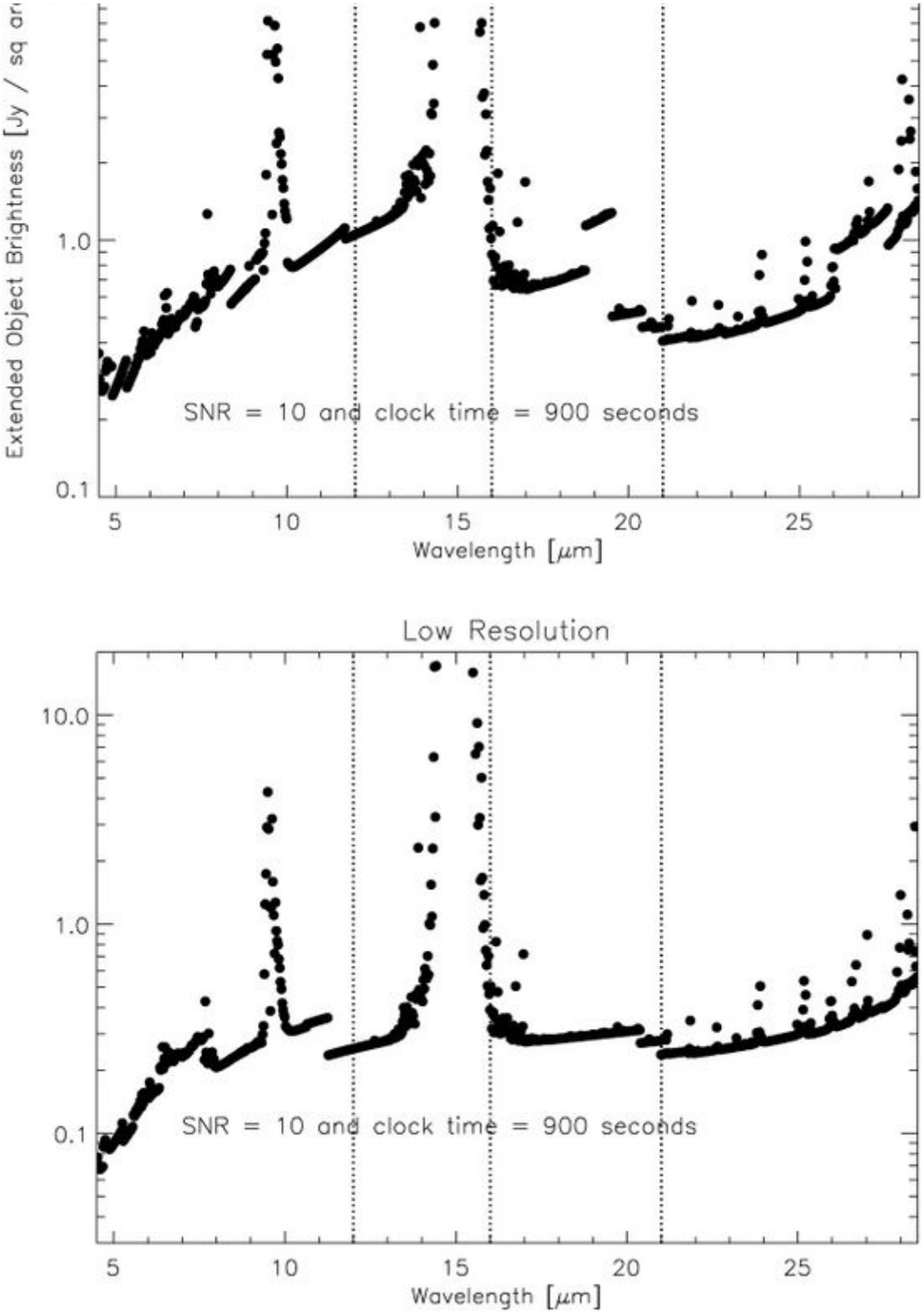

9 Figure 2-4. The minimum detectable extended source flux as a function of wavelength for the Medium (top) and Low (bottom) configurations, assuming the conditions mentioned at the end of . The vertical dotted lines show the boundaries between the slit widths used (1.4", 1.9", 2.4", 3.2").

In configurations using the medium resolution grating (Medium and HIGH_MED), the single setting spectral coverage ranges between 0.03 µm at the shortest wavelengths, and 0.3 µm at longer wavelengths (Figure 2-5). For the low resolution grating (the LOW and HIGH_LOW configurations) this is 0.2–0.8 µm. Note that while HIGH_LOW and HIGH_MED have the same spectral resolution, the larger wavelength coverage of HIGH_LOW comes at the expense of a smaller slit length, which is illustrated in Figure 2-6.

Figure 2-5.

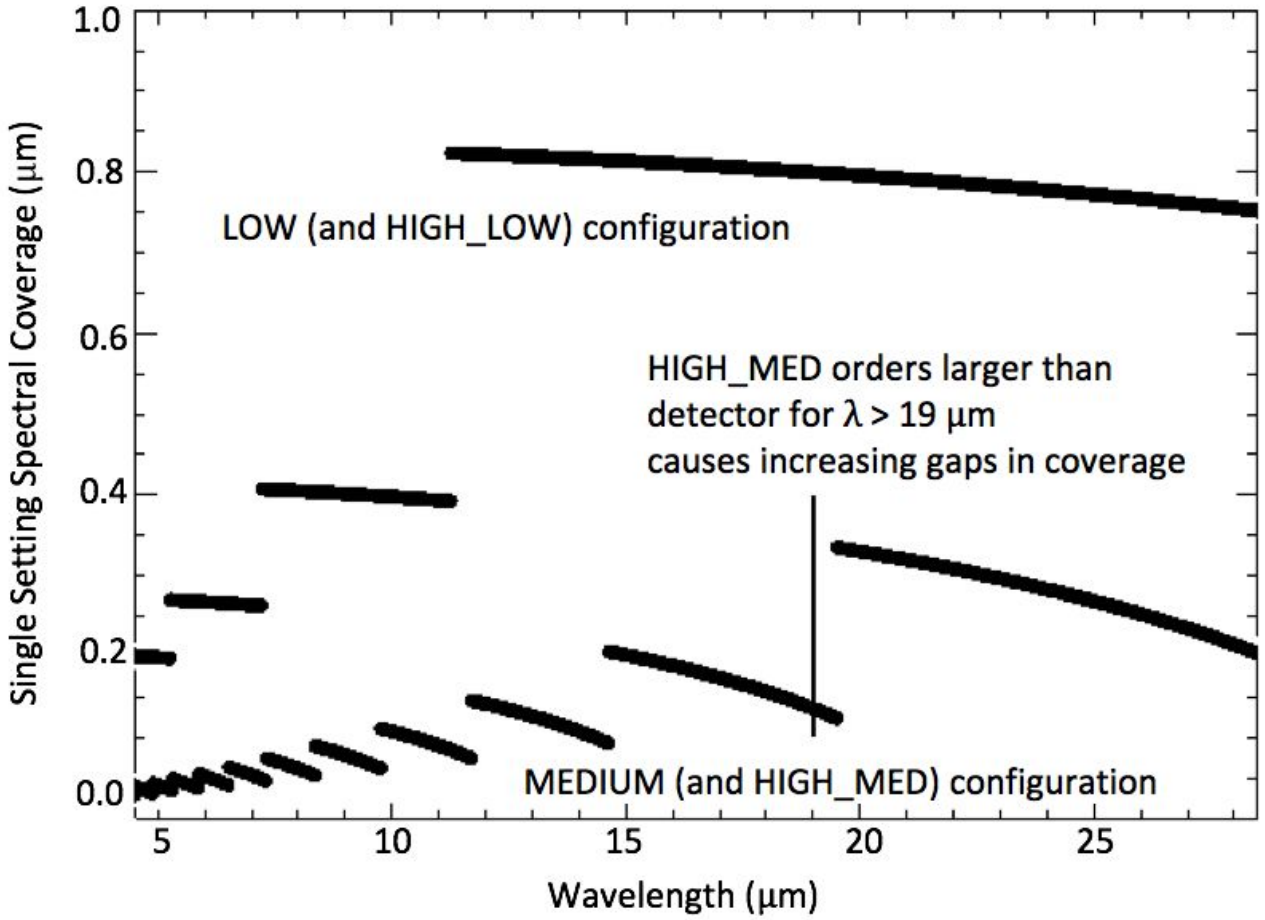

10 Figure 2-4. The minimum detectable extended source flux as a function of wavelength for the Medium (top) and Low (bottom) configurations, assuming the conditions mentioned at the end of . The vertical dotted lines show the boundaries between the slit widths used (1.4", 1.9", 2.4", 3.2").

Proposers should choose a single line of interest for each observation. Fine tuning of the bandpass to observe lines at the extreme edges of a single setting should be done in consultation with the EXES team to see if existing data indicates such tuning is possible.

The slit orientation on the sky depends upon the time when the target is observed and therefore the position angle cannot be specified.

Figure 2-6.

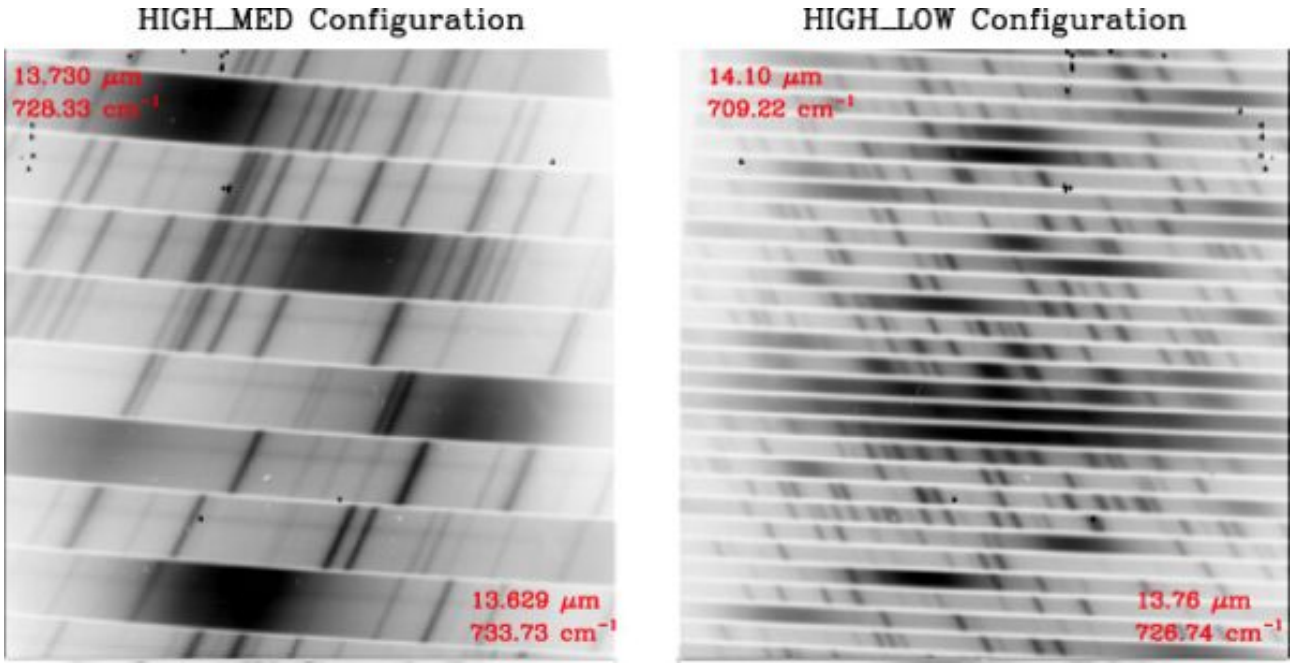

11 Figure 2-6. Comparison of raw 2D spectra of EXES in the HIGH_MED (left) and HIGH_LOW (right) configurations obtained during commissioning flights. The spectra are not nod-subtracted, highlighting the sky emission lines (dark). This comparison shows that, while the HIGH_MED and HIGH_LOW configurations have the same spectral resolution, HIGH_LOW has a much larger spectral coverage at the expensive of a shorter slit to be able to pack more orders on the array. In contrast, the Low and Medium configurations (not shown) have the same spectral coverage as HIGH_LOW and HIGH_MED, respectively, but a lower spectral resolution without cross dispersion. The approximate start and end wavelengths are indicated in red.
EXES will not use the secondary for chopping in any of its observations. Rather, only nodding and mapping modes will be implemented.

In a nod mode (either Nod On Slit or Nod Off Slit), the telescope is moved to a new position in order to remove the sky background. For point sources observed with a sufficiently long slit, the telescope is moved such that the object remains on the slit (Nod On Slit mode). For sources larger than about a quarter of the slit length, the telescope is moved such that the object is not on the slit (Nod Off Slit mode). The time between telescope motions will depend on the sky variation, the telescope settling time, and the integration time. The goal is to maximize the signal-to-noise per clock time. For observations of point sources, the detectable flux plots (Figures 2-1 and 2-2) and the ETC include assumptions regarding whether nodding off the slit is required due to short slit lengths. For nodded observations of extended objects, proposers should contact the EXES team to check if nodding on the slit is possible. If not, the observing time required should be doubled. Unless specific nod parameters are requested for such observations, the instrument team will define the nod amplitude, direction, and frequency. The sensitivities for extended source observations shown in Figures 2-3 and 2-4 assume that the source is nodded off-slit and take into account the variation in spatial resolution with wavelength. The atmospheric and overhead factors for nodding are included. If the source is small relative to the slit length, then it may be possible to nod along the slit. In this case, the source brightness given in the figures is for a SNR of 10 in 450 seconds.

In Map mode, the telescope is moved sequentially such that a series of positions along straight lines on the sky (i.e. along stripes) are observed to create a map. The sky background is taken from the first positions and, depending on the size of the map, from the last positions. In general, we anticipate the telescope motions to be half the slit width to create a well-sampled map. Proposers should specify the number of steps in a map and the step size. Map steps are generally assumed to be perpendicular to the slit. The first three positions for taking data in a map must be blank sky. These could be the first three positions of the map or at a separate sky offset position specified by the user. It is recommended that additional blank sky positions are observed at the end of the map on the other side of the object. For all maps, the instrument software returns to the sky offset position for three final sky observations at the end of the observation. Proposers should specify the required clock time based on the flux limit desired, using

the values in Figures 2-3 and 2-4, including any assumptions regarding binning of map positions to yield the final required SNR. The SNR for a single map position can be estimated by assuming that the required time is similar to that for nodding an extended object on slit, i.e. 10σ in 450 seconds for a given source brightness. If any spatial binning is required—at least a two-step sum is recommended—then the SNR will improve by the square root of the number of steps in the sum. The online ETC allows the user to specify the number of steps and bins according to the predicted image quality in producing a clock-time estimate.

Return to Table of Contents

2.2.1 Wavelength Calibration

Wavelength calibration with EXES will be performed by applying the grating equation to atmospheric lines observed in the source spectra. As long as there is a single telluric feature in the bandpass with depth of at least 5%, the wavelength calibration is expected to be accurate to $\cong$ 0.5 km s^{-1}.

If atmospheric models show no telluric features within the EXES instantaneous band pass for a given observation, then obtaining a good wavelength solution will require a few additional steps. Note that the absence of telluric features from SOFIA suggests the observation may be better done from the ground. First, the order sorting filter (OSF) is rotated so that a different order from the echelle is observed that includes a suitable telluric line. The grating equation can then be applied, providing wavelength calibration accuracy down to ≈ 1 km s^{-1}. The process of rotating the OSF, observing blank sky, and rotating the OSF back to the original orientation should take less than 5 minutes of additional time. A demonstration of this procedure can be found in Harper et al. (2009, ApJ, 701, 1464).

Return to Table of Contents

2.2.2 Flux Calibration and Atmospheric Line Correction

For every EXES science observation, the EXES temperature-controlled black body source and a nearby blank sky field will be observed. From these, a calibration spectrum will be constructed that will correct for response variations and provide flux calibration after division over the science observations. In principle, division by the calibration spectrum would also correct for telluric absorption lines (see Lacy et al., PASP volume 114, issue 792, p. 153), but this is presently not the case because of the large difference between the blackbody and sky temperatures. The flux calibration is expected to be better than 20% but the true accuracy is currently uncertain. Experiments focused on line profile information and those that can normalize the continuum level (or use past observations for setting the continuum) will likely be more successful. Projects requesting a telluric calibration object, in particular those observing lines near strong telluric features or those observing relatively broad lines, will need to include the observation time required in their proposal. Because of the difficulty of scheduling a given telluric calibrator with the science target in a given flight, the specific calibrator will need to be chosen at the time of flight planning in consultation between the program proposer, the instrument PI, and the SMO support scientist. For wavelengths below 8–10 μm this will most likely be a hot, bright star (e.g., Vega or Sirius) and at longer wavelengths an asteroid. Galilean moons will also be considered, provided they are well separated from Jupiter. For the proposal, a separate observation entry should be entered via USPOT with name `Cal_target` where *target* is the name of the associate science target (e.g., `IRC+10216` and `Cal_IRC+10216`) and given the coordinates RA:00:00:00, Dec:+00:00:00. The observing time for such a telluric standard observation will depend on the instrument configuration and wavelength observed as well as on the signal-to-noise level needed. Proposers must use the EXES ETC to estimate this, assuming a continuum brightness of 100 Jy below 10 μm and 150 Jy above 10 μm for the HIGH_MED and HIGH_LOW configurations. For the Medium and Low configurations the proposer should assume at all wavelengths a brightness of 50 Jy and 25 Jy, respectively. Proposers are urged to limit the EXES clock times on the telluric standard at a given wavelength and instrument configuration to less than about 30 minutes. Further improvement of the removal of telluric absorption features may be achieved by employing models of the Earth's atmospheric transmission.

Return to Table of Contents

2.2.3 Overheads

The treatment of overheads for EXES differs from that of most other SOFIA instruments: instead of on-source times, users are required to specify wall clock times (i.e. total elapsed time) in USPOT, which is the on-source time plus all overheads except those related to acquisition and instrument set-up. The overheads include time on empty sky in the off-slit nodding and mapping modes as well as read-out and other telescope and instrument inefficiencies. The ETC and the figures in this manual give the clock times needed. The figures in this manual only give clock times. USPOT will add an additional 15 minutes for peak-up, wavelength optimization, flux calibration, and flat field overheads in the HIGH_MED, Medium, and Low configurations and 20 minutes in HIGH_LOW. In all configurations, an extra 3 minutes of peak-up time is needed for the narrow (1.4 arcsec) slit. If no peak-up is necessary (i.e., after a wavelength change on the same target, if the source is extended, or if the continuum emission is too weak), the overheads can be reduced by using the **No Peak-Up** option in USPOT. Overheads can also be reduced if multiple sky positions are observed in the same wavelength setting. In this case, click the **No Wavelength Setup** button in USPOT. Note that the time on a given target on a single flight is limited to 90–180 minutes, so full overheads may be needed again once the sum of AOR times exceeds 90 minutes. Conversely, if a single observation takes more than 90 minutes it may need to be split into multiple AORs, each with full overheads. Please consult the EXES and SOFIA staff in these cases.

Return to Table of Contents

2.2.4 As a Principle Investigator Instrument

EXES is a Principal Investigator (PI) class instrument. The proposer is encouraged (but not required) to contact the Instrument PI before preparing or submitting the proposal, since the PI has the most up to date information about the instrument capabilities. However, it is recommended that they do so, in order to get the most up to date information about instrument capabilities. The data collection and reduction will be done by the instrument team, and it is expected that data analysis and preparation of the results for publication will be done by the proposers in collaboration with the instrument team.

Return to Table of Contents

3. FIFI-LS

To export the handbook as a PDF, click on the three dots in the upper right, then choose "Export with Scroll PDF Exporter". In the Template drop-down menu, choose "Handbook Template", and then click "Export".

3.1 Specifications

3.1.1 Instrument Overview

The Far Infrared Field-Imaging Line Spectrometer (FIFI-LS) is an integral field, far infrared spectrometer. The instrument includes two independent, simultaneously operating grating spectrometers sharing one common field-of-view (FOV). Each spectrometer has a detector consisting of 400 pixels of Germanium Gallium-doped photoconductors. The short wavelength spectrometer (blue channel) operates at wavelengths between 50 µm and 125 µm, while the long wavelength spectrometer (red channel) covers the range from 105 µm up to 200 µm. One of two dichroics has to be selected for an observation affecting the wavelength range of both channels in the overlap region.

The projection onto the sky of the 5x5 pixel FOVs of both channels is concentric (10 arcsec offset), but the angular size of the FOVs differs. The red channel has a pixel size of 12x12 arcsec yielding a square 1 arcmin FOV and the blue channel has a pixel size of 6x6 arcsec, which yields a square 30 arcsec FOV.

The resolving power of both channels varies between 1000 and 2000 dependent on the observed wavelength. The higher values are reached towards the long wavelength ends of each spectrometer.

The detectors are cooled down to about 1.7 K with super fluid helium. The spectrometers and all mirrors are cooled down to 4 K with liquid helium. The exception is the entrance optics featuring a K-mirror (see Section 3.1.1.3) and an internal calibration source. These optical components are cooled to about 80 K with liquid nitrogen.

Return to Table of Contents

3.1.1.1 Integral Field Concept

The integral field unit (IFU) allows FIFI-LS to obtain spectra at each point in its FOV; this is in contrast to a spectrometer with a slit, which only provides spectra along the slit. Both channels in FIFI-LS have an IFU, which consists of 15 specialized mirrors to separate the two dimensional 5x5 pixel FOV into five slices (of five pixels length each) which are then reorganized along a (one dimensional) line (25x1 pixel). This line forms the entrance slit of the actual spectrometer. The diffraction grating disperses the incoming light in the spectral dimension. Finally the dispersed light reaches the 16x25 pixel detector array. The result is a data cube with 5x5 spatial pixels (spaxels) and 16 pixels in the spectral dimension. Figure 3-1 shows the concept.

Figure 3-1.

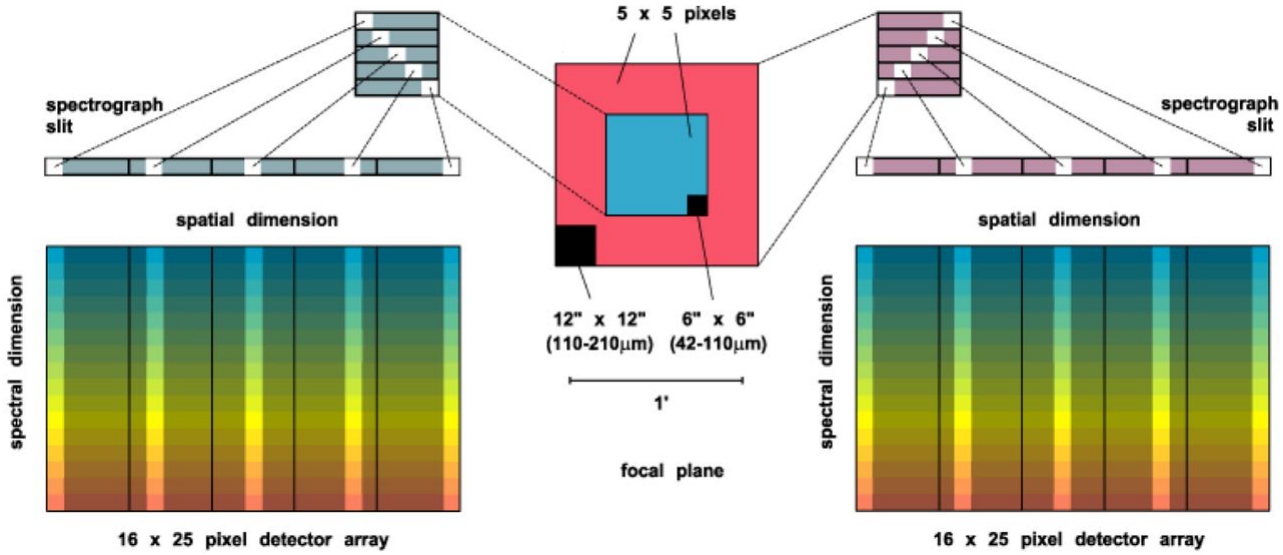

12 Figure 2-6. Comparison of raw 2D spectra of EXES in the HIGH_MED (left) and HIGH_LOW (right) configurations obtained during commissioning flights. The spectra are not nod-subtracted, highlighting the sky emission lines (dark). This comparison shows that, while the HIGH_MED and HIGH_LOW configurations have the same spectral resolution, HIGH_LOW has a much larger spectral coverage at the expensive of a shorter slit to be able to pack more orders on the array. In contrast, the Low and Medium configurations (not shown) have the same spectral coverage as HIGH_LOW and HIGH_MED, respectively, but a lower spectral resolution without cross dispersion. The approximate start and end wavelengths are indicated in red.

Return to Table of Contents

3.1.1.2 Selection of the Dichroic

The two channels have an overlap in their wavelength range. That is necessary because a dichroic splits the light between the two channels allowing the common FOV for both channels. The drawback is that a dichroic has a transition region where neither the transmission nor the reflection is good. Thus, FIFI-LS has two dichroics with transitions at different wavelengths. The The D105 cuts off the blue channel at about 100 µm and opens the red at about 115 µm. The D130 cuts off the blue channel at 120 µm and opens the red at 130 µm. Figure 3-2 should be used to choose the best dichroic and line combinations. The proposer needs to pair up wavelengths so that each pair can be observed efficiently with one of the dichroics. Typically, the D105 is used unless a wavelength between 100 and 115 µm is observed.

Figure 3-2.

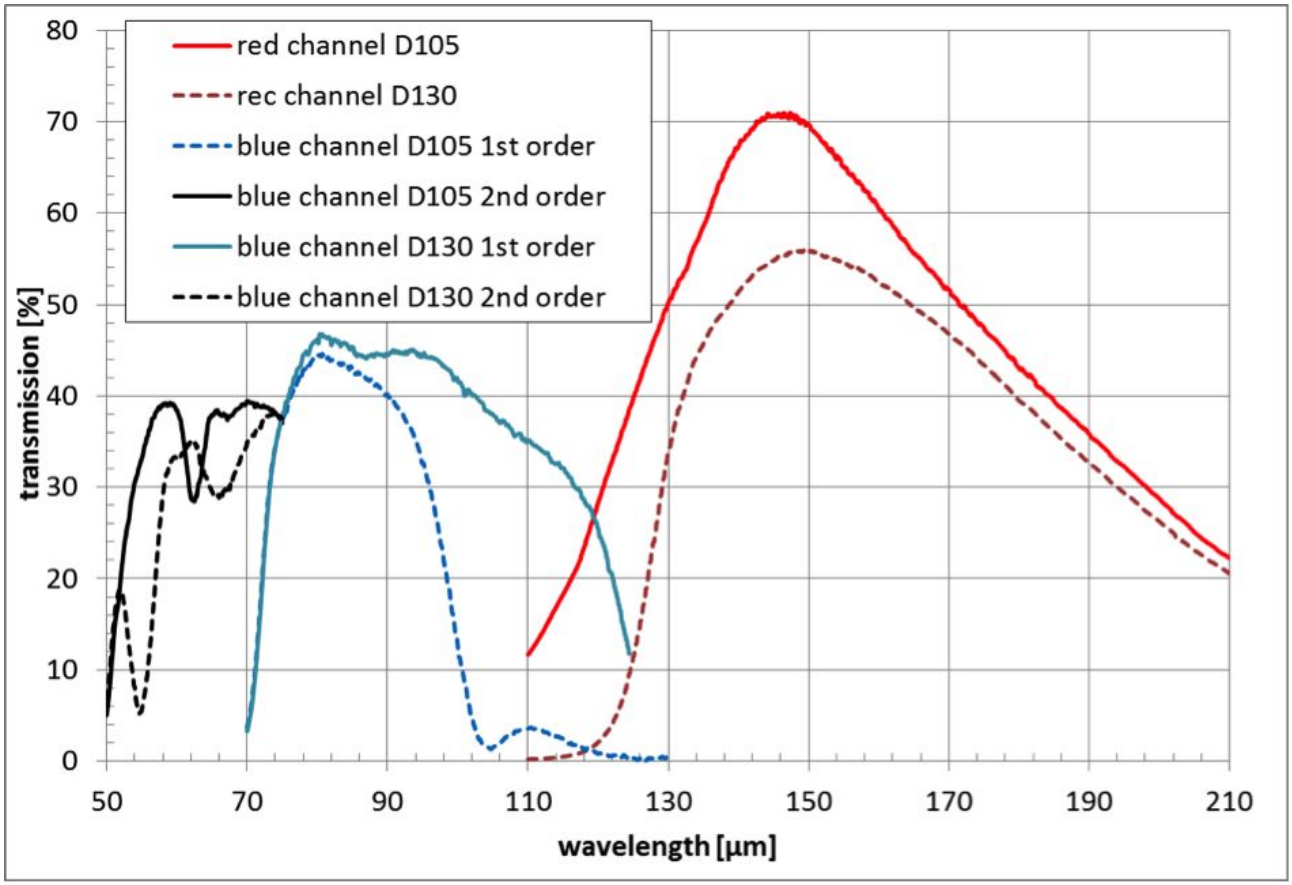

13 Figure 3-2. Throughput of optical system—here the transmission of the overall optical system is shown for the six possible optical configurations using two dichroic beam splitters (D105 and D130) and both grating orders (blue channel only).

Return to Table of Contents

3.1.1.3 Beam Rotator

The SOFIA telescope is essentially an Alt-Az-mounted telescope. Thus, the field of view on the sky rotates while tracking an object. However, the telescope can rotate around all three axes, but the amount it can rotate in cross-elevation and line-of-sight is limited. Thus, the normally continuous sky rotation is frozen-in for some time while the telescope is inertially stabilized. When the telescope reaches its limit in line-of-sight rotation, it needs to rewind, resulting in a rotated FOV of the telescope.

FIFI-LS has a beam rotator (K-mirror) that rotates the instrument's FOV, counteracting the sky rotation experienced by the SOFIA telescope. When a rewind happens, the FIFI-LS beam rotator will automatically rotate the FOV of the instrument, so that the position angle of the instrument's FOV on the sky is maintained. An additional benefit is that the beam rotator enables the observer to line up the FOV with e.g. the axes of a galaxy and keep the alignment. The desired position angle of the FOV can be specified in Phase II of the proposal process.

Return to Table of Contents

3.1.2 Performance

3.1.2.1 Comparison with the PACS Spectrometer

The FIFI-LS design is very similar to the Herschel/PACS-spectrometer sharing much of the design. The detectors are basically the same and the optical design is very similar (same sized gratings in Littrow configuration, same IFU). The difference is that FIFI-LS features two grating spectrometers whereas the PACS-spectrometer had only one. The two gratings make it possible to observe two different wavelengths simultaneously and independent of each other (one in each channel). This design also allows different pixel sizes (6 arcsec vs 12 arcsec) in each spectrometer, which means a better match to the beam size. The spectral range of FIFI-LS also goes down to 51 µm whereas PACS did not routinely observe the [OIII] 52 µm line.

Return to Table of Contents

3.1.2.2 Spectral Resolution

The blue spectrometer operates in 1st and 2nd order. An order-sorting filter blocks the unwanted order. The red spectrometer only operates in 1st order. The spectral resolution of FIFI-LS depends on the observed wavelength. It ranges from $R = \lambda/\Delta\lambda$ ~500 to 2000 corresponding to a velocity resolution of 150 to 600 km/s. The top panel of Figure 3-3 shows the spectral resolution in velocity and in R vs. wavelength, also given in Table 3-1 for selected spectral lines.

FIFI-LS has 16 pixels in the spectral direction. The wavelength range covered by these 16 pixels also depends on the observing wavelength. The bottom panel of Figure 3-3 shows the instantaneous spectral coverage or bandwidth (BW) in micron.

Table 3-1

Line	Rest λ (micron)	Channel	R	FWHM (km/s)	Inst. Cov. (km/s)	Inst. Cov. (micron)
[OIII]	51.8	blue	950	320	1840	0.32
[NIII]	57.3	blue	1050	280	1540	0.29
[OI]	63.2	blue	1300	230	1240	0.26
[OIII]	88.4	blue	600	490	2340	0.69
[NII]	121.9	red	750	390	2340	0.69
[NII]	121.9	blue	1050	290	1350	0.55
[OI]	145.5	red	1000	300	1800	0.87
[CII]	157.7	red	1150	260	1560	0.82

Line	Rest λ (micron)	Channel	R	FWHM (km/s)	Inst. Cov. (km/s)	Inst. Cov. (micron)
more to come CO lines						

Spectral resolution and instantaneous coverage for selected spectral lines

Figure 3-3.

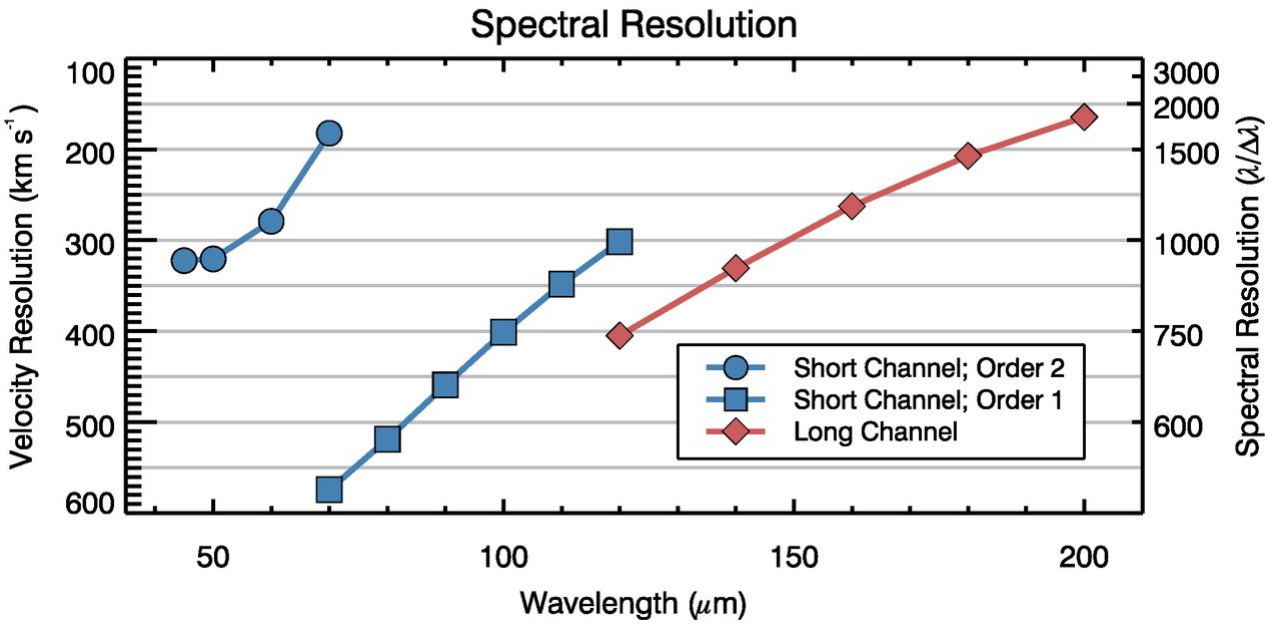

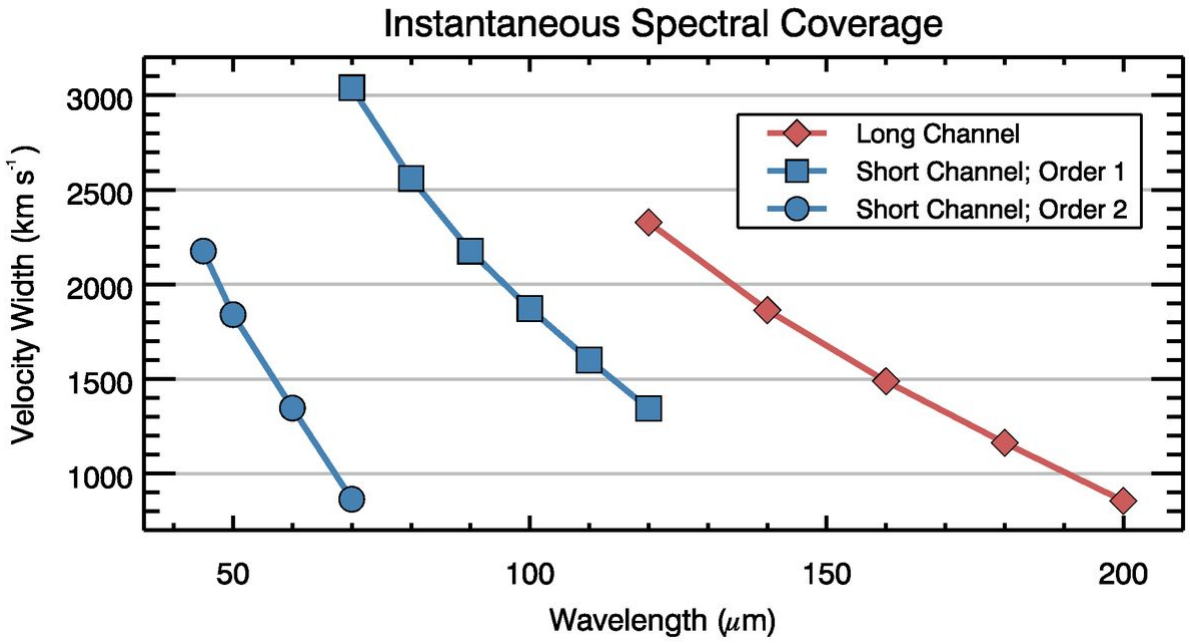

14 Figure 3-3. Top, The spectral resolution in km/s and λ/Δλ for both channels; Bottom, The instantaneous wavelength coverage in km/s of the 16 spectral pixels vs. wavelength.
Return to Table of Contents

3.1.2.3 Sensitivity

FIFI-LS will operate such that the detectors are always background-limited, infrared photodetectors. Under this assumption, the overall performance of FIFI-LS as a function of wavelength has been estimated. Further assumptions about the emissivity of the telescope, optics, and baffling, the efficiency of the detectors had to be made. Figure 3-4 shows the resulting sensitivities for continuum and unresolved lines as minimum detectable fluxes per pixel, i.e. detected with a signal to noise ratio (SNR) of 4 and an on-source integration time of 900 s or 15 min.

The SOFIA Instrument Time Estimator (SITE) should be used to estimate the on-source exposure times used in proposals and observing preparation. The time estimator calculates the on-source integration time per map position for a source flux, *F* and a desired SNR using Eq. 3-1:

(Eq.3-1)

$$t_{\rm on} = l\left(\frac{\rm SNR/4}{\alpha \rm F/MDF(\lambda)}\right)^2 900 \text{ s}$$

where MDF(λ) is either the Minimum Detectable Continuum Flux (MDCF) in Jy per pixel or the Minimum Detectable Line Flux (MDLF) in W m^{-2} per pixel at the entered wavelength (see Figure 3-4).

Figure 3-4.

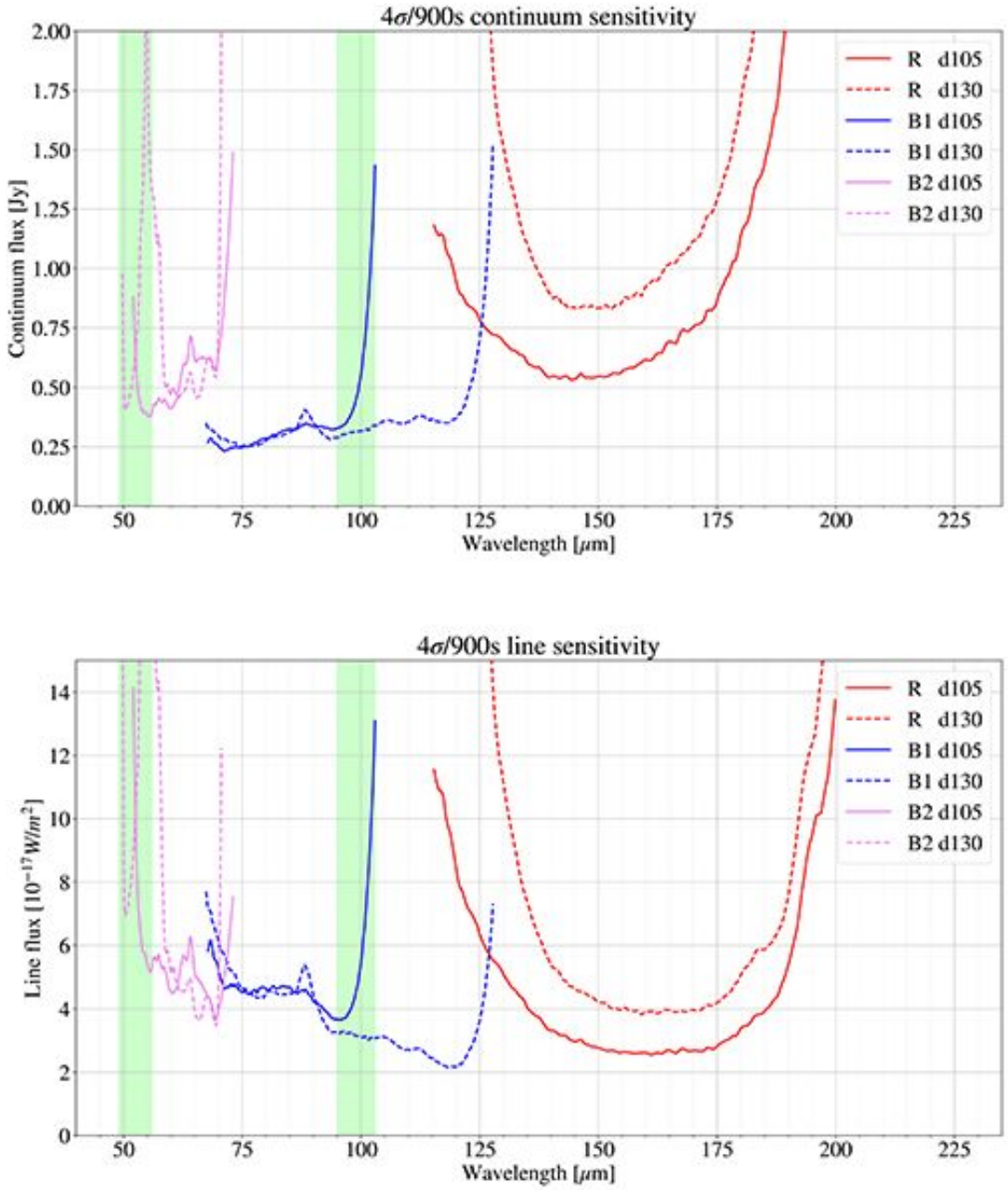

15 Figure 3-4. Continuum and emission line sensitivities for a monochromatic point source: The values are calculated for a SNR of 4 in 900 s. The MDCF is in Jy per pixel and the MDLF is in Wm-2 per pixel. Both sensitivity values scale as SNR / √(t), where t is the on-source integration time.

Return to Table of Contents

3.2. Planning Observations

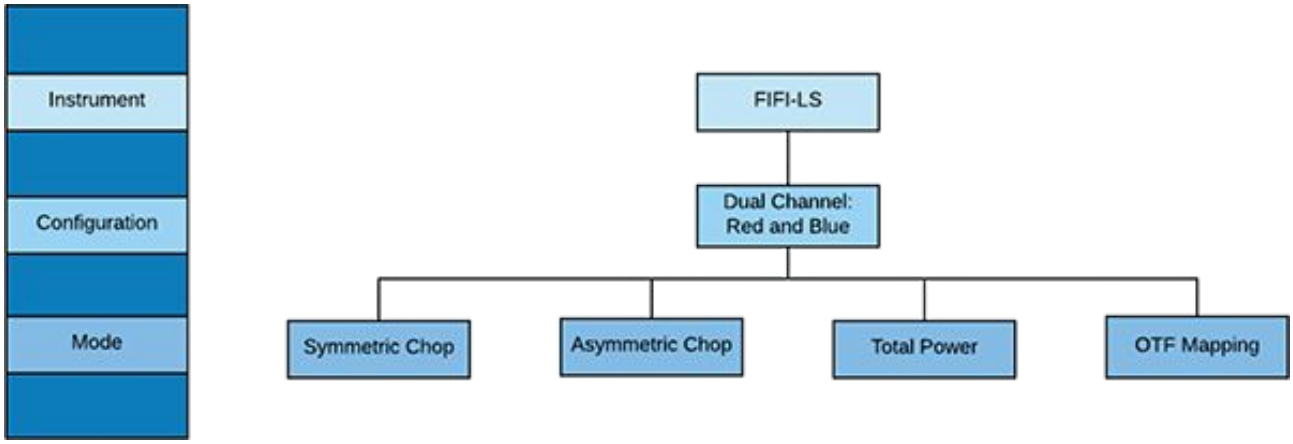

3.2.1 Observing Modes

The high sky background in the far infrared requires careful subtraction. That is achieved by chopping with SOFIA's secondary mirror and/or by nodding the telescope.

In the chopped modes (symmetric and asymmetric chop) the secondary chops at 2 Hz to efficiently remove the sky emission. To remove residual background not canceled by chopping, the telescope is nodded typically every 30s either to move the source to the other chop-beam or to an off-position. Since the instrument telescope communications and the telescope move take 8s, a whole nod-cycle for a symmetrically chopped observation typically takes 76s. In the unchopped modes (OTF and total power) integration times vary between 10 and 30s to ensure a sufficiently short nod interval.

Symmetric chopping is the most commonly used observing mode with FIFI-LS since it combines the best background subtraction offered by chopping with good observing efficiency. Asymmetric chopping becomes necessary for extended sources but does also allow for shorter on source integration times for bright sources. Total Power observations are used for even larger sources that do not enable chopping at all. On the fly mapping (OTF) is a new mode that that enables good spatial sampling and observing efficiencies for extended maps.

The following sections describe the possible observing modes. In the discussion of the overheads, N is the number of map positions and ton is the on-source exposure time per map position. Details like the exact chop throw and angle do not need to be fixed until Phase II of the proposal process, but proposers should attempt to determine if their chosen mode is feasible for their targets as moving to a different mode, often with a higher overhead, after time has been allocated can give less integration time on the targets and thus affect the feasibility of the program. Information on how the parameters for each mode is to be entered into USPOT during Phase II of the proposal process can be found on the FIFI-LS USPOT web page.

Return to Table of Contents

3.2.1.1 Symmetric Chop

This mode combines chopping symmetrically around the telescope's optical axis with a matched telescope nod to remove the residual telescope background. This mode is also known as nod match-chop (NMC) (cf. Section 5.2.1) or beam switching (BSW, cf. Section 7.2.1).

When observing using a symmetric chop the target is imaged off the optical axis. Large chop amplitudes therefore degrade the image quality due to the introduction of coma. This effect causes asymmetric smearing of the Point Spread Function (PSF) in the direction of the chop. However, the effect is small (with an effect on the Signal to Noise Ratio (SNR) of less than 10%) in the red channel for all permitted chop throws and in the blue channel for total chop throws less then 6 arcmin and wavelengths longer than 63 µm. For wavelengths shorter than 63 µm, we

recommend total chop throws of less than 4 arcmin, although observations have been made successfully with larger throws – please contact the SOFIA helpdesk (sofia_help@sofia.usra.edu) to discuss this if it is necessary for your observations. Generally, it is recommended to use a chop as small as possible while keeping the FOV in the off positions outside of any detectable emission.

The position angle of the chop can be specified relative to equatorial coordinates or telescope coordinates (e.g. horizontal). Keep in mind that the telescope nod matched to the chop creates two off-positions symmetric to the on-position (Figure 3-5). Horizontal chopping is preferred when it is possible, i.e. for relatively small sources without any other sources of emission in the surrounding field and for which the position angle of the chop is thus unimportant.

The total overhead in this mode is about 1.6 N ton + 300s, since the source is only observed during 50% of the observation and additional time is required for telescope moves, plus 300s for the setup. This overhead estimate assumes that the on-source exposure time per map position ton is 30s; ton can be set to any value between 15 and 30s in this mode but for values less than 30s the overhead calculated by USPOT will be larger than given here as the fixed time for the telescope moves becomes more important. If the desired on-source exposure time per map position ton is less than 15s, the asymmetric chop mode or the on the fly mapping mode should be used.

Figure 3-5.

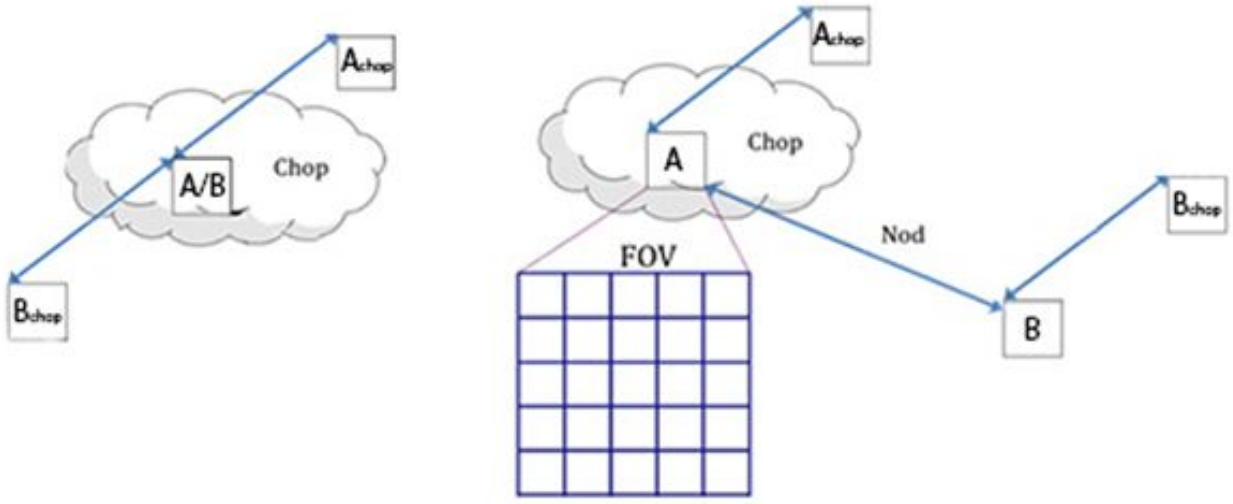

16 Figure 3-5. The geometry of chopping and nodding in the Symmetric Chop mode (left) and the Asymmetric Chop mode (right).

Return to Table of Contents

3.2.1.2 Asymmetric Chop

If the target's size or environment does not allow the Symmetric Chop mode to be used, e.g. if it is not possible to find clean symmetric chop positions on opposite sides of the source, the Asymmetric Chop mode allows larger chop throws and needs an emission free field only in direction from the source. The maximum chop throw is ~10 arcmin for all wavelengths. It also allows for faster mapping of extended sources. The asymmetric chop keeps the on-beam on the optical axis in most cases, resulting in an image unaffected by coma. Consequently, the off-beam is off-center by twice the amount of a symmetric chop with the same chop throw, resulting in twice as much coma in the off – but as the off-beam should only see empty sky this does not affect the observations. The telescope is nodded to an off position where the same chopped observation is executed to provide the residual background subtraction. Figure 3.5 illustrates this geometry.

The 'classical' asymmetric chop uses an ABBA nod pattern, for most cases a modified ABA nod pattern, which is the default in this mode, is recommended, For the fastest mapping an AABAA nod pattern is available. In both of these modified nod patterns, the B (off) nod is longer than the individual A (on) nods. For the ABA pattern, the B is 1.5

times the length of the A and for the AABAA pattern the B is 2 times the length of the A. These modified nod patterns are beneficial on very bright objects, where the estimated on-source exposure time per map position is 15 s or less so that the total observing time is dominated by telescope movements. The actual patterns are thus ABA′ and AA′BA″A‴, i.e. the A positions are all different. In this mode, the total overhead is 3.3 N ton + 300s assuming an on-source exposure time per map position of 15s for the ABA pattern and 3.0 N ton + 300s, assuming an on-source exposure per map position of 10s for the AABAA pattern. The overhead increases with shorter integration times, thus USPOT may return different overheads from those given here if different observing times are used. These modified nod patterns should also be used for any source with asymmetric chop as long as the line is narrow enough to fit within the instrument's instantaneous spectral coverage.

If the line is very wide the ‘classical’ mode has to be used. Here the total overhead in this mode is about 4.1 N ton + 300s, since the source is observed during 25% of the observation plus additional time for telescope moves and 300s for the setup. This overhead estimate assumes that the on-source exposure time per map position ton is at least 15s.

Return to Table of Contents

3.2.1.3 Total Power

Sometimes the target’s environment does not allow even a single chop position to be used, in these cases it is still possible to make observations of bright targets using the unchopped Total Power mode. This uses the same ABA pattern used for the asymmetric chop mode above but without any chop being made. This can lead to potentially poorer background subtraction as the only off-source position is the B nod, so there is some additional risk. In stable atmospheric conditions it can give results as good as the symmetric chop mode. In this mode, the total overhead is 1.9 N ton + 300s assuming an on-source exposure time per map position of 10s.

Return to Table of Contents

3.2.1.4 On-the-fly mapping

The On The Fly Mapping (OTF) Mode can be used to map large areas of bright emission efficiently. This is a new mode that is still undergoing commissioning and development so is offered as shared-risk observing only. Overhead and sensitivity calculations may change so observers should be conservative when estimating the observing time needed for this mode.

In OTF mode, the telescope is driven across the source, taking data ‘on the fly’. No chopping is done, so the same caveats that apply for the total power mode (above) apply to OTF. An ‘off’ nod position is taken at the end of each scan through the source, with a time of √N tsample, where N is the number of independent samples in the scan and tsample is the integration time for each of these samples. This off is used for all of the samples in the scan.

Each scan takes 30s and the length is determined by the scan speed. The map is built up by scans spaced by the width of the array being used (30” for blue, 60” for red) and (if desired) by crossing scans at right angles. As this mode is still under development, potential users should contact the helpdesk (sofia_help@sofia.usra.edu) to discuss their planned observing strategy prior to submitting a proposal.

In contrast to the other observing modes, this mode targets spectral features much wider than the bandwidth (see Section 3.1.2.2) like solid state features. The problem is a good atmospheric calibration over the whole observed wavelength range. The spectrum has to pieced together from many different exposures. The best way to take such data and how to reduce it is still being investigated. If this observing mode is considered, the Help-Desk must be contacted well in advance to allow for time to calculate overheads.

Return to Table of Contents

3.2.2 Integration Time Estimates

The SOFIA Instrument Time Estimator (SITE) should be used to estimate the on-source exposure times used in proposals and observing preparation. The time estimator requires the following input:

Instrument Properties

Wavelength
(in microns, between 51 and 203 µm): default 157.741 µm (rest wavelength of the [CII] line)
Specify the rest wavelength of the requested transition.

Bandwidth
(in km/s or microns): default 0 km/s
Enter the desired width of the spectrum. The width should allow for sufficient baseline on both sides of the expected line/spectral feature to allow a good estimate of the underlying continuum telluric and astronomical. This value enters the time estimate as the factor *I*. If the desired spectrum is wider than the instantaneous bandwidth, *I* is the ratio of the requested width of the spectrum and the bandwidth (Figure 3-3). Otherwise *I* is equal to 1.

Observer Velocity
(VLSR in km/s): default 0 km/s
In many cases, the default value of zero can be used. However, if the observing wavelength is near a strong narrow telluric feature, the Earth's velocity relative to the LSR becomes important, e.g. for galactic sources and the [OI] line at 145.525 µm. Then either enter the velocity directly or have it computed by entering time, date, source coordinates, and SOFIA's location (boxes for these are shown if Compute Velocity is checked). The Doppler-shift due to the source's and the observatory's velocity is important to estimate the atmospheric extinction, discussed further below.

Calculation Method

Signal to Noise Ratio or Total Integration Time (s)
default S/N ratio resulting from a Total Integration Time of 900 s
SITE can either calculate the resulting signal to noise ratio given an integration time or the integration time to reach a signal to noise ratio. Select one of these parameters to be calculated and specify the value of the other parameter. For continuum observations, SNR is based on averaging over the *entire* spectrum.

Astronomical Source Definition

Source Flux
default 2.087e-17 W m^{-2} line flux (MDLF per pixel for [CII])
Specify the expected source flux *per FIFI-LS pixel* either as integrated line flux in W/m^2 or as continuum flux density in Jansky and select 'line' or 'continuum' as appropriate. Make it obvious in the technical feasibility section of the proposal that the referenced flux estimates have been converted to FIFI-LS pixels sizes.

Source Velocity
(in km/s): default 0 km/s
Enter the radial velocity of the source relative to the local standard of rest (LSR).

Observing Condition Constraints

Elevation Angle
(20, 40 or 60 deg): default 40
For northern sources an elevation of 40° is okay, but sources south of a declination of -15° will most likely be observed at a respectively lower elevations unless an observation from the southern hemisphere is required.

Altitude
(in feet; 35 – 45,000 ft): default 41,000 ft
This value is used in ATRAN to derive the atmospheric absorption. For more details about ATRAN see Section 1.3.

On a typical SOFIA flight, observations start at 38,000 ft or 39,000 ft and 43,000 ft are reached 3.5 h before the observations end. The default value of 41,000 ft represents an average altitude. If you want to be conservative, using a value of 38,000 ft should ensures that time estimate does not underestimate the water vapor overburden. If an observation is rather sensitive to the water vapor, a higher altitude can be entered and justified in the proposal. In Phase II, select **Low** or **Very Low** for **Requested WV Overburden** in the **Observing Condition** panel in USPOT, if the altitude used in the time estimation is 41,000 ft or 43,000 ft, respectively. Note, that this limits the schedulability of the observation to the last 5.5 h or 3.5 h of observations.

Zenith Water Vapor Overburden
(in microns)
This is automatically set to a typical value for the altitude selected, e.g. selecting an altitude of 39,000 ft will set the water vapor to 9.6 microns.

The time estimator calculates the on-source integration time per map position for a source flux, *F* and a desired SNR using Eq.3-1 (see also Figure 3-4).

The factor α is the transmission of the atmosphere for the observing wavelength derived by ATRAN. The on-line time estimator includes a plot of the transmission of the atmosphere at full spectral resolution and smoothed to the spectral resolution of FIFI-LS at the observing wavelength over the bandwidth. Two integration times are calculated using the transmissions from each curve. The value derived from the unsmoothed curve applies to an observation of a very narrow line, while the value from the smoothed curve applies to a continuum source or a line broader than the instrument's spectral resolution. If the atmospheric transmission is smooth near the observing wavelength, the two values will not differ much and the more conservative or appropriate observing time should be chosen. Furthermore, the observing time will not depend strongly on the source velocity. The velocity correction can be rounded to 100km/s and the earth's velocity can be ignored.

However, if there is a telluric feature near the observing wavelength, one has to carefully check the feasibility of the observation (a special warning is displayed if the ratio of the derived observing times exceed 1.5). This usually happens when the observing wavelength is near a strong and narrow atmospheric feature. A typical example is the [OI] line at 145.525 µm, which is near a narrow and strong telluric feature at 145.513 µm or at -25 km/s relative to the [OI] line. In such a case, it is crucial to enter a good estimate of the source velocity accurate to ~1 km/s. The source velocity needs to be the combination of the source velocity relative to the LSR or another reference frame *and* earth's velocity relative to that reference frame, which depends on the observing date and target location. Therefore the time estimator includes a calculator for the earth's velocity relative to the LSR. It may be necessary to add a time constraint for the observation to avoid an adverse earth's velocity relative to the source.

If the observing line is near a strong and narrow telluric feature, not only the observing time estimate needs greater care, but the correction for the atmospheric absorption of an observed line flux will have a large uncertainty. To derive the correction factor, the atmospheric transmission curve would need to be integrated while weighted with the intrinsic line profile of the observed emission line with the correct relative Doppler-shift. In most cases FIFI-LS will not be able to resolve the line profile and cannot resolve the atmospheric feature. Any attempt to correct the measured line flux would depend strongly on assumptions of the source's line shape and position and assumptions of the water vapor content and shape of the telluric feature. In short, expect a large uncertainty of a line flux measured near a strong and narrow telluric feature.

The exposure time estimator returns the *on-source* exposure time *per map position* t_{on}. If mapping is planned, this values has to be multiplied with *N*, the number of map positions, to derive the total on-source observing time. More on mapping can be found in Section 3.2.3. *The total on-source observing time N x t_{on} has to be entered into USPOT* during Phase I of the proposal process. The overhead depends on the observing mode (Section 3.2.3) and is automatically added by USPOT.

Be conservative with the time estimates! Unforeseen issues like thunderstorms or computer crashes may cut the observing time short. Better to aim for 5σ and get a 3σ result, than aim for a 3σ and then wonder, what to do with a 1.8σ signal.

Return to Table of Contents

3.2.3 Spectral Dithering

Spectral dithering is always employed for self flat-fielding and increased redundancy. Spectral dithering implemented via a grating scan. The grating is moved in small steps, so that the spectrum moves over different pixels in the spectral dimension of the detector array.

The default pattern to cover the instantaneous bandwidth (BW, Section 3.1.2.2) is to move the grating 12 steps, each corresponding to half a spectral pixel width. This pattern results in a spectrum about 30% wider than the BW. The central 70% of the BW are observed during the whole observing time reaching the full SNR, while the remaining 15% on each side of the BW should reach on average 86% of the SNR. The SNR reached on the extra 30% should still be 46% on average based on the observing time for each part of the spectrum. For wider spectral coverage, the step size and number of steps of the grating scan will be adjusted by the instrument operators to achieve the desired spectral coverage. The steps will be evenly distributed over the nod-cycles.

Return to Table of Contents

3.2.4 Mapping

3.2.4.1 Raster Mapping

Raster Mapping is supported by the Symmetric Chop, Asymmetric Chop and Total Power observing modes; OTF Mapping is a dedicated mapping mode that is covered separately below.

Raster mapping can be done on a rectangular grid with a user-defined spacing and extent. It is also possible to supply a list of mapping positions to achieve a map with a custom shape optimized to the source geometry. These details need to be specified only in Phase II of the proposal process (see the FIFI-LS USPOT chapter). In Phase I, the effective map area needs to be entered in USPOT and the proposal should explain the suggested mapping strategy. The on-source integration time per cycle entered in USPOT is the on-source integration time per cycle per raster point. This gives a total on-source exposure time for the AOR of this number multiplied by the number of raster map points Ncycle Npoint ton.

For chopped observations: If the source geometry allows the chopped beams to be positioned symmetrically on both sides of the source, then one should use the more efficient Symmetric Chop mode for mapping. If that is not possible the Asymmetric Chop mode has to be used; for short integrations, one of the modified nod patterns (ABA or AABAA) is preferred. Figure 3-6 illustrates mapping with an asymmetric chop. The chopped map (positions A1chop to A3chop in the example) covers an area with the same form as the on-source map, offset by the chop throw. If this is undesirable (e.g. if part of the chopped map would overlap a region of possible emission), the map needs to be broken up into sub-maps with varying chop parameters (which can be specified in Phase II). Breaking the map up into individual sub-maps requires a separate AOR for each map. If there are more than five AORs in a map, all with short integration times, it may be desirable to toggle the flag for combining multiple short AORs in USPOT, which enables an alternative calculation of overheads with a lower fixed overhead per AOR.

When estimating the on-source integration time (Section 3.1.2.3), take into account the differing overlap of the red and blue FOV at the desired raster map spacing. The SNR entered into the calculation of ton is the SNR for a single raster map point. The final SNR for a point in the map should reach √n * SNR with n being the number of raster points from which a point is covered by the respective FOV. For example in Figure 3-6, the area of the spaxel in the middle (dark orange) is covered by 3 FOVs while 16 spaxels (light orange) are covered by 2 FOVs and the outer parts of the map (yellow) are covered by 1 FOV. The noise level in the area covered by the central spaxel should thus be √3 lower than in the outer parts and the SNR (for the same signal) thus √3 times higher. (Note that this is an example map, not a suggested mapping strategy.)

Figure 3-6.

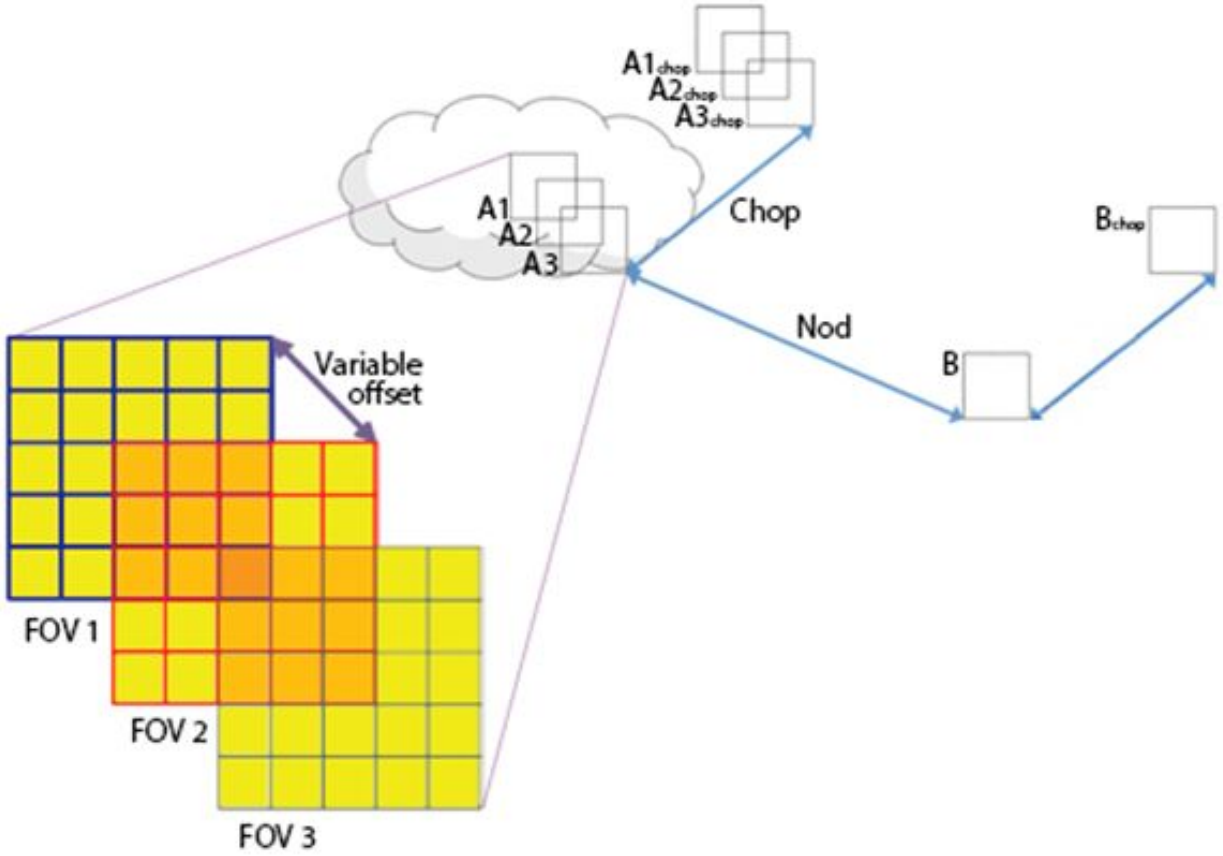

17 Figure 3-6. The geometry of chopping and nodding while mapping using the asymmetric chop mode.

Return to Table of Contents

3.2.4.2 On The Fly Mapping

On The Fly (OTF) Mapping involves taking data while the telescope is in motion, in contrast to the hop-and-dwell approach of raster mapping where the telescope only moves between integrations. It allows fast, well-sampled maps to be made of bright, extended sources.

During an OTF scan the FIFI-LS field of view is rotated at 11.3 degrees to the direction at which the telescope is being driven, giving an equal spacing of the spaxels in the cross-scan direction. Combined with integrations of 1/8th of a second as the telescope moves, this builds up a dense array of points at which data have been taken giving a good sampling of the spatial PSF.

As each point is crossed by 5 spaxels, the effective integration time per spaxel (i.e. what should be put into SITE to estimate the SNR) is given by 5 * spaxelsize/scanspeed in each scan direction. For a standard 30s scan, the length of the scan (and thus the size of the map) is also given by the scanspeed. As the data is taken while the telescope is in motion, higher scan speeds could result in smearing of the beam in the direction of the scan.

An example OTF map is shown in Figure 3-7. This shows six scans (three in each direction) for the blue array with a speed of 4”/s (giving a scan length of 2’). The on-source time for this map is estimated as 6 * 0.5 = 3 minutes and the variable overhead as 1.5 * 6 * 0.5 = 4.5 minutes. Adding in the fixed overhead of 5 minutes gives a total time of 12.5 minutes. The integration time per spaxel (reached within the red box, covering 1.5’ by 1.5’) is 5 * 6”/4”/s = 7.5s in

each scan direction, for a total of 15s. A map of this size would normally take 9 pointings. With an integration time of 15s/pointing this would take 16.4 minutes in symmetric chop mode (2.25 minutes on-source, 9.15 minutes variable overhead, 5 minutes fixed overhead), which would not give any dithering.

Figure 3-7.

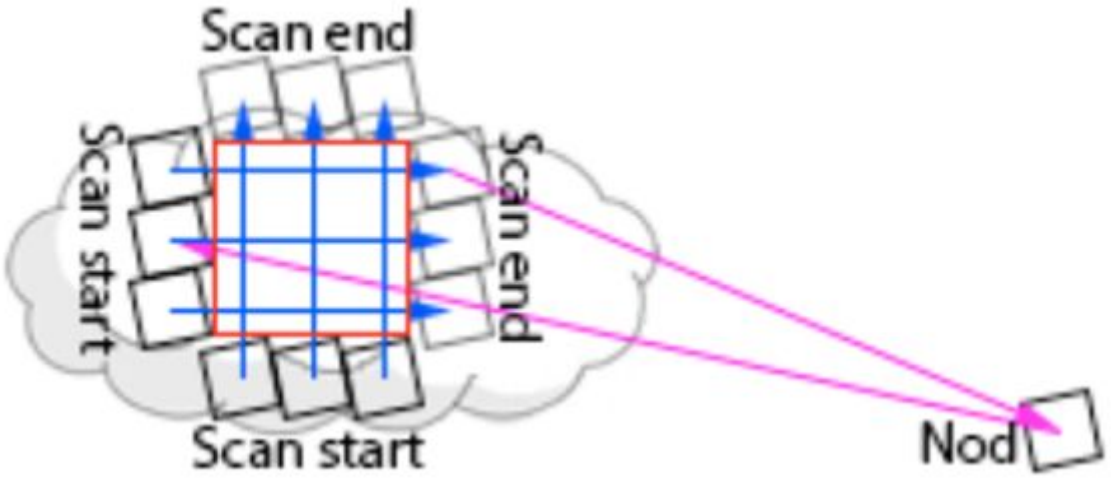

18 Figure 3-7. Example of mapping with the OTF mode.

Return to Table of Contents

4. FORCAST

To export the handbook as a PDF, click on the three dots in the upper right, then choose "Export with Scroll PDF Exporter". In the Template drop-down menu, choose "Handbook Template", and then click "Export".

4.1 Specifications

4.1.1 Instrument Overview

The **F**aint **O**bject infra**R**ed **CA**mera for the **S**OFIA **T**elescope (FORCAST) is a dual-channel mid-infrared camera and spectrograph sensitive from 5–40 µm. Each channel consists of a 256x256 pixel array that yields a 3.4x3.2 arcmin instantaneous field-of-view with 0.768 arcsec pixels, after distortion correction. The Short Wavelength Channel (SWC) uses a Si:As blocked-impurity band (BIB) array optimized for $\lambda < 25$ µm, while the Long Wavelength Channel's (LWC) Si:Sb BIB array is optimized for $\lambda > 25$ µm. Observations can be made through either of the two channels individually or, by use of a dichroic mirror, with both channels simultaneously across most of the range. Spectroscopy is also possible using a suite of six grisms, which provide coverage from 5–40 µm with a low spectral resolution of $R = \lambda/\Delta\lambda \sim 200$. The instrument has space for cross dispersing grisms allowing for high resolution cross-dispersed (XD) spectroscopy at R ~ 800–1200 in the 5–14 µm range. The availability of the XD configuration during a given cycle is published in the Call for Proposals.

Return to Table of Contents

4.1.1.1 Design

The FORCAST instrument is composed of two cryogenically cooled cameras of functionally identical design. A schematic of the instrument layout is provided in Figure 4-1 below. Light from the SOFIA telescope enters the dewar through a 7.6 cm (3.0 in) caesium iodide (CsI) window and cold stop and is focused at the field stop, where a six position aperture wheel is located. The wheel holds the imaging aperture, the slits used for spectroscopy, and a collection of field masks for instrument characterization. The light then passes to the collimator mirror (an off-axis hyperboloid) before striking the first fold mirror, which redirects the light into the LHe-cooled portion of the cryostat.

The incoming beam then reaches a four-position slide, which includes an open position, a mirror, and two dichroics, one for normal use and the other as a spare. The open position passes the beam to a second fold mirror, which sends the beam to the LWC, while the mirror redirects the light to the SWC. The magnesium oxide (MgO) dichroic reflects light below 26 µm to the SWC and passes light from 26–40 µm to the LWC. The light then passes

through a Lyot stop at which are located two filter wheels of six positions each, allowing combinations of up to 10 separate filters and grisms per channel. Well characterized, off-the-shelf filters can be used, since the filter wheel apertures have a standard 25 mm diameter (see Section 4.1.2.2).

Finally, the incoming beam enters the camera block and passes through the camera optics. These two-element catoptric systems are composed of an off-axis hyperboloid mirror and an off-axis ellipsoid mirror that focuses the light on the focal plane array. Also included is an insertable pupil viewer that images the Lyot stop on the arrays to facilitate alignment of the collimator mirror with the telescope optical axis and to allow characterization of the emissivity of both the sky and telescope.

Figure 4-1.

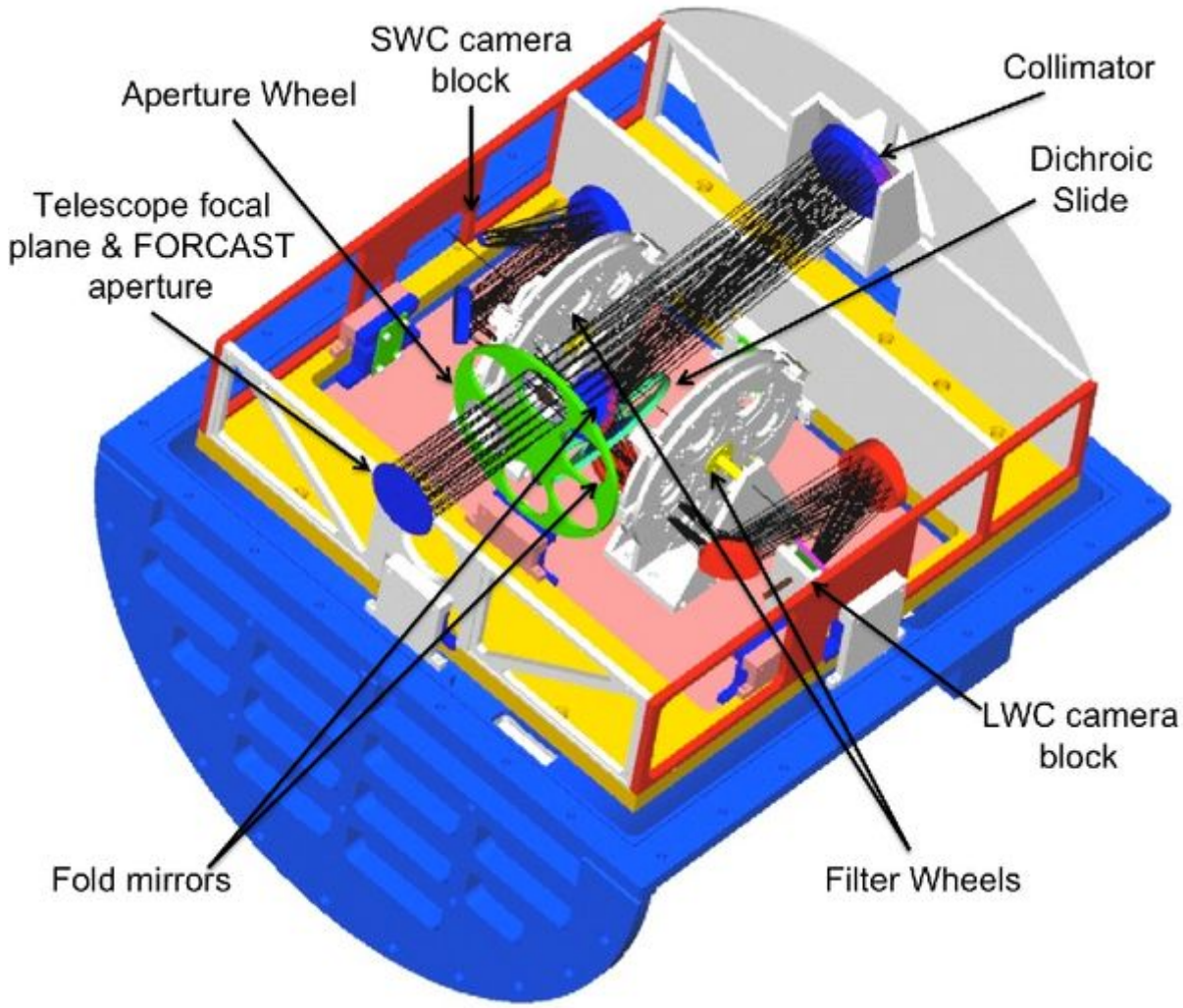

19 Figure 4-1. A schematic of the FORCAST layout.
Return to Table of Contents

4.1.2 Performance

4.1.2.1 Camera Performance

The SWC and LWC arrays were selected to optimize performance across the 5–40 μm bandpass. Both arrays have a quantum efficiency (QE) greater than 25% over most of their spectral range. The cameras can be operated with

variable frame rates and in either high or low capacitance modes (which are characterized by well depths of 1.8x107 and 1.9x106 e- respectively), depending upon the sky background and source brightness.

The best measured image quality (IQ) obtained by FORCAST on SOFIA is in the 7–11 µm range with a FWHM PSF (point spread function) of ~2.7 arcsec. This measured image quality in-flight is limited by telescope jitter arising from vibrations of the telescope itself (e.g., due to wind loading in the cavity), turbulence, and tracking accuracy. Presented in Figure 4-2 is a sample of FWHM IQ measurements made during a single observatory characterization flight during the winter of 2010 in comparison to the theoretical diffraction limit calculated for a 2.5 m primary with a 14% central obstruction combined with the FWHM telescope jitter, here assumed to be 2.08 arcsec (1.25 arcsec rms).

Figure 4-2.

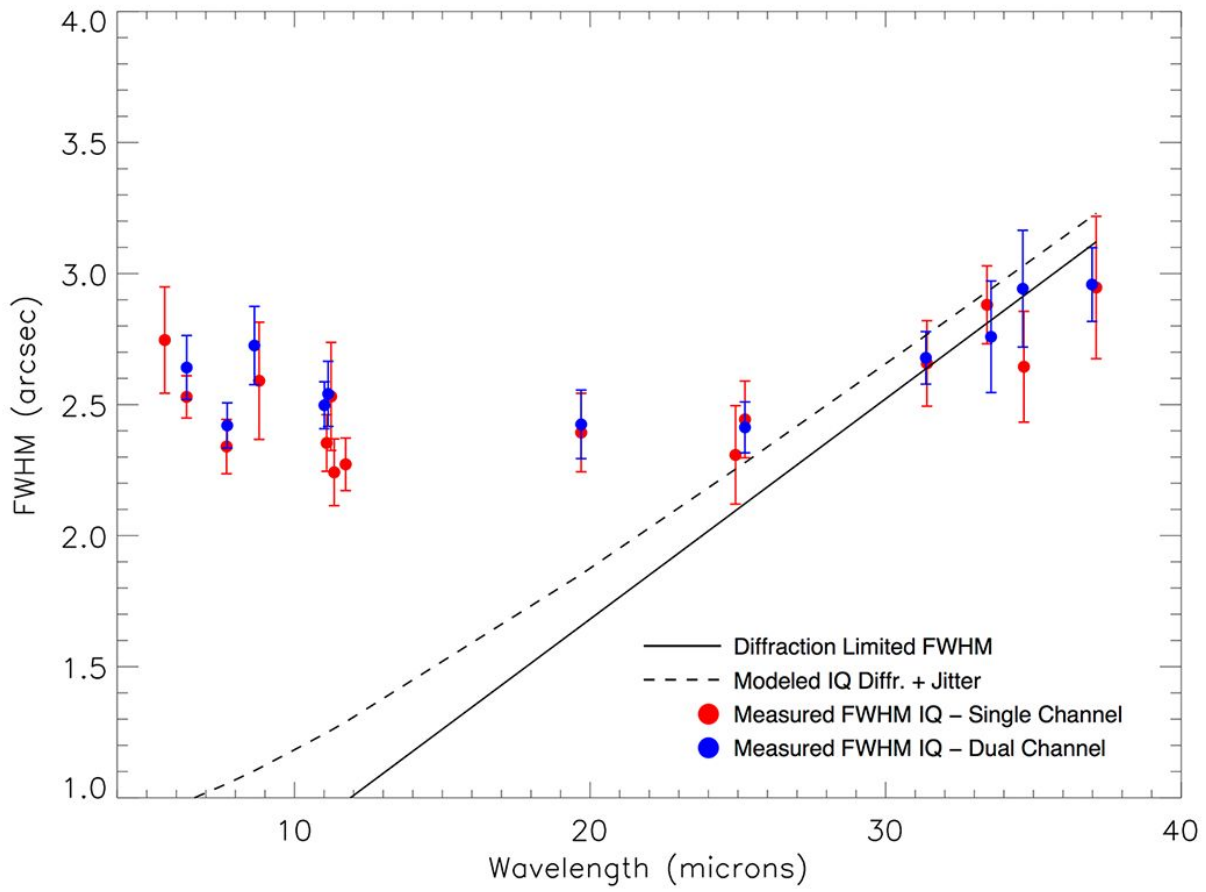

Representative FWHM PSF for the FORCAST camera in select filters as measured during Cycle 7. Also shown are the diffraction limited FWHM (*solid line*; calculated for a 2.5-m primary with a 14% central obstruction) and the modeled IQ *(dashed line)*, which includes shear layer seeing and 0.5 arcsec rms telescope jitter (corresponding to 0.83" FWHM).

Return to Table of Contents

4.1.2.2 Filter Suite

Imaging with FORCAST can be performed in either a single channel or in both the SWC and LWC channels simultaneously (dual channel configuration). In a single channel configuration, any one of the available filters may

be used. In the dual channel configuration, a dichroic is used to split the incoming beam, directing it to both the SWC and LWC.

The dichroic reduces the overall throughput. Table 4-1 shows the throughput with the dichroic in (dual channel configuration) relative to that for the single channel configuration. The degradation of the system throughput by the dichroic can have a significant effect on the instrument sensitivities as discussed in more detail in Section 4.1.2.3. In addition, since there are more short wavelength filters available than slots in the SWC filter wheels, some short wave filters will be housed in the LWC. The final filter wheel configuration for each observing cycle will be driven by proposal pressure. Depending on the final filter configuration, it is possible that not all LWC filters will be able to be used in the dual channel configuration due to the cutoff in the dichroic transmission at short wavelengths. The N' broadband filter (FOR_F112) is only offered in single-channel mode.

Table 4-1: Dichroic Throughput

Bandpass	Throughput
5-10 µm	60%
11-25µm	85%
25-40 µm	40%

The filters in the SWC are standard Optical Coating Laboratory, Inc. (OCLI) thin-film interference filters. These filters are stacked with blocking filters to prevent light leaks. The only exception is the 25.4 µm (FOR_F253) University of Reading filter, which is a custom double half-wave (three mesh) scattering filter stacked with a diamond scattering blocking filter to provide blue-light rejection. The 33.6 (FOR_F336), 34.7 (FOR_F347), and 37.1 µm (FOR_F371) filters in the LWC are LakeShore custom double half-wave (three mesh) scattering filters. The 31.5 µm filter is a Fabry-Perot Interferometer filter.

The central wavelengths, bandwidths, and the typical FWHM IQ in each of the filters are given in Table 4-2 below. The first column under the Imaging FWHM column (single channel) heading presents the best measured FWHM IQ in single channel configuration. These values are representative of the IQ observed since Cycle 3. The second column (dual channel) contains the average measured FWHM IQ in dual channel configuration. Not all of the filters have measured IQ values, but we expect that they will be comparable to those with measured values that are of similar λ_{eff}. Figure 4-3 shows the filter transmission profiles (normalized to their peak transmission) over-plotted on an ATRAN model of the atmospheric transmission. The filter transmission curves (text tables) are available as a zip file or individually from Table 4-2.

Due to the limited number of slots available in the filter wheels, not all of the filters listed in Table 4-2 are available at any one time. For Cycle 9, there will be a nominal filter set (indicated by ***bold italic type*** in Table 4-2). Other filters can be requesed for use, but a convincing scientific argument must be made to justify swapping out the existing filters. A filter swap during the cycle may be permitted dependent upon proposal pressure; more details are available in the Call for Proposals.

Table 4-2: Filter Characteristics

Channel	Filter	λ_{eff} (µm)	Δλ (µm)	Imaging FWHM (arcsec)		Profiles
				Single Channel	Dual Channel	

SWC	FOR_F054	5.4	0.16	_[b]	–	txt file
	FOR_F056	***5.6***	***0.08***	–	–	txt file
	FOR_F064	***6.4[a]***	***0.14***	***2.9***	***2.9***	txt file
	FOR_F066	6.6	0.24	2.9	3.1	txt file
	FOR_F077	***7.7***	***0.47***	**3.0**	**3.0**	txt file
	FOR_F088	***8.8***	***0.41***	•	-	-
	FOR_F111	***11.1***	***0.95***	***2.8***	***2.9***	txt file
	FOR_F112	***11.2***	***2.7***	-	-	-
	FOR_F197	***19.7***	***5.5***	***2.4***	***2.5***	txt file
	FOR_F253	***25.3***	***1.86***	***2.3***	***2.1***	txt file
LWC	FOR_F113	11.3	0.24	2.6	–	txt file
	FOR_F118	11.8	0.74	2.6	–	-
	FOR_F242	24.2	2.9	2.6	-	txt file
	FOR_F315	***31.5***	***5.7***	***2.8***	***2.8***	txt file
	FOR_F336	***33.6***	***1.9***	***3.1***	***3.3***	txt file
	FOR_F348	***34.8***	***3.8***	***3.1***	***3.0***	txt file
	FOR_F371	***37.1***	***3.3***	***2.9***	***3.4***	txt file

[a] Entires in bold are expected to be part of the default filter set for Cycle 9.

[b]IQ values for some filters have not been measured at this time, but it is expected that they will be similar to those of similar λ_{eff} with measured values.

Figure 4-3.

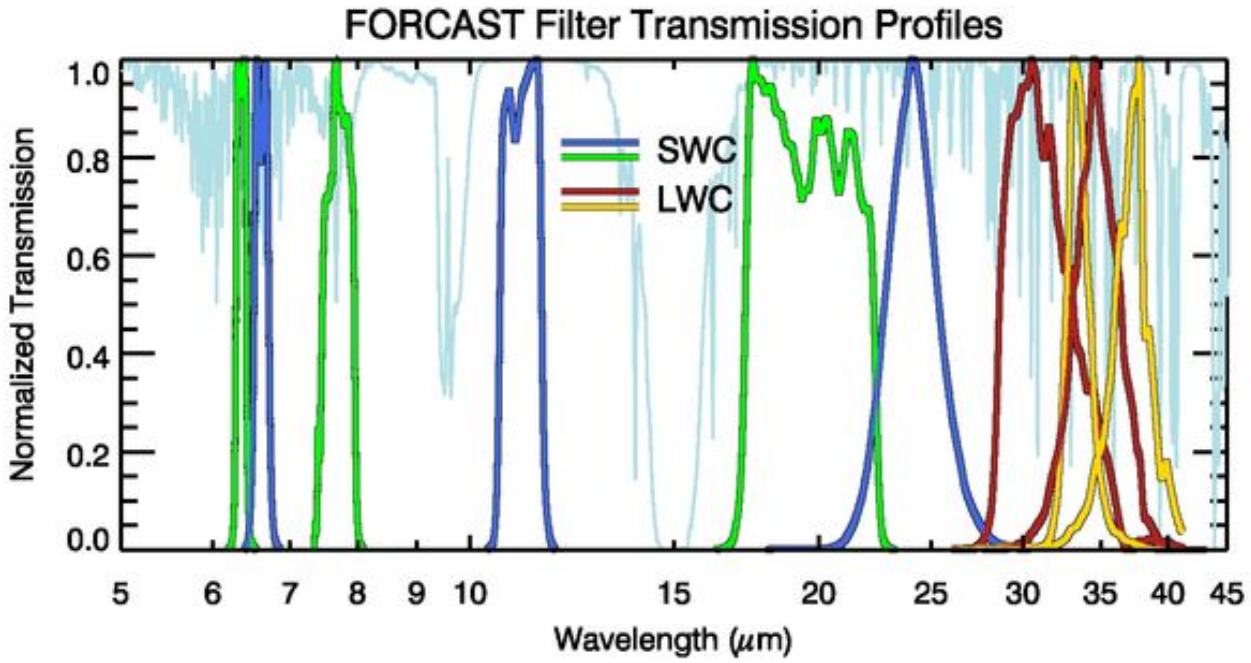

20 Figure 4-3. FORCAST filter transmission profiles along with an ATRAN model of the atmospheric transmission across the FORCAST band (assuming a zenith angle of 45 degrees and 7 µm of precipitable water vapor). For clarity, the filter profiles have been normalized to their peak transmission. SWC filters alternate between green and blue, while LWC filters alternate between red and yellow.

Return to Table of Contents

4.1.2.3 Imaging Sensitivities

The FORCAST imaging sensitivities for a continuum point source for each filter are presented in Table 4-3 and Figure 4-4. The Minimum Detectable Continuum Flux (MDCF; 80% enclosed energy) in mJy needed to obtain a S/N = 4 in 900 seconds of on-source integration time is plotted versus wavelength. The MDCF scales roughly as (S/N) / √(t) where t = net integration time. The horizontal bars indicate the effective bandpass at each wavelength. At the shorter wavelengths the bandpass is sometimes narrower than the symbol size.

Atmospheric transmission will affect sensitivity, depending on water vapor overburden. The sensitivity is also affected by telescope emissivity, estimated to be 15% for Figure 4-4.

Observations with FORCAST are performed using standard IR chop-nod techniques. Chop/nod amplitudes can be chosen such as that they are small enough to leave the source on the array in each position or large enough that the source is positioned off the chip for one of the chop positions. For background-limited observations, as is the case with FORCAST on SOFIA, chopping and nodding off-chip in nod-match-chop (NMC; see Section 4.2.1) will generally result in the same signal to noise (S/N) as chopping and nodding on-chip in nod-perp-chop (NPC; see Section 4.2.1). Calculations of S/N for various chop-nod scenarios are provided here.

Table 4-3: Filter Sensitivities

Filter	Channel	Single Chan. MDCF (mJy)	Dual Chan. MDCF (mJy)
FOR_F054[a]	SWC	41.5	575

Filter	Channel	Single Chan. MDCF (mJy)	Dual Chan. MDCF (mJy)
FOR_F056[b]	SWC	58.1	225
FOR_F064	SWC	39.5	54.7
FOR_F066	SWC	58.8	77.7
FOR_F077	SWC	49.5	59.8
FOR_F088	LWC	64.5	68.0
FOR_F111	SWC	79.4	74.5
FOR_F112	SWC	51.2	62.6
FOR_F113	LWC	173	-
FOR_F118	LWC	108	-
FOR_F197	SWC	59.7	60.1
FOR_F242	LWC	75.7	-
FOR_F253	SWC	115	128
FOR_F315	LWC	90.3	123
FOR_F336	LWC	181	266
FOR_F348	LWC	137	195
FOR_F371	LWC	189	290

[a] MDCF values shown are those measured from Cycle 4 data.

[b] No observations were available to test the theoretical MDCF values.

Figure 4-4.

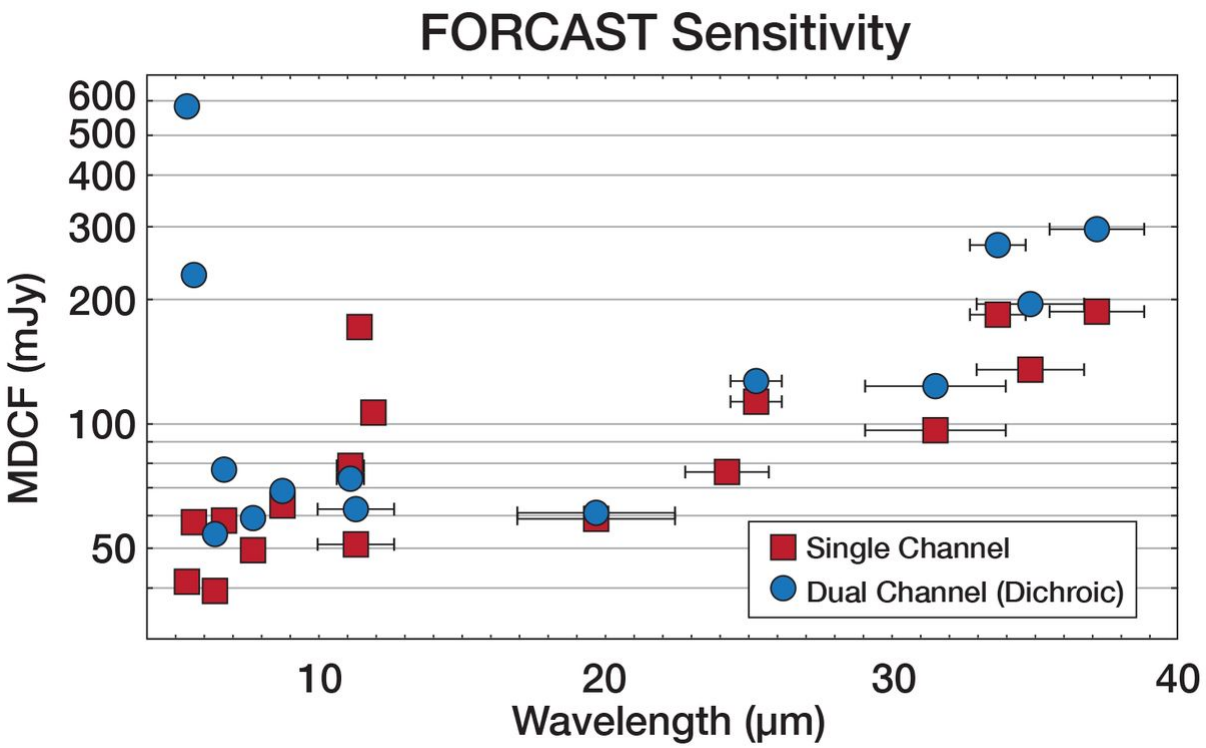

21 Figure 4-4. Cycle 9 continuum point source sensitivities for single and dual channel modes. Values are for S/N = 4 in 900 s under nominal conditions. Investigators are encouraged to use the for their calculations.
Return to Table of Contents

4.1.2.4 Grisms

The suite of 6 grisms available for FORCAST provide low to medium resolution coverage throughout most of the range from 5–40 μm (see Table 4-4). The grisms are situated in the four filter wheels: two in each SWC wheel and one in each LWC wheel. The arrangement is chosen to minimize the impact on the imaging capabilities of the instrument. The grisms are blazed, diffraction gratings used in transmission and stacked with blocking filters to prevent order contamination. A summary of the grism properties is provided in Table 4-4. *Note that during Cycle 9, the cross-dispersed XD configuration will not be available. The information on XD configuration below is for informational purposes, only.*

Grisms FOR_G063, FOR_G227, FOR_G329, and the FOR_XG063 dispersing grism provided by the University of Texas at Austin, are made of silicon to take advantage of its high index of refraction, which allows optimum spectral resolution. However, these grisms suffer from various absorption artifacts precluding their use in the 8–17 μm window. Coverage in this region is provided by the FOR_G111 grism (and its cross-dispersing counterpart), constructed of KRS-5 (thallium bromoiodide) by Carl-Zeiss (Jena, Germany). These latter two grisms have a lower spectral resolution due to the lower index of refraction of the KRS-5 material.

Three slits have been designed for FORCAST: two long slits (2.4 x 191 arcsec, 4.7 x 191 arcsec) and a short slit (2.4 x 11.2 arcsec). The narrow slits yield higher resolution data. All of the slits are located in the aperture wheel of the instrument. The cross-dispersed spectra are obtained by using the short slit and passing the beam first through the low-resolution grism (either FOR_G063 or FOR_G111), followed by a disperser.

Although grisms are available in both cameras, during Cycle 9 grism spectroscopy will be available only in single channel configuration.

It is important to note that due to the fixed position of the slits in the aperture wheels, the lack of a field de-rotator, and the fact that SOFIA behaves in many respects as an Alt-Az telescope, the orientation of the slit on the sky will be dependent on the flight plan and will not be able to be predetermined. Furthermore, the slit orientation rotates on the sky with each telescope Line-of-Sight (LOS) rewind (see Section 1.2.4). These limitations may be especially important to consider when proposing observations of extended objects.

Table 4-4: Grism Characteristics

Channel	Grism	Material	Groove Sep. (μm)	Prism Angle (°)	Order	Coverage (μm)	R (λ/Δλ)[a]
SWC	FOR_G063	Si	25	6.16	1	4.9 - 8.0	120[c]/180
	FOR_XG063[b]	Si	87	32.6	15 - 23	4.9 - 8.0	1170[d]
	FOR_G111	KRS-5	32	15.2	1	8.4 - 13.7	130[c]/260
LWC	FOR_G227	Si	87	6.16	1	17.6 - 27.7	110/120
	FOR_G329	Si	142	11.07	2	28.7 - 37.1	160/170[b]

[a] For the 4.7'' x 191'' and the 2.4'' x 191'' slits, respectively

[b] Not available during Cycle 9

[c] The resolution of the long, narrow-slit modes is dependent on (and varies slightly with) the in-flight IQ

[d] Only available with the 2.4'' x 11.2'' slit

Return to Table of Contents

4.1.2.5 Spectroscopic Sensitivity

Tables 4-5 and 4-6 provide samples of the MDCF and Minimum Detectable Line Flux (MDLF) calculated at three different wavelengths across each grism bandpass for each of FORCAST's spectroscopic configurations. The data are provided for point sources only. The MDCF and MDLF estimates are for the raw integration time of 900 seconds and do not include observing overheads, but do account for a a two-position chop (perpendicular to the slit).

Figure 4-5 presents the continuum point source sensitivities for the FORCAST grisms. The plots are the MDCF in Jy needed for a S/N of 4 in 900 seconds at a water vapor overburden of 7 μm, an altitude of 41K feet, and a zenith angle of 60°. The rapid variations with λ are due to discrete atmospheric absorption features (as computed by ATRAN).

To determine the required integration time necessary to achieve a desired S/N ratio for a given source flux, the SOFIA Instrument Time Estimator (SITE) should be used. SITE also allows for calculation of the limiting flux for a given integration time and required S/N. Since FORCAST observations are background limited, the values given in Tables 4-5 and 4-6 and Figure 4-5 can be used to make an estimate of the required integration time using Equation 4-1:

(Eq. 4-1)

$$\frac{[\mathrm{S/N}]_{\mathrm{req}}}{4} = \frac{F_{\mathrm{src}} \cdot \sqrt{t_{\mathrm{exp}}}}{\mathrm{MDCF} \cdot \sqrt{900}}$$

where $[S/N]_{req}$ is the desired signal-to-noise ratio, F_{src} is the continuum flux of the target, t_{exp} is the exposure time on source (without taking into consideration observational overheads), and the MDCF is taken from the tables for the point-source sensitivities or estimated from the figures. For emission lines, simply use the line flux for F_{src} and use the MDLF value instead of the MDCF. *However, these tables may not contain the most recent or best determined sensitivity values and therefore the on-line calculator results should be used in the actual proposal.*

Table 4-5: Long Slit Point Source Sensitivities

Grism	λ (μm)	R = (λ/Δλ)	MDCF (mJy)	MDLF (W m^{-2})	R= (λ/Δλ)	MDCF (mJy)	MDLF (W m^{-2})
		4.7'' Slit			**2.4'' Slit**		
FOR_G063	5.1	120	79	2.3E-16	180	98	2.9E-16
FOR_G063	6.4	120	219	5.2E-16	180	268	6.3E-16
FOR_G063	7.7	120	496	5.2E-16	180	724	6.3E-16
FOR_G111	8.6	130	419	4.9E-16	300	532	6.2E-16
FOR_G111	11.0	130	449	4.1E-16	300	575	5.2E-16
FOR_G111	13.2	130	593	4.5E-16	300	764	5.8E-16
FOR_G227	17.8	110	715	8.6E-16	140	936	1.1E-15
FOR_G227	22.8	110	834	7.9E-16	140	989	9.3E-16
FOR_G227	27.2	110	1979	1.6E-15	140	2586	2.0E-15
FOR_G329	28.9	160	1365	6.5E-16	220[a]	1899	9.0E-16
FOR_G329	34.1	160	1408	5.6E-16	220[a]	1994	8.0E-16
FOR_G329	37.0	160	1763	5.6E-16	220[a]	2439	8.0E-16

[a] The 2.4 arcsec long slit mode for G329 will not be available during Cycle 9.

Table 4-6: Cross-Dispersed Point Source Sensitivities[a]

Grism	λ (μm)	R = (λ/Δλ)	MDCF (mJy)	MDLF (W m^{-2})
		2.4'' x 11.2'' Slit		
FOR_XG063	5.1	1200	238	1.2E-16
FOR_XG063	6.4	1200	703	2.8E-16
FOR_XG063	7.7	1200	918	3.0E-16

[a] XD configurations are not available during Cycle 9.

Figure 4-5.

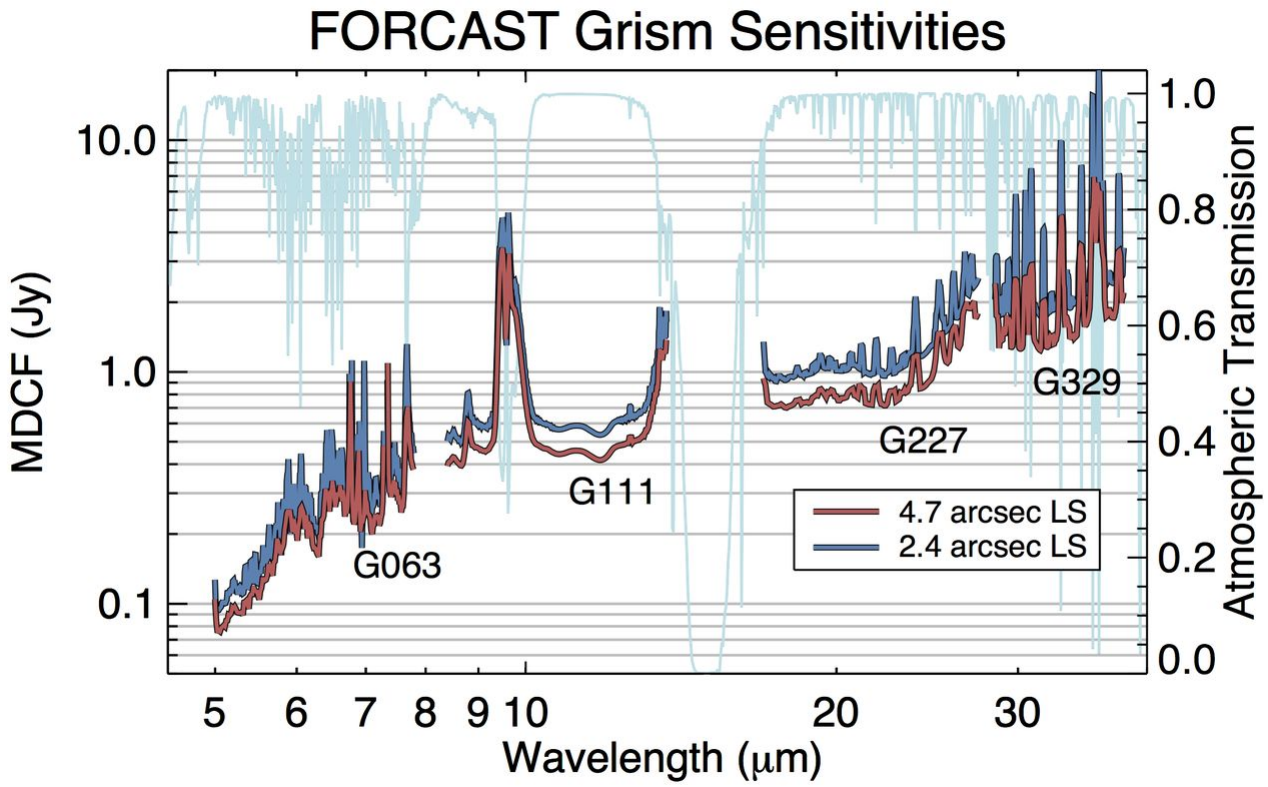

22 Figure 4-5. Cycle 7 grism continuum point source sensitivities for both wide and narrow long slits overlaid on an atmospheric transmission model (light blue). Values are for S/N = 4 in 900 s under nominal conditions.
Return to Table of Contents

4.2 Planning Observations

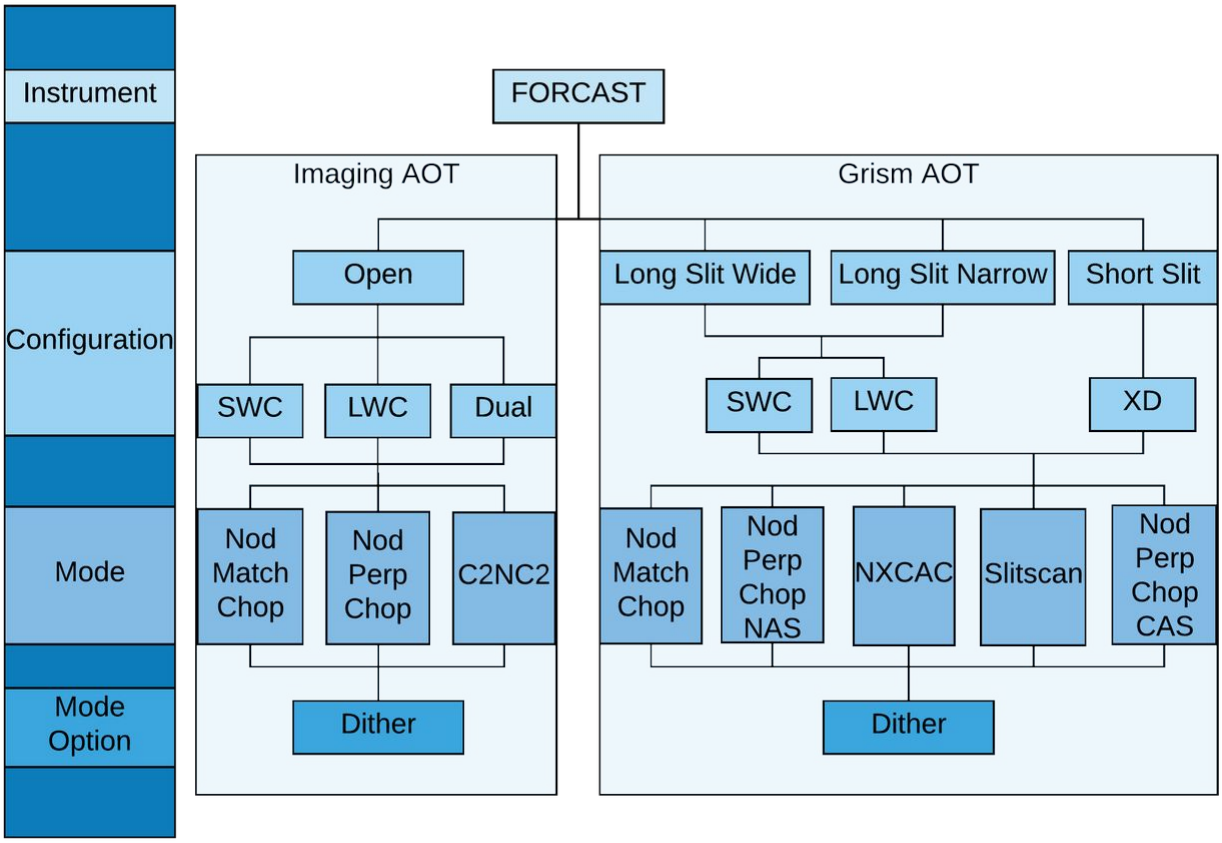

As is the case with ground based observations at mid-IR wavelengths, individual FORCAST exposures will be dominated by the sky and telescope background. Therefore chopping and nodding are essential for each observation. Selection of the observing mode and its parameters, including the distance and direction of chop and nod throws, depend on the details of the field of view around the target. The source(s) of interest may be surrounded by other IR-bright sources or may lie in a region of extended emission, which needs to be avoided to ensure proper background subtraction. Presented in this section is a discussion of how to best plan FORCAST observations in order to optimize the success of observations.

Return to Table of Contents

4.2.1 Imaging Observations

Proposers are strongly encouraged to familiarize themselves with the basics of techniques for performing background limited observations covered in Section 1.3. In brief, the imaging observation modes for FORCAST include the following:

NMC Mode
Nod Match Chop mode consists of a chop symmetric about the optical axis of the telescope with one of the two chop positions centered on the target. The nod throw is oriented 180° from the chop, i.e. anti-parallel, such that when the telescope nods, the source is located in the opposite chop position. The chop/nod subtraction results in two negative beams on either side of the positive beam, which is the sum of the source intensity in both nod positions and therefore has twice the intensity of either negative beam. This mode uses

the standard ABBA nod cadence. An example of an observation taken in this mode is presented in the left panel of Figure 4-7.

NPC Mode
Similar to NMC, Nod Perpendicular to Chop mode also uses a chop that is symmetric about the optical axis, but in this case the nod is perpendicular to the chop. The final images produced using NPC show four sources arranged in a parallelogram with alternating positive and negative beams. Unlike NMC, each beam in NPC has the same relative intensity. This mode also uses the standard ABBA nod cadence. The right side of Figure 4-7 shows data obtained using NPC. *This mode will not be supported in Cycle 9.*

C2NC2 Mode
In Chop-Offset Nod mode, the chop throw is asymmetric, such that one chop position is centered on the optical axis (and the target) while the second (sky) position is off-axis. Rather than nodding, the telescope then slews to an offset position free of sources or significant background and the same chop pattern is repeated. Observations in C2NC2 mode follow a nod cadence of ABA and, by default, are dithered to remove correlated noise. This mode is particularly useful for large extended objects, smaller objects that are situated within crowded fields, or regions of diffuse emission with only limited sky positions suitable for background removal.

Since only a single chop position out of a full chop/nod cycle is on source, NMC and NPC have a much greater efficiency than C2NC2. A sample mosaic demonstrating how a C2NC2 observation might be designed for a large, extended object is provided in Figure 4-8, and it is immediately apparent from the figure that C2NC2 has an efficiency of only ~20%. However, while mosaicking cna be performed for any of the available obseving modes, proposers should keep in mind that the effects of coma may compromise the image severely for fields requiring large chop amplitudes when chopping symmetrically (NMC or NPC modes). If the source has an angular extent large enough that multiple pointings are required, the central position of each FORCAST field must be specified, with due consideration of the desired overlap of the individual frames. For more on mosaicking, see Section 5.3 in the USPOT Manual.

Figure 4-7.

23 Figure 4-7. Each source position (solid line) with its associated asymmetric chop position (dashed line) have matching colors. After a full chop cycle at each position, the telescope is slewed to a location off of the source, shown in black and labeled with the coordinates (600, 600). The chop throw and angle at that position is the same as it is for the source position to which it is referenced (not shown in the figure).
Figure 4-8.

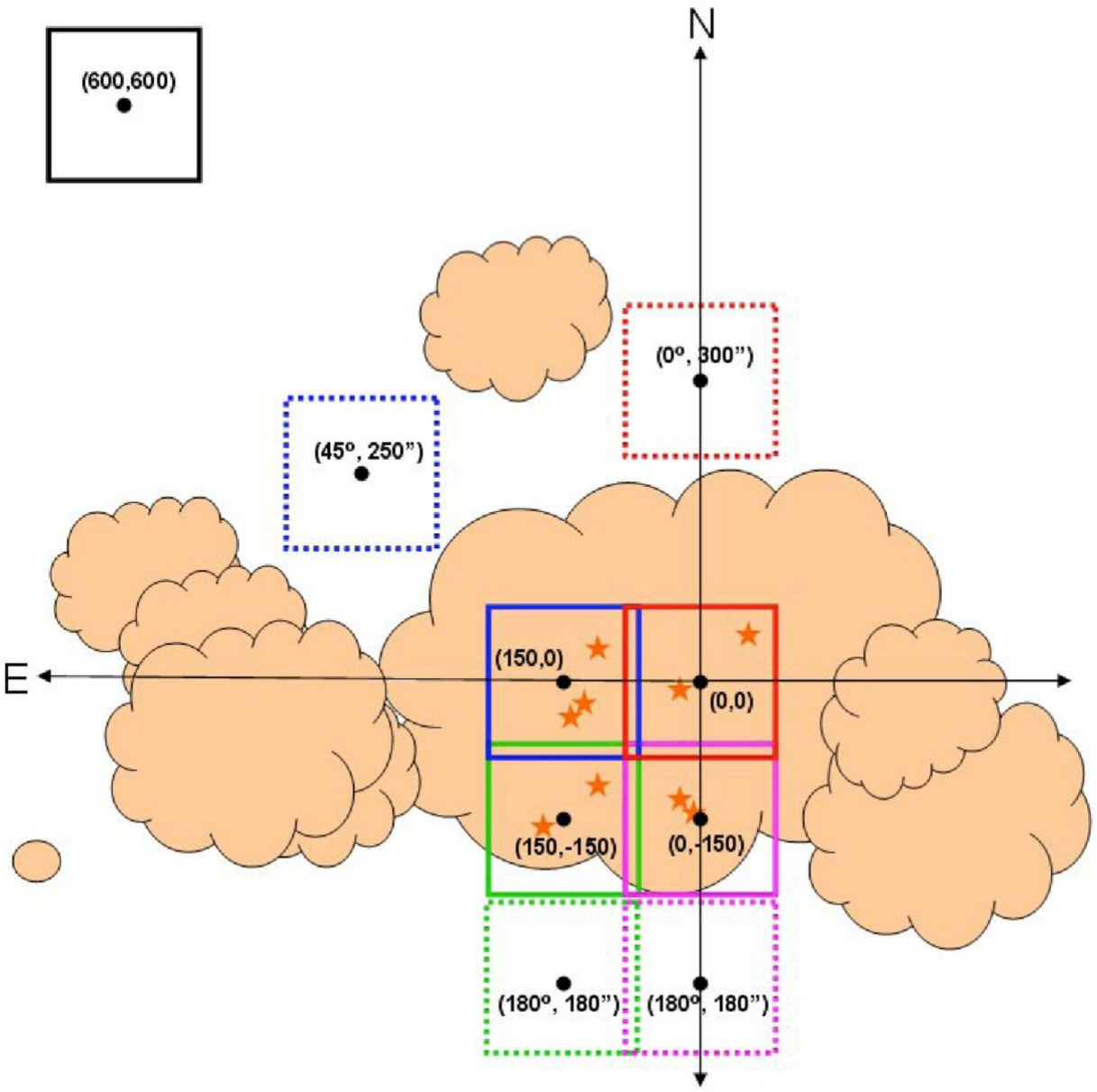

Once a proposal has been accepted, the proposer, in collaboration with the SMO instrument scientist, will specify the details of chopping and nodding for each observation using the SOFIA observation preparation tool (USPOT). Experienced proposers are encouraged to design their observations using USPOT *before* writing their proposals to prevent the loss of observing time that might occur if, during Phase II, the observations are discovered to be more challenging than expected.

Following are a few of the most important issues to consider when preparing a FORCAST Imaging proposal:

Check a Database
It is recommended that a near-IR or mid-IR database (e.g., 2MASS, *Spitzer* , *WISE* , MSX or IRAS) be checked to see if the target of interest is near other IR sources of emission. In the case of extended sources, where on-chip (i.e., on the detector array) chop and nod is not possible, it is necessary to pick areas free of IR emission for the chop and nod positions to get proper background subtracted images.

For Emissions Less than ~1.6 arcmin
If the IR emission from the region surrounding the source is restricted to a region smaller than half the FORCAST field of view (i.e. ~1.6 arcmin), then the chop and nod can be done on-chip. Observations performed in NMC mode either on-chip or off-chip yield a S/N equal to or slightly better than that obtained in NPC mode. For additional discussion of this point, see the calculations of S/N for various FORCAST chop-nod scenarios provided here.

Chop Throw Constraints
When using a symmetric chop, chopping and nodding can be performed in any direction for chop throws less than 584 arcsec. When using an asymmetric chop, the maximum possible chop throw is 420 arcsec. However, some chop angles (as measured in the instrument reference frame) are not allowed for asymmetric chop throws between 250 arcsec and 420 arcsec. Since the orientation of the instrument relative to the sky will not be known until the flight plan is generated, Those requesting chop throws between 250–420 arcsec are required to specify a range of possible chop angles from which the instrument scientists can choose when the flight plan is finalized.

Additionally, large chop amplitudes may degrade the image quality due to the introduction of coma. This effect causes asymmetric smearing of the PSF parallel to the direction of the chop at a level of 2 arcsec per 1 arcmin of chop amplitude.

For large, extended objects, it may not be possible to obtain clean background positions due to these limitations on the chop throw.

For Faint Targets
Currently, the longest nod dwell time (that is, the time spent in either the nod A or nod B position) for FORCAST is 30 sec in the SWC-only and dual channel configurations and up to 120 sec in the LWC-only configurations (depending on the filter). Run the exposure time estimator to determine if the object will be visible in a single A-B chop-subtracted, nod-subtracted pair, with an exposure time of 30 sec in each nod position. If the object is bright enough to be detectable with S/N greater than a few, it is recommended that dithering be used when observing in NMC or NPC mode. The dithering will mitigate the effects of bad pixels when the individual exposures are co-added.

If the object is not visible in a single A-B chop/nod-subtracted pair, with a nod dwell time of 30 sec in each nod position (60 sec integration), then dithering should *not* be used.

Return to Table of Contents

4.2.1.1 Estimation of Exposure Times

The exposure times for FORCAST imaging observations should be estimated using the SOFIA Instrument Time Estimator (SITE). SITE can be used to calculate the signal-to-noise ratio (S/N) for a given total integration time, or to calculate the total integration time required to achieve a specified S/N. The total integration time used by SITE corresponds to the time actually spent integrating on-source without overheads. These integration times are used as input for USPOT, which will automatically calculate the necessary overheads. The format of the S/N values output by SITE depends on the source type. For Point Sources, the reported S/N is per resolution element, but for Extended Sources, it is the S/N per pixel.

For mosaic observations the total integration time required for a single field should be multiplied by the number of fields in the mosaic to obtain the total time, which is to be entered in USPOT.

An important consideration in planning observations is whether FORCAST should be used in single channel configuration, or in a dual channel configuration, since one gains the extra filter observation at the cost of lower system throughput in the individual bands. On the SITE form, a single channel configuration is specified by selecting the filter of interest for one channel and selecting **None** on the other channel in the Instrument properties section.

Return to Table of Contents

4.2.2 Spectroscopic Observations

Proposers are strongly encouraged to familiarize themselves with the basics of techniques for performing background limited observations covered in Section 1.3. In brief, the spectroscopic observation modes for FORCAST include the following:

NMC Mode
As with FORCAST imaging observations, Nod Match Chop mode consists of a chop symmetric about the optical axis of the telescope with one of the two chop positions centered on the target. See Section 4.2.1 or Section 1.3.

NPC CAS and **NPC NAS Modes**
Grism Nod Perpendicular to Chop observations can be performed either in a Chop Along Slit mode (NPC CAS) or Nod Along Slit mode (NPC NAS). As with FORCAST imaging observations, FORCAST's grism NPC modes also impliment a chop that is symmetric about the optical axis–however, unlike in NMC mode, the nod is perpendicular to the chop. The final images produced using NPC CAS or NAS show two sources arranged along the slit with one positive and one negative beam. Unlike NMC, each beam in NPC has the same relative intensity.

NXCAC Mode
Nod not related to Chop with Asymmetric Chop mode is the grism version of C2NC2, i.e., an asymmetric chop with dithering along the slit. See Section 4.2.1 or Section 1.3.

Slitscan Mode
In Slitscan mode, the slit is moved across a target in discrete steps using dithers perpendicular to the slit axis to yield a spectroscopic map of an entire area of sky.

During Cycle 9, grism spectroscopy with FORCAST will only be available in single channel, long-slit configurations (SWC and LWC). By default, observations will be set up using NMC aligned along the slit in Long Slit configurations and perpendicular to the slit in XD configuration. Due to the size of the PSF, neither chopping or nodding along the slit nor dithering are possible for high-resolution XD observations. For larger sources and for targets embedded in crowded fields it is advised to use C2NC2 mode.

The observing efficiency for FORCAST spectroscopic observations depends on a number of factors, including the observing mode, chop frequency and nod cadence, the detector frame rate, and LOS rewind cadence. The typical observing efficiency as measured from NMC and NPC observations is 50–75% of clock time. Work is ongoing to optimize the mode-dependent efficiency values. These efficiency estimates are built-in to USPOT and do not need to be specified.

It is important to note that due to the fixed position of the grisms/slits in the filter/aperture wheels, the orientation of the slit on the sky will be dependent on the flight plan and will not be able to be predetermined. Further, the slit orientation rotates on the sky with each telescope Line-of-Sight (LOS) rewind (Section 1.1). These limitations may be especially important to consider when proposing observations of extended objects.

Return to Table of Contents

4.2.2.1 Estimation of Exposure Times

The exposure times for FORCAST Grism spectroscopic observations should be estimated using the SOFIA Instrument Time Estimator (SITE). SITE can be used to calculate the signal-to-noise ratio (S/N) for a given total integration time, to calculate the total integration time required to achieve a specified S/N, or to estimate the limiting flux for a desired S/N.

In either case, *overheads should not be included*, as USPOT calculates them independently.

Return to Table of Contents

5. FPI+

To export the handbook as a PDF, click on the three dots in the upper right, then choose "Export with Scroll PDF Exporter". In the Template drop-down menu, choose "Handbook Template", and then click "Export".

5.1 Specifications

5.1.1 Instrument Overview

The Focal Plane Imager (FPI+) is the standard tracking camera for the SOFIA telescope, utilizing a science grade CCD sensor. Since the FPI+ is a subsystem of the SOFIA tracking system, it is permanently installed on the telescope. Therefore, it can be operated on every observing flight, either stand-alone or in parallel with any science instrument that is mounted on the telescope.

As a science instrument, the FPI+ is intended to be used as a fast framerate imaging photometer in the visual wavelength range. The highly configurable readout modes of the camera can be adapted to the proposed observation needs. Examples for the scientific use of the FPI+ include observations of stellar occultations and exo-planet transits. The observations of stellar occultations benefit from SOFIA's mobility, e.g. the abilities to fly into the shadow path and to avoid cloud cover. The observation of exo-planet transits benefit from the much reduced scintillation noise at flight altitude, resulting in higher signal-to-noise ratios in the light curves compared to ground based measurements.

Return to Table of Contents

5.1.1.1 Design

Most of the visual light passes SOFIA’s tertiary beam splitter (M3-1) before it is reflected into the Nasmyth tube by the fully-reflective tertiary (M3-2). A significant amount of visual light is not transmitted, but rather absorbed or reflected along with the longer, infrared wavelengths. However, in the range between 480 nm to 800 nm, where the visual-light CCD cameras are most sensitive, more than 50% of the light is transmitted to the FPI+. The visual light continues through a set of four silver-coated folding mirrors inside the so called *delay line assembly* of the telescope. This setup allows focusing the FPI+ independently from the instrument at the telescope science instrument flange. A pair of windows is installed between the Nasmyth tube and the delay line that create the boundary between the stratospheric conditions in the telescope cavity and cabin conditions inside the delay line assembly. Two eyepiece lenses are used to collimate the telescope beam. Close to the camera is a pellicle beam splitter made of a nitrocellulose membrane with 85% transmission. The beam splitter can be used to reflect a

reticle into the light path for camera alignment purposes. The last optical element in front of the camera is an industrial ZEISS 1.4/85 mm Planar T* IR photo lens.

A double-carousel, filter wheel with six positions on each carousel is installed between the reticle beam splitter and the ZEISS lens.

Return to Table of Contents

5.1.1.2 Angular Resolution

The image quality at visible wavelengths on SOFIA is dominated by seeing and image motion. The major source of seeing is the turbulent shear layer across the telescope cavity, which causes scattering of the light from density fluctuations. These fluctuations are strongly dependent on the mean static air density and the Mach number. The resulting wavefront error is smaller at longer wavelengths. An average image size between 3.5 arcseconds FWHM and 4 arcseconds FWHM can be expected for the FPI+, depending on flight altitude and observed wavelength.

The CCD sensor of the FPI+ is an e2v CCD201-20 1024 x 1024 pixel frame transfer EMCCD with a plate scale of 0.51 arcsec/pix and a square field of view (FOV) of 8.7 x 8.7 arcmin. The unvignetted FOV is a circular beam of approximately 9 arcmin diameter centered on the FPI+ sensor. Pixel binning of 2x2, 4x4, etc. is available and can be used to increase the frame rate and reduce the effective readout noise. In flight, the seeing blur size of the observatory is at about 4 arcsec diameter. Therefore, a reduction of the angular resolution by binning up to 4x4 (2x2 arcsec^2) still provides critical sampling of the seeing element.

Return to Table of Contents

5.1.2 Performance

5.1.2.1 Filter Suite

The wavelength range of the FPI+ is 360 nm to 1100 nm. Six spectral filters are available within this range. These are five Sloan Digital Sky Survey filters u'g'r'i'z' and a Schott RG1000 near-IR cut-on filter. Additionally, three neutral density (ND) filters can be used to attenuate bright stars. The ND filters are required for the tracking function of the FPI+ and the optical densities are chosen in such a way that stars within the brightness range of 0 < V mag < 16 can be imaged with an exposure time of 1 second. The Daylight filter is also a requirement for telescope tracking to be able to acquire bright guide stars in twilight.

Table 5-1: Filter Wheel Configuration

Carousel 1	Carousel 2
OPEN	OPEN
Sloan u'	ND 1
Sloan g'	ND 2
Sloan r'	ND 3
Sloan I'	Daylight

Carousel 1	Carousel 2
Sloan z'	Blocked

Table 5-1 shows the configuration of the FPI+ double filter wheel. Filters from carousel one and two can be combined freely with a few exceptions. The daylight tracking filter from carousel two can only be used with the OPEN position of carousel one to avoid non-overlapping wavelength bands. The Blocked position cannot be selected for observations, but instead is used for taking calibration data (bias frames, dark frames).

Filter Throughput

Figure 5-1 shows a plot of the FPI+ total system throughput, which includes a model for atmospheric extinction, the calculated SOFIA telescope throughput, and the instrument quantum efficiency. The filter spectral response has been measured and is added to the plot. At the wavelengths where the Sloan u' filter is transparent, other elements in the FPI+ light path (dichroic tertiary mirror, protected silver coatings, ZEISS lens) are nearly opaque. This results in a very low throughput (~0.5%) for the selection of the FPI+ with the Sloan u' filter.

Figure 5-1.

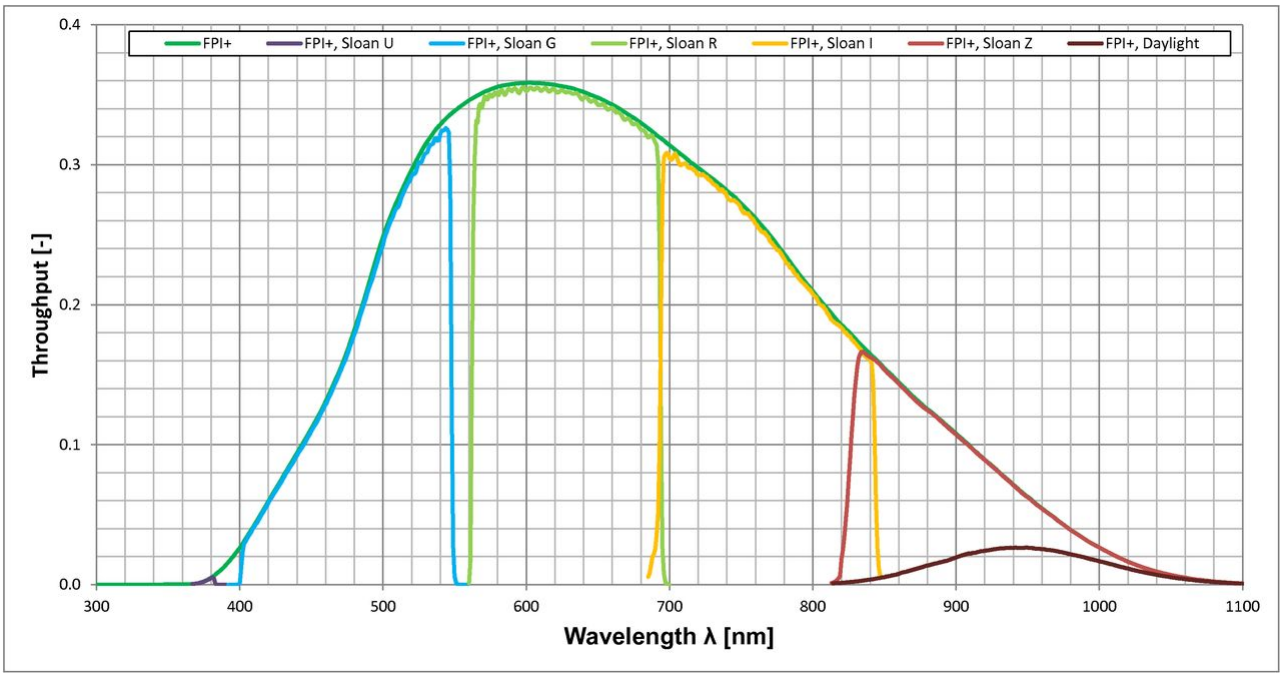

24 Figure 5-1. Total system throughput for Sloan filters, the Schott RG1000 (daylight) filter and the OPEN FPI+ configuration.

Figure 5-2 is a plot of the neutral density filter transmittance vs. wavelength for the three installed ND filters. Over the entire wavelength range of the FPI+, the ND filters have the average optical density listed in Table 5-2. However, there is a wavelength dependence of the optical density of all ND filters that has to be considered when using the ND filters in conjunction with the Sloan filters. All filters are par focal despite their different thicknesses, because they are installed in the parallel beam in front of the Zeiss lens.

Figure 5-2.

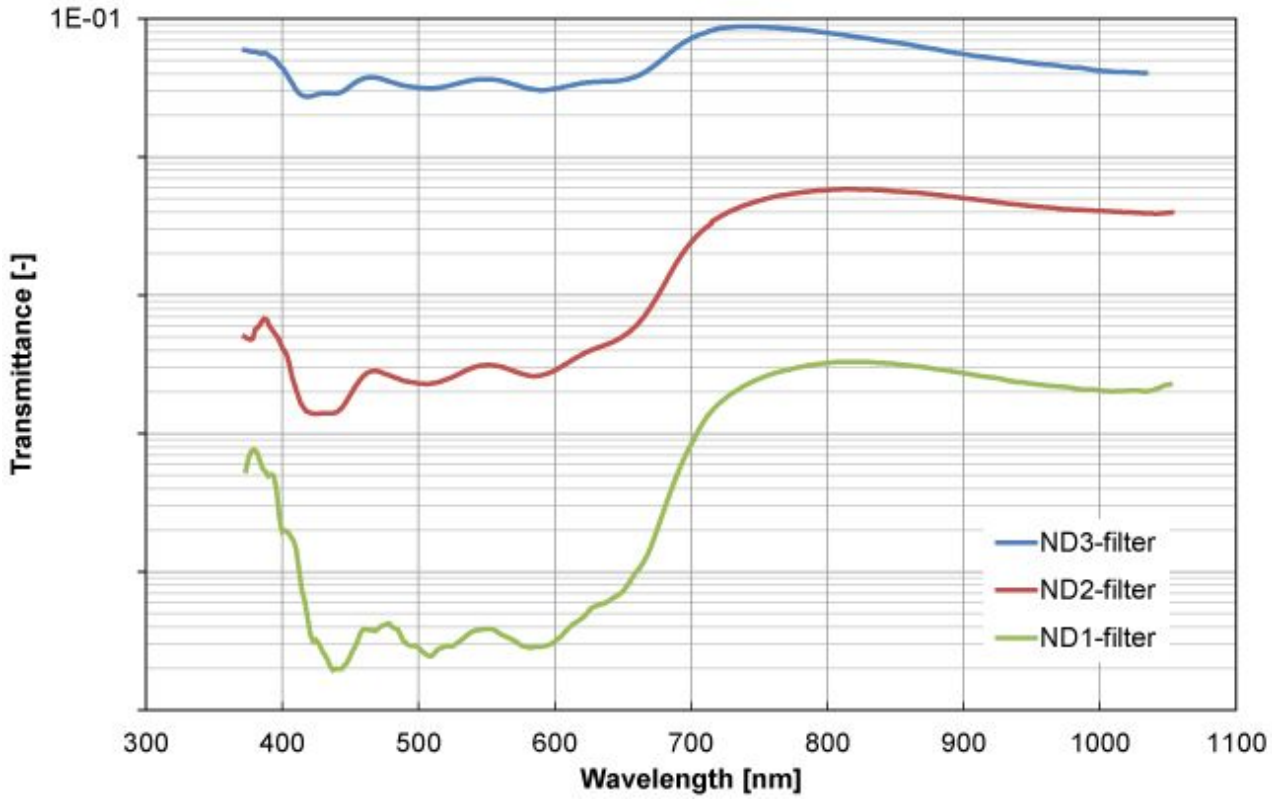

25 Figure 5-2. Transmittance curves of the FPI+ neutral density filters.

Table 5-2: Neutral Density Filter Properties

Filter name	Glass Type	Thickness	Average Optical Density
ND1	Schott NG9	4.0mm	4
ND2	Schott NG3	3.5mm	2.6
ND3	Schott NG4	2.8mm	1.3

Return to Table of Contents

5.1.2.2 Imaging Sensitivities

The instrument sensitivity and resolution is provided to analyze the feasibility of scientific investigations. The sensitivity of the FPI+ in its different Sloan filters was measured in-flight as part of the camera upgrade verification. The selected star field had targets with a wide range in V mag brightness (11.1 < V mag < 16.7). The full-frame images were acquired with an exposure time of one second without pixel binning. The SNR values in Figure 5-3 are calculated with the measured signal values and the known noise sources. Displayed are the results of the OPEN configuration and the Sloan filters u', g', r', i', z' and DAYLIGHT.

Figure 5-3.

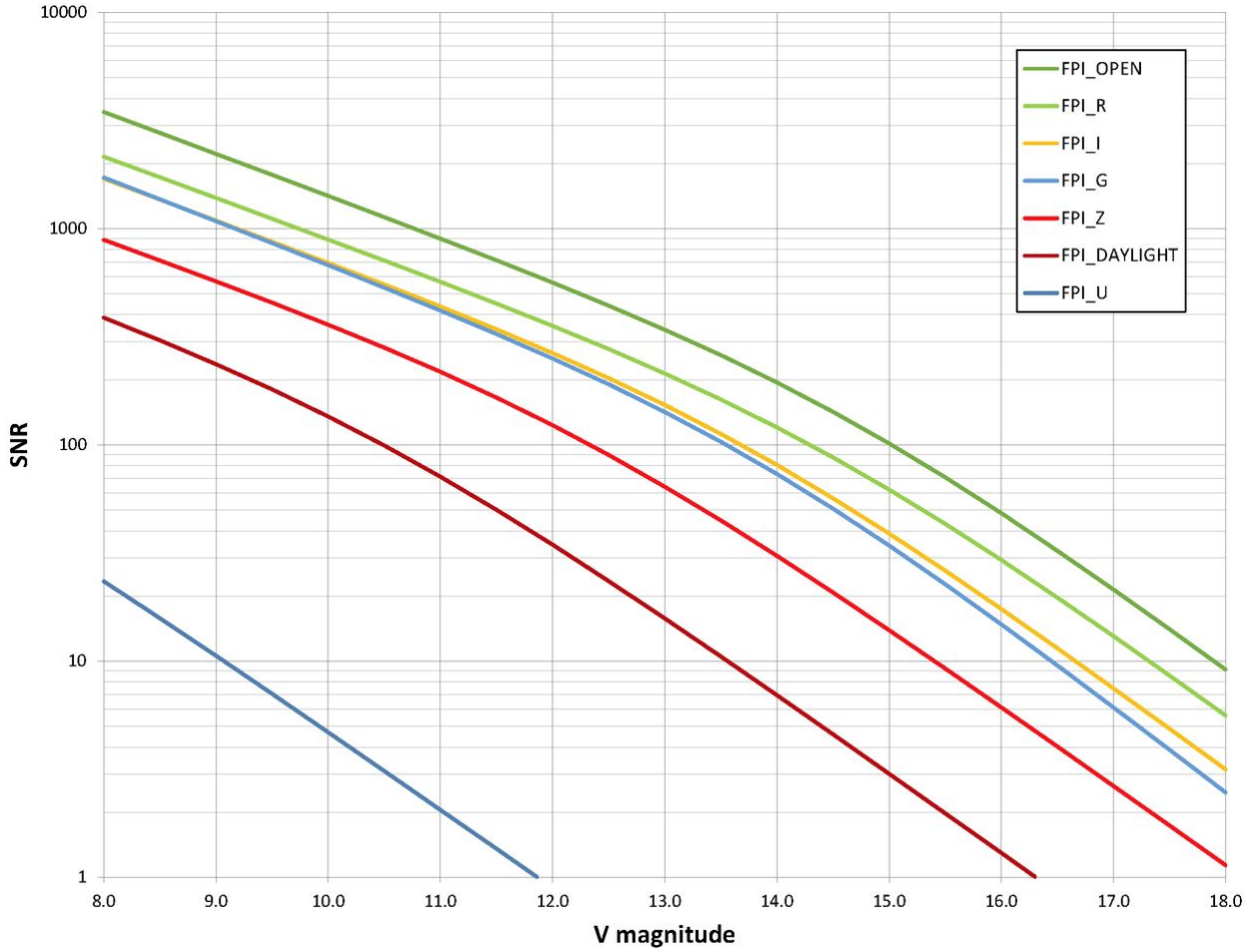

26 Figure 5-3. Signal to Noise Ratio (SNR) for point sources imaged with FPI+ at texp = 1 sec. Displayed is the OPEN broadband configuration as well as the spectral Sloan filters u', g', r', i', z' and the FPI+ DAYLIGHT filter.
Return to Table of Contents

5.1.2.3 Camera Performance

Table 5-3: Camera Modes and Performance

FPI+ Observing Mode	Horizontal Clock Rate	Bit Depth	Gain [e-/DU]	Minimum Read Noise	FPI+ Tracking Possible
FAST_STARE	10 MHz	14 bit	10.7	45.9 e- rms	No
FPI_TRACK_MEDIUM_STARE	5 MHz	14 bit	8.9	36.1 e- rms	Yes
FPI_TRACK_SLOW_STARE	1 MHz	16 bit	0.7	6.0 e- rms	Yes

With the camera's multi-stage thermo-electric cooler, it is possible to achieve sensor temperatures of 100˚ C below ambient temperature. The measured dark current rate at a sensor temperature of -85˚ C, the recommended setting, is 0.001 e-/pixel/second.

The frame rates listed in Table 5-4 are for the full frame. When sub-frames are used (without FPI+ tracking) the achievable rates can be increased. The frame rate then depends on the sub-frame size and its position on the sensor.

Table 5-4: Frame Rates (frames per sec) for the Acquisition of Full Frames

Size	FAST_STARE	MEDIUM_STARE	SLOW_STARE
1x1	8.9	3.8	0.9
2x2	17.5	6.9	1.7
4x4	33.6	11	3.2

Return to Table of Contents

5.2 Planning Observations

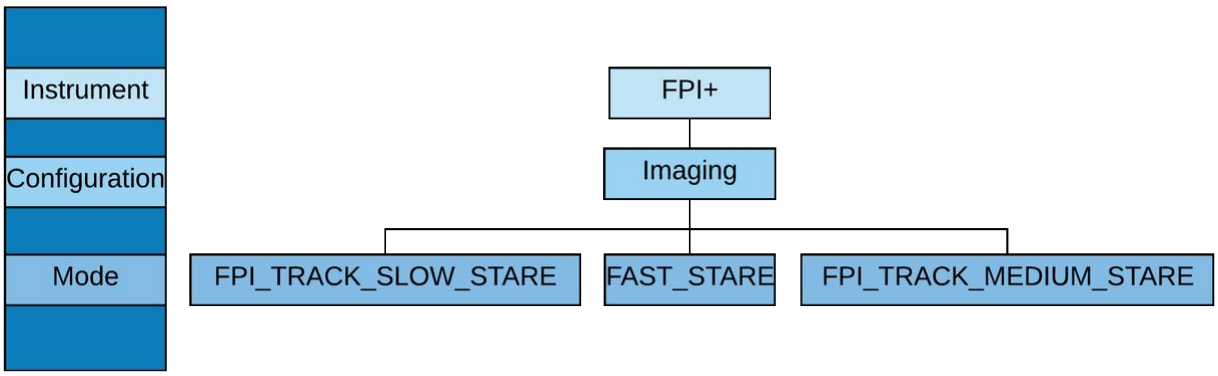

5.2.1 Observing Modes

FPI+ is the standard tracking camera for the SOFIA telescope, and therefore does not require background ellimination techniques to be employed. The FPI+ science instrument offers one imaging configuration with three observing modes: FPI_TRACK_SLOW_STARE, FPI_TRACK_MEDIUM_STARE and FAST_STARE. There is no slit for spectroscopy available. The observing modes are described below.

FPI_TRACK_SLOW_STARE (1 MHz)
Allows image acquisition while tracking on the same images. The parallel tracking requires a reasonably bright guide star in the field of view and exposure times should not exceed 4000 milliseconds.

FPI_TRACK_MEDIUM_STARE (5MHz)
The higher readout rate results in a higher associated readout noise but also in faster frame rates. The parallel tracking requires a reasonably bright guide star in the field of view and exposure times should not exceed 4000 milliseconds.

FPI_TRACK_FAST_STARE (10 MHz)
The fastest readout currently possible with FPI+. This mode does not allow FPI+ tracking on the science images--however FFI tracking can be used.

The two slower observing modes offer, but do not require, tracking in the FPI+ in parallel to the acquisition of science data. However, simultaneous FPI+ tracking does impose certain restrictions on the camera acquisition setting. Acquisition setting restrictions for simultaneous FPI+ tracking are as follows:

- Image frame size: Full frame
- Pixel binning: 1x1, 2x2, 4x4
- Exposure time: between 100 and 4,000 ms for best tracking performance
- Target: Track star available in FPI+ field of view

With simultaneous FPI+ tracking, a target position accuracy of 0.17 arcsec rms has been measured over a two hour time period. There is no positional drift of the target evident.

Alternatively, all of the three observing modes can be used with tracking in the Fine Field Imager (FFI; the tracking camera on the telescope front ring) or without any tracking at all. This allows the selection of an arbitrary sub-frame and binning factors along with the choice of very short (or longer) exposure times in the FPI+. With FFI tracking, positional drifts of the target of 3.9 arcsec per hour have been observed.

Return to Table of Contents

5.2.2 Estimation of Exposure Times

The sensitivities of the FPI+ with all spectral filter options have been implemented into the SOFIA Instrument Time Estimator (SITE). This online tool allows the estimation of exposure times to achieve a desired signal to noise ratio.

Return to Table of Contents

5.2.3 Overheads

Generally, observations can be set up very efficiently and overheads are small. For each observation, bias frames and dark frames will be acquired for image calibration. These calibration acquisitions will result in additional overheads.

The overhead is the instrument set-up time per observation in minutes. It is calculated with:

$$\text{Overhead} = A * \text{Repeat} + B$$

where A = 0.013 sec, B = 200 sec, and Repeat is the total number of acquisitions with the specified exposure time.

The entire duration of the observation is:

$$\text{Duration} = \text{ExposureTime} * \text{Repeat} + \text{Overhead}$$

Observations are done in the frame transfer mode. This means parameter A represents the time for the charge transfer on the sensor and has a value of 1 to 3.4 µs.

The setup time is less than 20 seconds and approximately 3 minutes should be planned for the acquisition of bias and dark calibration frames.

Return to Table of Contents

6. GREAT

To export the handbook as a PDF, click on the three dots in the upper right, then choose "Export with Scroll PDF Exporter". In the Template drop-down menu, choose "Handbook Template", and then click "Export".

6.1 Specifications

6.1.1 Instrument Overview

The **G**erman **RE**ceiver for **A**stronomy at **T**erahertz Frequencies (GREAT) is a modular heterodyne instrument with multiple configurations (see below) that provide high resolution spectra (up to R = 10^8) in several frequency windows between 0.4900–4.7448 THz.

The front-end unit consists of two independent dewars that operate simultaneously. Each dewar contains one of the following channels:

upGREAT Low Frequency Array (LFA)
The LFA is a 14-pixel array with two polarizations (Horizontal and Vertical with 7 pixels each) with 6 pixels arranged in a hexagonal pattern around the central pixel. Both polarizations of the array (LFAH and LFAV) can be tuned to one simultaneous or two independent frequencies in the 1.835-2.007 THz range. Tuning the LFA polarizations to two independent frequencies is offered on a best effort basis. The [OI] 145 µm line can can only be observed in V polarization, which has an additional tuning range from 2.060 to 2.065 THz.

upGREAT High Frequency Array (HFA)
The HFA is a 7-pixel array arranged with 6 pixels in a hexagonal geometry around a central pixel. The local oscillator is a Quantum Cascade Laser with a narrow tuning range limited to the [OI] 63 µm frequency of 4.74477749 THz (with a tuning range of roughly + 250 km/s to -100 km/s in LSR velocity).

4GREAT
4GREAT consists of four co-aligned (to within a few arcsec) pixels at four different frequencies. The tuning ranges of these pixels are: 491-635 GHz (4G1), 890-1092 GHz (4G2), 1240-1525 GHz (4G3), and 2490-2590 GHz (4G4).

The GREAT instrument uses eXtended bandwidth Fast Fourier Transform Spectrometers (XFFTS) as backends. Each XFFTS has a bandwidth of 4 GHz and 16,384 channels, thus providing a resolution of 244 kHz (note that the useful bandwidth depends on the tuning and the atmospheric transmission). The beam size is close to the diffraction limit —about 14 x (1.9/ ν THz) arcsec, where ν is the frequency observed in THz.

A detailed description of the GREAT instrument and its performance during the 2011 Basic Science flights can be found in the GREAT special issue of Astronomy & Astrophysics (Heyminck et al. 2012, A&A, 542, L1). The upGREAT arrays are described in Risacher et al. (2016, A&A, 595, A34) and Risacher et al. (2018, JAI 7, 1849914). 4GREAT is described in Duran et al. (in prep.). Additional information about the instrument can be found on the GREAT website.

Return to Table of Contents

6.1.1.1 Design

Heterodyne receivers work by mixing the signal from a source on the sky at a given frequency ν_s with the signal from a local oscillator (LO) at a specified (and precisely controlled) frequency ν_{LO}. This signal mixing results in two frequency bands on the sky called the signal and image bands being folded into the intermediate frequency (IF) band in the few GHz range, which is amplified and then spectrally analyzed. These bands are located symmetrically on either side of the LO frequency ν_{LO}, and they are separated from that LO frequency by an intermediate frequency $\nu_{IF} = |\nu_s - \nu_{LO}|$. GREAT operates in a double sideband mode (DSB), which means that both the image and signal bands are not separated and are equally sensitive to incoming radiation. By definition, the band containing the spectral line of interest is always the signal band and the opposite band is the image band. This signal band can be chosen to be either above (Upper Sideband, USB) or below (Lower Sideband, LSB) the LO frequency; see Figure 6-1. For sources rich in spectral lines, care has to be taken so that a spectral line in the image band does not overlap or blend with the line of interest in the signal band. This can be achieved by fine-tuning the local oscillator frequency.

4G1 and 4G2 use Superconductor-Insulator-Superconductor (SIS) mixing devices providing an IF band from 4 to 8 GHz. 4G3 and 4G4 and the upGREAT arrays employ Hot-Electron-Bolometer (HEB) mixers with IF bands of 0.1 to 4 GHz. The optics of GREAT generally utilize beam splitters to overlay the LO and sky signal. However - due to LO power limitations - 4G4 uses a diplexer, which reduces the usable IF band to 1.4 to 2.8 GHz.

Figure 6-1.

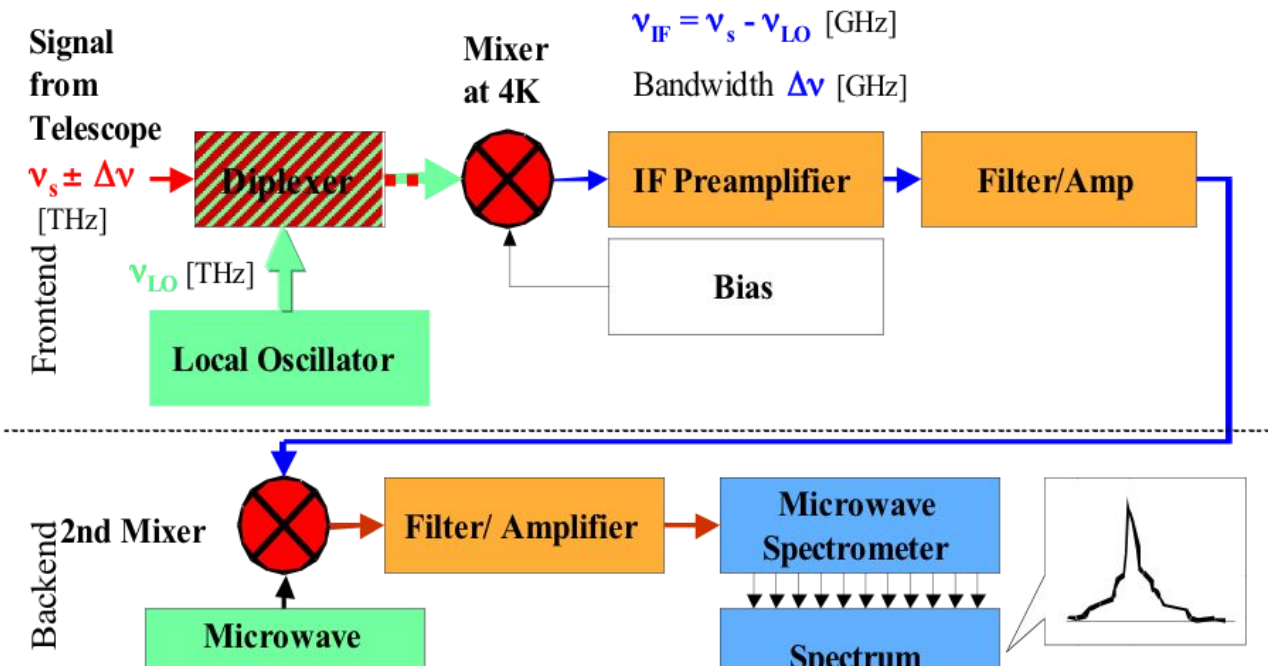

27 Figure 6-1. Schematics of a GREAT receiver channel. Only 4G4 uses a diplexer, all other channels have a beam-splitter. The second IF mixing process is optional and is only used when the mixer output range and the backend input range do not match.

Return to Table of Contents

6.1.1.2 Configurations

The channels that are currently operational are listed in Table 6-1. Not every frequency in each tuning range has been checked, so there may be gaps where the LOs do not provide enough power to pump the mixer or regions where the receiver temperature deviates from the average values quoted in the table.

Table 6-1

GREAT Configurations

Front-End	Frequencies (GHz)	Lines of Interest	DSB[6] Receiver Temperatures (K)	Main beam efficiencies
HFA [1]	4744.77749	[OI] 63 µm	1250	0.63
LFAH [2]	1835–2007	[CII] 158 µm, CO, OH, $^2\Pi_{1/2}$, ^{12}CH, ^{13}CH	1000	0.69
LFAV [2]	1835–2007 2060–2065	Same as LFAH, plus [OI] 145 µm		

Front-End	Frequencies (GHz)	Lines of Interest	DSB[6] Receiver Temperatures (K)	Main beam efficiencies
4G4	2490–2590	OH $^2\Pi_{3/2}$, ^{18}OH $^2\Pi_{3/2}$	3300	0.57
4G3	1240–1395 1427–1525	[NII] 205 µm, CO, OD, HCN, SH, H_2D^+	1100	0.70
4G2 [3,4]	890–984 990–1092	CO, CS	> 600 300	0.59
4G1 [4]	491–555 560–635	NH_3, [CI] 609 µm, CO, CH	< 150	0.51

1. One 7-pixel array. Quantum Cascade Laser LO with very small tuning range near the [OI] 63 µm line.
2. Two 7-pixel arrays at two polarizations (H,V). Both polarizations can be tuned to the same frequency (LFAH range), or two separate frequencies on a best effort basis. The [OI] 145 µm line is only tunable with the V-array LO.<
3. Strong degradation below 900 GHz.
4. For 4G1 and 4G2, the gaps in the center of the LO tuning correspond to frequency ranges blocked by the low atmospheric transmission.

In Cycle 9, GREAT offers two configurations:

upGREAT LFA with upGREAT HFA
This configuration employs the Low Frequency Array (LFA) in one dewar and the High Frequency Array (HFA) in the second dewar. The LFA consists of two polarizations (H and V) with 7 pixels each, and the HFA consists of 7 pixels. Both polarizations of the array (LFAH and LFAV) can be tuned simultaneously in the 1.835-2.007 THz range (and specifically the [CII] line at 1900.536 GHz), or alternatively they can each be tuned to a different frequency on a best effort basis. The [OI]145 µm line can only be observed in V polarization.

4GREAT with upGREAT HFA
This configuration implements 4GREAT in one dewar and the HFA in the second dewar. The 4GREAT pixels are coaligned on the sky to within a few arcseconds, and operate simultaneously.

Return to Table of Contents

6.1.2 Performance

6.1.2.1 Sensitivities

The GREAT sensitivities and integration times are calculated with the SOFIA Instrument Time Estimator (SITE). This section presents the background for these calculations as well as some worked-out examples. Because heterodyne receivers are calibrated by measuring the receiver temperature T_{rx} with a hot and a cold load, the logical intensity unit for a heterodyne observation is temperature expressed in Kelvin (K). Typically, measurements are expressed either with antenna temperature T_A^* or main brightness temperature T_{mb}.The asterisk for the antenna temperature T_A^* refers to values corrected for atmospheric transmission, telescope losses, and rearward spillover (see Kutner & Ulich, 1981, ApJ, 250, 341) . Similarly, the noise (ΔT_A * or ΔT_{mb}) is also expressed in units of temperature. The

sensitivity, or signal-to-noise ratio, of the observations is given by the ratio between the source temperature and the root mean square (rms) temperature of the spectrum. In order to calculate these quantities, we first estimate the single sideband (SSB) system temperature T_{sys} which includes the noise from the thermal emission of the telescope and the sky, and refers to the brightness temperature scale on the sky:

(Eq.6-1)
$T_{sys} = 2 \times [T_{rx} + \eta_{tel} \times T_{sky} + \eta_{tel} \times T_s + T_{tel}] / (\eta_{tel} \times \eta_{sky})$,

where T_{rx} is the dual sideband (DSB) receiver temperature;
T_{sky} is the radiation temperature of the sky;

T_s is the continuum temperature of the source, which is usually negligible unless observing an extremely bright object such as Jupiter, Saturn, or Sgr B2, and is therefore set to zero in the GREAT time estimator;

T_{tel} is the radiation temperature of the telescope;
η_{sky} is the atmospheric transmission;
η_{tel} is the efficiency of the telescope, which includes ohmic losses and spillover.

All temperatures in Equation 6-1 are Rayleigh-Jeans equivalent "radiation" temperatures, and not physical temperatures.

The factor 2 in Equation 6-1 assumes that the noise temperature is the same in both signal and image band, which is true for the HEB and SIS mixers used by GREAT. The atmospheric transmission η_{sky} can be estimated using the transmission code ATRAN for the altitude, observing frequency, and airmass of the planned observations. The GREAT time estimator in SITE automatically accounts for the attenuation of the signal in the atmosphere by calling ATRAN. The radiation temperature T_{sky} depends on η_{sky} and the ambient temperature T_{atm} of the sky:

(Eq. 6-2)
$T_{sky} = T_{atm,RJ} \times (1 - \eta_{sky})$,

where $T_{atm,RJ}$ is the Rayleigh-Jeans (RJ) equivalent mean temperature of the atmosphere. The relationship between T_{atm} and $T_{atm,RJ}$ is given by:

(Eq. 6-3)
$T_{atm,RJ} = c^2 \times B(\nu, T_{atb}) / (2 \times k_B \times \nu^2)$,

where $B(\nu, T_{atm})$ is the flux density derived from Planck's law of blackbody radiation for a temperature T_{atm} at a frequency ν, c is the speed of light, and k_B is the Boltzmann constant. As an example, assuming an ambient temperature T_{atm} of 220 K (a typical temperature of the atmosphere at 41,000 ft), we find $T_{atm,RJ}$ = 177.5 K at 1.9 THz.

Likewise, the telescope temperature T_{tel} is related to η_{tel} by the following equation:

(Eq. 6-4)
$T_{tel} = T_{TA,RJ} \times (1 - \eta_{tel})$,

where $T_{TA,RJ}$ the Rayleigh-Jeans (RJ) equivalent temperature of the telescope assembly. For a physical temperature T_{TA} of 230 K for the telesope assembly, and using Equation 6-3, we find $T_{TA,RJ}$ = 187.4 K at 1.9 THz. If the telescope efficiency η_{tel} is 0.92, then the radiation temperature T_{tel} of the telescope is 14.8 K.

As an example, let us calculate the system temperature for the [CII] fine structure line at 157.74 µm (1.9005369 THz). In this example, we assume typical observing conditions at the beginning of a flight. Specifically, we suppose an altitude of 39,000 ft and a source elevation of 30 degrees. For a standard atmospheric model this corresponds to a sky transmission η_{sky} of 0.76, which gives T_{sky} = 42.6 K. For a receiver temperature T_{rx} = 1000 K, Equation 6-1 therefore predicts a single sideband system temperature T_{sys} = 3015 K from the background contribution of the sky alone.

Now we are ready to calculate the sensitivity. The rms antenna temperature ΔT_A^*, which is corrected for the atmospheric absorption and telescope losses, is given by the following equation:

(Eq. 6-5)
$\Delta T_A^* = (2 \times T_{sys} \times \kappa) \times (t \times \Delta\nu)^{-0.5}$,

where k is the backend degradation factor, t is the total integration time on each pair of on and off positions, and $\Delta\nu$ is the frequency resolution of our spectra. Strictly speaking, $\Delta\nu$ is the noise bandwidth which can be slightly different than the frequency resolution depending on the design of the spectrometer. For this example, we suppose the Full Width at Half Maximum (FWHM) of the line to be only a few km/s wide, and so we choose a velocity resolution of 1 km/s (or 6.3 MHz) for the calculation. Since the GREAT backends have a much higher resolution (244 kHz), we can easily bin the spectrum to our desired velocity resolution. For an integration time of 240 seconds, and assuming a backend degradation factor k of 1, we find a rms antenna temperature ΔT_A^* of 0.155 K.

The relationship between the antenna temperature T_A^* and the brightness temperature T_R^* is expressed as:

(Eq. 6-6)
$T_R^* = T_A^* / \eta_{fss}$,

where η_{fss} is the forward scattering efficiency, which is $\eta_{fss} = 0.97$ for GREAT. A rms antenna temperature $\Delta T_A^* = 0.155$ K therefore corresponds to a rms brightness temperature $\Delta T_R^* = 0.160$ K. Please note that the GREAT time estimator uses the brightness temperature T_R^*, and not the main beam brightness temperature $T_{mb} = T_R^* \times \eta_{fss} / \eta_{MB}$, where η_{MB} is typically 0.65 for the LFA and 0.63 for the HFA resulting from the large central blockage in the folded Nasmyth optics of the SOFIA telescope.

For some projects, it may be necessary to instead convert the antenna temperature T_A^* into a flux density S_ν, such as to compare the line intensity with the continuum level of the source. The flux density S_ν can be obtained from the antenna temperature T_A^* using the following standard relation:

(Eq. 6-7)
$S_\nu = 2 \times k_B \times \eta_{fss} \times T_A^* / A_{eff}$,

where k_B is the Boltzmann constant, and A_{eff} is the effective collecting area of the telescope. A_{eff} is related to the geometrical surface area A_g of the telescope by the aperture efficiency η_a such as $A_{eff} = \eta_a \times A_g$. For a main beam efficiency η_{MB} of 0.67 and assuming a Half Power Beam Width (HPBW) of 14.1± 0.3 arcsec, we find an aperture efficiency η_a of 0.55 ± 0.02. For the 2.5 m telescope of SOFIA, the measured flux density for a [CII] line can be expressed as:

(Eq. 6-8)
$S\,(Jy) = 992 \times T_A^*\,(K)$ or, within errors, $S(Jy) \sim 1000 \times T_A^*\,(K)$.

We can also use Equation 6-8 to convert the units of line intensities from Jy to W/m^2, which may be a more familiar unit for the far-infrared community. If we assume that the [CII] line we are observing has a Gaussian profile with a Full With Half Maximum (FWHM) of = 5 km/s, or 31.8 MHz, then the integrated line intensity is given by $1.065 \times T_{peak} \times \Delta\nu$ with $\Delta\nu = 31.8$ MHz. If we take T_{peak} equal to our rms antenna temperature $\Delta T_A^* = 0.155$ K, we find using Equation 6-8 that a four minutes integration corresponds to a one sigma brightness limit of 5.2×10^{-17} W/m^2 for a line width of 5 km/s at a 1 km/s resolution. For a detection experiment, the resolution could even be degraded to 2 km/s instead. In this case, we gain a square root of 2 and our one sigma detection limit becomes 3.7×10^{-17} W/m^2.

Return to Table of Contents

6.1.2.2 Examples

Single point observation
When writing a proposal, investigators often already know what sensitivity is needed given the expected width and brightness of the line to be observed, and they are instead interested in calculating the required integration time. For example, we can calculate the integration time needed to detect the [CII] 158 µm line toward T Tauri, a young low-mass star. Based on Herschel PACS observations, Podio et al. (2012, A&A, 545, A44) find a line intensity of 7.5 x 10^{-16} W m^{-2}. However, the line width was not resolved due to the ~240 km/s resolution of PACS. In this case, the high velocity resolution of GREAT would determine if the line is dominated by an outflow or by the circumstellar disk, or both. If we assume the line is outflow dominated with a FWHM of 20 km/s (or 127.2 MHz), and using Equation 6-8, we find a peak antenna temperature T_A^* of 0.56 K or a brightness temperature T_R^* of 0.58 K. Assuming a SNR of 10 and a resolution of 1 km/s are needed for this project, we can now calculate the required integration time.

If these observations are taken at an altitude of 41,000 ft and at a target elevation of 40 degrees, the ATRAN transmission tool predicts an atmospheric transmission η_{sky} of 0.86 integrated over the received bandpass. According to Equation 6-2, the sky temperature T_{sky} is therefore 24.9 K for an ambient temperature T_{atm} of 220 K. For a receiver temperature T_{rec} of 1000 K, Equation 6-1 then provides a system temperature T_{sys} of 2623 K. To achieve a signal to noise ratio of 10 for the observed line, we then need to integrate until we reach a rms antenna temperature ΔT_A^* of 0.056 K. We can now solve for the integration time t using Equation 6-5, where we set the frequency resolution $\Delta\nu$ to be 6.338 MHz (or 1 km/s). In this case, we find the required integration time t to be 1385 s (or 23.1 minutes). Depending on the sideband chosen as the signal band, SITE provides two comparable solutions, 1465 s and 1456 s, which differ slightly due to the atmospheric transmission in each sideband and the star's Local Standard of Rest (LSR) velocity of ~25 km/s.

Since the PACS data show the emission in T Tauri to be compact, the GREAT observations could be achieved with a single pointing in Dual Beam Switching mode (DBS; see Section 6.2.1.1) using the default chop throw of 60 arcsecond. The overheads for both the DBS and Total Power (TP) modes are estimated to be 100%, and they are automatically included when setting up the observations in USPOT. The duration of the observations would therefore be 48.5 minutes.

Since this example applies specifically to [CII] 158 µm line measurements toward an object with low LSR velocity, both LFA polarizations would contribute equally to the observations. This effectively halves the required observing time to be 24.3 minutes instead (including overheads). However, please note that this additional step is only valid for lines in the 1.835-2.007 THz range when both polarizations of the LFA are tuned to the same line. Prospective investigators should contact the SOFIA help desk if they have any question on how to use both LFA polarizations in their sensitivity calculations.

On The Fly mapping
Sensitivity calculations are done a bit differently in the case of an On The Fly map (OTF), where data is acquired as the telescope is continuously scanning the sky.

Let's take the example of a 5 x 5 $arcmin^2$ map to measure extended [CII] 158 µm line emission in a star-forming region. For OTF maps using the LFA, we typically sample the beam every 6 arcsec (slightly oversampled compared to the ~14 arcsec HPBW of a LFA pixel). The number of map points N_{on} for a single 5 arcmin-wide scan would therefore be 50. If the on-source exposure time t_{on} per point is 0.5 s, then the total on-source time for each line is 25 s. In Total Power mode, the off-source time t_{off} is then t_{on} x $N_{on}^{0.5}$, which in this case would be 3.5 s. The integration time for each line is therefore 28.5 s, and the total integration time to complete all 50 lines of the entire map is 23.8 minutes. Assuming overheads of 100%, which are automatically added when designing observing plans in USPOT, the total observing time for this 5 x 5 $armin^2$ map in Total Power mode would be 47.6 minutes.

In Dual Beam Switching mode, the off-source time is equal to the on-source time, and so the total observing time (including overheads) for the entire map would be 83 minutes instead. The Dual Beam Switching mode is rarely used for OTF maps due to its lower observing efficiency relative to the Total Power mode, and is typically reserved for observations of faint lines (T_R^* < 0.5 K) with large FWHMs (> 30 km/s) where a stable receiver baseline is crucial.

For an OTF map, each map point is covered once by each pixel of the array. For the LFA and the HFA, this effectively means that the integration time per point is multiplied by a factor 7. In addition, if both LFA polarizations are tuned to the same frequency, they can be combined to further multiply the integration time per point by a factor 2. The effective on-source integration time per point T_{on} can therefore be estimated with:

(Eq. 6-9)
$T_{on} = n_{cycle} \times n_{pix} \times n_{pol} \times t_{on}$,

where n_{cycle} is the number of times the map is repeated, n_{pix} is the number of pixels contributing to the map position, n_{pol} is the number of array polarizations tuned to the observed line, and t_{on} is the on-source exposure time.

Back to our previous example of a 5 x 5 arcmin^2 OTF map of [CII] 158 µm line emission, the effective integration time per point T_{on} would therefore be T_{on} = 1 x 7 x 2 x 0.5 s = 7 s. Assuming typical observing conditions (i.e., an altitude of 41,000 ft and an elevation of 30 degrees), the GREAT time estimator calculates a rms temperature ΔT_R^* of 0.43 K for a resolution of 1 km/s. This means that any [CII] line emission larger than 4.3 K in the map will be detected at a 10-sigma level or higher.

Finally, in contrast to classic OTF maps, each map point in an Array OTF or a Raster map are only covered by a single pixel of the array instead (i.e., n_{pix} = 1 in Equation 6-9). To reach comparable effective T_{on} integration times, Array OTF or Raster maps need longer exposure times t_{on} per point or multiple repetitions.

Return to Table of Contents

6.2 Planning Observations

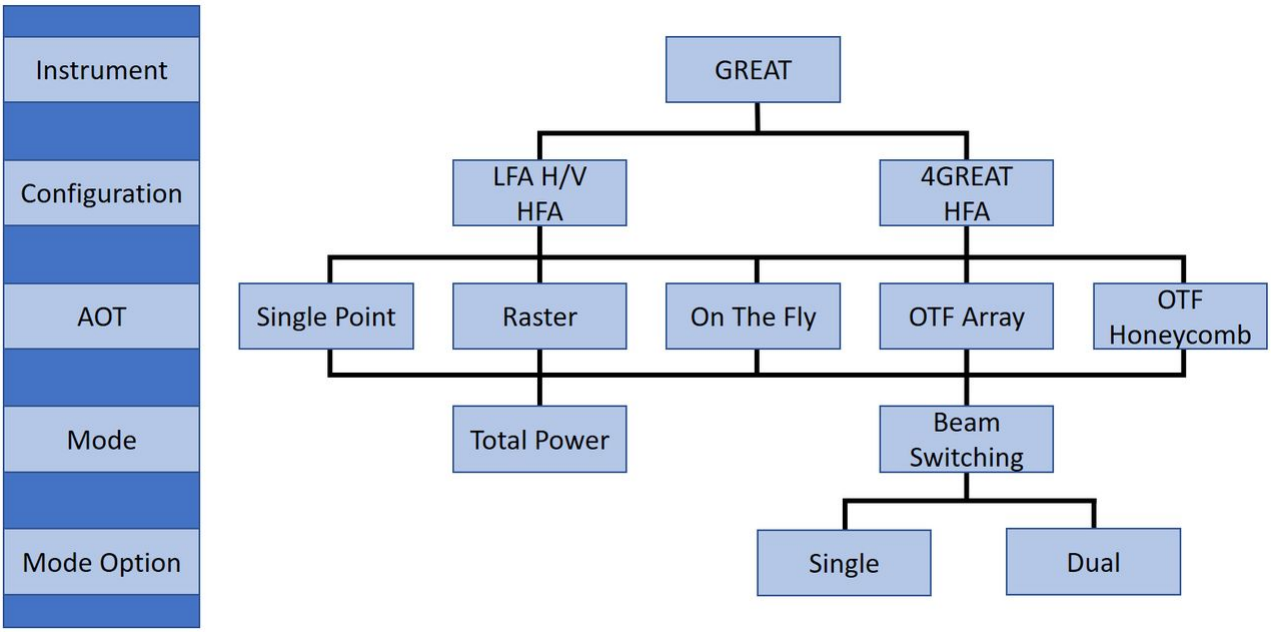

This section describes the GREAT instrument and the available observing modes. It also contains additional information to estimate observing times in individual modes.

If the frequency of interest is not listen in Table 6-1, please contact the GREAT team to ensure the feasibility of the observations. There may be gaps where the broadband Local Oscillators do not provide enough power to pump the mixers.

Note: Allan variance affects the capabilities of GREAT and requires special attention when planning observations, see Section 6.2.1.2 for details.

Return to Table of Contents

6.2.1 Observing Modes Overview

Two observing modes are currently offered: Total Power (TP) and Beam Switching (BSW), the latter of which is available as either Single Beam Switching (SBS) or Dual Beam Switching (DBS).

Total Power Mode
In Total Power mode, the telescope alternates between the target and a nearby reference position that is free of emission. The GREAT software then produces a spectrum from the difference between measurements on the target (ON) and reference (OFF) positions. The optimal integration time in this mode depends on the stability of the receiver and the rate of atmospheric fluctuations. Typically, the recommended integration times on the ON position are < 30 s for the LFA and < 20 s for the HFA. Shorter integration times provide a better cancellation of atmospheric fluctuations, but at the cost of a reduced observing efficiency due to overheads. The ON-OFF cycle is repeated until the required sensitivity is reached.

Total Power mode is most often used to maximize the observing efficiency of On The Fly maps, as well as for single point observations in crowded regions with significant extended emission. Reference positions that are far from the target position may result in poor baselines due to temporal fluctuations in the sky background. If a reference position cannot be identified within 30 arcmin of the target, an intermediate reference position can be selected instead even if it potentially has some emission from the line of interest. This intermediate position will then be measured against a faraway reference position with no line emission. Any contamination in the original spectrum due to line emission in the intermediate reference position can then be accounted for and removed.

Beam Switching Mode (BSW)
In Single Beam Switching (SBS) mode, the telescope is pointed at an intermediary position between the target and reference positions while the secondary mirror is chopped. The main parameters for this mode are the chop throw, which is the angular distance between the target and reference position, and the chop angle relative to the chosen reference frame (i.e., sky coordinates or telescope assembly).

In Dual Beam Switching (DBS) mode, there are instead two reference positions placed symmetrically around the target position. In addition to chopping the secondary mirror like for the SBS mode, the telescope nods between two intermediary positions so that the target is measured against each reference position alternatively.

While using either beam switching modes, the secondary mirror typically chops at a rate between 1.0 and 2.5 Hz. The maximum chop throw allowed is 5 arcmin due to the physical limitations of the secondary mirror. Because the time between the ON and OFF Positions is short (~1 s), this mode typically results in better sky cancellation, and better baseline stability.

Beam switching modes are most often used for point or compact sources for which there is a nearby reference position clear of emission. Smaller chop throws between 60 and 180 arcsec are usually preferred to limit pointing errors and beam distortions (coma).

Return to Table of Contents

6.2.1.1 Astronomical Observation Templates (AOTs)

GREAT offers five standard Astronomical Observation Templates (AOTs) in USPOT: Single Point, Raster Mapping, On The Fly (OTF) Mapping, OTF Array Mapping, and OTF Honeycomb Mapping. Each AOT can be run in either Total Power or Beam Switching modes.

Single Point
The Single Point AOT is used to observe a single position on sky. It is typically used to observe faint sources that require long integration times.

Raster
Raster mapping is essentially a collection of single point observations used to create small maps where a relatively long integration time per map point is needed.

On the Fly
In an OTF map, the telescope scans along a series of rows while the back-ends are continuously integrating the incoming signal. An average is recorded after the telescope has moved a specific distance on the sky. Typically, the size of these steps is half of the beam width. Using default mapping parameters (see Section 6.2.3), each point in the central region of an OTF map will be covered at least once by each pixel of the array (either the HFA or the LFA). The size of this central region changes as a function of the mapping parameters, and it can be assessed easily with USPOT's visualization options (see Section 6.2.3.2).

In Total Power mode, each row scan is preceded by a measurement of the reference position. The integration time t_{OFF} on this reference position before each scan is $t_{OFF} = N_{ON}^{0.5} \times t_{ON}$, where N_{ON} is the number of steps in the row and t_{ON} is the on-source exposure time per point. In this mode, the size of a scan row is limited by the stability of the receiver and by atmospheric fluctuations. The recommended time to complete a single row is under 30 seconds for the LFA and 20 seconds for the HFA. In addition, the typical on-source exposure times per point are between 0.3 s and 2.0 s. Large maps (> 10 arcmin for the LFA and > 3 arcmin for the HFA) should therefore be divided into smaller sub-maps to ensure receiver stability during observations.

In Beam Switching mode, the secondary mirror chops while the telescope is scanning along each row. No dedicated reference position is needed, and so the telescope can immediately start the next row. However, the times spent integrating on the source and reference positions are equal, and so the observing efficiency of the Beam Switching mode is still lower than for the Total Power mode. This mode is rarely used for OTF maps, but it can nonetheless be useful for small maps of compact regions where a stable baseline is needed for the detection of the line observed.

OTF Array
An OTF Array map is created in a similar fashion to a regular OTF map; the telescope scans along a series of rows while the back-ends are continuously integrating the incoming signal. The main difference is that the distance between scan rows is not constant, and is instead designed so that each map point is covered by a single pixel of the array (assuming default mapping parameters; see Section 6.2.3.3). OTF Array maps are typically a combination of several scan "blocks", and are often used to observe relatively compact regions expected to have bright line emission.

OTF Honeycomb
An OTF Honeycomb map is the preferred solution for compact objects that are comparable in size to the array used (either the LFA or HFA). Instead of scanning rows, the telescopes follows a small 25-points hexagonal pattern in order to fully-sample the gaps between each array pixel on the sky (see Section 6.2.3.4). This avoids the issue of wasted integration time outside the region of interest, which can be an issue for OTF and OTF Array maps depending on the size and geometry of the target.

Like OTF Array maps, OTF Honeycomb maps can be tiled together to map larger regions. However, OTF and OTF Array maps are recommended for regions larger than a few times the array size in order to obtain a more homogeneous noise map by covering each map point with different array pixels.

Return to Table of Contents

6.2.1.2 Spectroscopic Stability Limitations

As mentioned in Section 6.2.1, the spectroscopic stability (e.g., Allan variance) sets limits to the operation of a heterodyne instrument like GREAT.

Beam Switching modes typically operate with a chop frequency around a few tenths of a Hz to a few Hz, which is relatively fast, and so the observing limitations are mainly set by the atmospheric stability. As such, on-source integration times of 30 s for the LFA and 20 s for the HFA are typically implemented to achieve optimal spectroscopic stability. A Dual Beam Switching mode is recommended, when possible, in particular for projects

aiming to measure weak and/or broad lines. Some performance decrease has been observed when using a Single Beam Switching mode instead, but it is a viable alternative for crowded regions.

For a Total Power mode, the situation is more complicated and multi-dimensional. Observing line widths larger than a few hundreds MHz and using a reference position farther than 30 arcmin from the source position may negatively impact the stability of the spectroscopic baseline. These impacts depend on the frequency observed, the weather conditions, the stability of the sky background, the elevation of the source, and the arrays used. Please contact the SOFIA help desk if your Total Power observations require a faraway reference position and/or if the line of interest is expected to be weak and broad.

Return to Table of Contents

6.2.2 Estimation of Exposure Times

Estimations of exposure times for GREAT can be made using the SOFIA Instrument Time Estimator (SITE). SITE is a web-based tool that calculates either the signal-to-noise ratio for a given line brightness and integration time, or the integration time needed to reach a certain RMS noise level for either one point on the sky or per map position for an OTF map in Total Power mode. These integration times do not include tuning, chopping, slewing, and other observatory overheads. The total time, including all overheads, is determined in USPOT after entering the time calculated by SITE. SITE is also useful to determine which sideband is the best to use as the signal band by taking the atmospheric transmission into account. System temperatures for the line in the USB or LSB are given, as well as a plot showing the line locations for either Local Oscillator tuning compared to the atmospheric transmission.

The time estimator calculates the time required to reach an RMS brightness temperature ΔT_R^* for a line at a frequency ν by solving the standard radiometric formation for a single point observation. As a reminder, the relation between the brightness temperature T_R^* and the antenna temperature T_A^* is:

$$T_R^* = T_A^* / \eta_{fss} ,$$

where η_{fss} is the forward scattering efficiency which is equal to 0.97 for GREAT. The antenna temperature T_A^* is corrected for ohmic losses and rear spillover. The RMS temperatures ΔT_R^* and ΔT_A^* follow the same relation. The RMS antenna temperature ΔT_A^* is obtained from:

$$\Delta T_A^* = (2 \times T_{sys}) / (t \times \Delta\nu)^{0.5} ,$$

where Tsys is the single sideband system temperature, t is the integration time, and $\Delta\nu$ is the requested frequency resolution. This formula applies when $t_{ON}=t_{OFF}$, which is the case for single point Total Power observations and for all Beam Switching observations.

For On The Fly maps in Total Power mode, the RMS antenna temperature is instead:

$$\Delta T_A^* = T_{sys} (1 + (1 / N_{on})^{0.5})^{0.5} / (t \times \Delta\nu)^{0.5} ,$$

where t is the on source exposure time per point, and N_{on} is the number of on-source positions between measurements of the reference position.

SITE uses the most recent receiver temperatures measured by the GREAT team, and it calls the program ATRAN to estimate the atmospheric transmission for a given altitude, telescope elevation, and water vapor overburden. This transmission is used to calculate T_{sys} assuming an ambient temperature of 220 K for the atmosphere and a telescope assembly temperature of 230 K.

GREAT is a dual sideband receiver, which means that it simultaneously observes in two frequency bands: the upper sideband (USB) and the lower sideband (LSB). The transmission plot in SITE shows the locations of each sideband relative to the observed line, depending on which sideband is used as the signal band. The sidebands for the LFA, HFA, 4G3, and 4G4 are separated by +/- 1.5 GHz, while for 4G1 and 4G2 they are separareted by +/- 5.5 GHz for 4GREAT bands 1 and 2. The required integration times are calculated for both sidebands. The lowest value provided

by SITE should be typically used for the time estimate in a proposal. Differences in the calculated integration times for the LSB and USB are due to the frequency dependence of the atmospheric transmission.

Description of SITE Input Parameters

Type of Observation
Select "Single Point or Beam Switch OTF/Raster Map" for single point observations in either total power or beam-switched mode, and for OTF/Raster maps observations in beam-switched mode. Select "TP OTF/ Raster Map" for OTF/Raster maps in total power mode.

Rest Frequency
Enter the rest frequency (in THz, using 7 decimal places) of the line you wish to observe. The current tuning ranges for the GREAT receivers are listed in Table 6-1.

Frequency or Velocity Resolution
Enter the frequency (in MHz; select the "MHz" radio button) or velocity (in km/s; select the "km/s" radio button) resolution that is requested in the final spectrum.

Line Width
Enter the frequency (in MHz; select the "MHz" radio button) or velocity (in km/s; select the "km/s" radio button) window that will be used to calculate the atmospheric transmission. Modifying this parameter may be important if the line you wish to observe falls close to a narrow atmospheric feature.

Total Power Map Parameters
For OTF maps: Enter the number of ON positions (steps or dumps) in each OTF scan row in the N_{on} field, or have the time estimator calculate this value for you. If you choose to have the estimator calculate it, you should enter the dimensions of the map (in arcsec) and select a "Map Type" option (Classical OTF or Array OTF). For a Classical OTF map, the "Map Size" refers to the area mapped by the central pixel only. For an Array OTF map, the "Map Size" refers to the area that will be fully-sampled (i.e., the array width is added to the length of each scan). The Array OTF map should only be selected if the frequency falls within the tuning range of the LFA or HFA (see table above).

Using these inputs, the calculator evaluates scanning in both x- and y-directions, and selects the direction that has fewer scan lines. It then estimates N_{on} using the length of the scans and a frequency-based receiver stability time. The step sizes assumed for each frequency band are: 3 arcsec for the HFA, 6 arcsec for the LFA, 25 arcsec for 4G1, 12 arcsec for 4G2, 8 arcsec for 4G3, and 5 arcsec for 4G4. Note that there are many ways to configure a mapping observation, and the calculated value of N_{on} is only one of many possible values. For an OTF Honeycomb, N_{on} should be set to 25.

For Raster maps: Enter the number of on positions that will be used for each reference position in the N_{on} field. You may ignore the Map Size and Map Type fields.

Signal to Noise Ratio / Integration Time
If the SNR radio button is selected, enter the desired signal to noise ratio in this field and the estimated line strength in the Brightness Temperature field. The time estimator will calculate the integration time required to reach this SNR. If the Integration Time radio button is selected, enter the integration time (in seconds) for your observation. If your observation is a Total Power OTF map or a Total Power raster map, enter the effective on-source exposure time per map point. Otherwise, enter the ON+OFF integration time. The time estimator will calculate the 1-sigma rms sensitivity (in units of T_R^*) based on the input integration time.

Brightness Temperature T_R^* (K)
Enter the estimate of the peak brightness temperature of your line. This field is only used if the SNR radio button is selected (see above). As is the case for other heterodyne receivers that use hot and cold loads to measure the receiver temperature, the intensity units are Kelvin (K). The intensity scale used in the online tool is brightness temperature T_R^*. This relates to the measured antenna temperature as $T_R^* = T_A^* / \eta_{fss}$, and the

main beam temperature (corrected for losses in the side lobes) as $T_{MB} = T_A^* / \eta_{mb}$. The main beam efficiency has been measured from planetary observations, and has been determined to be 0.70 for the LFA and 0.63 for the HFA. For the latest 4GREAT main beam efficiencies, please contact the Help-Desk. A detailed description of the GREAT intensity calibration is given in Section 6.1.2.2, which also contains worked examples for different observing modes and unit conversions.

Source Velocity
Enter the source velocity (in km/s) in the Local Standard of Rest (LSR) reference frame.

Observer Velocity
Enter the velocity of the observatory with respect to the LSR on the date of the observation. If this is unknown, you may either leave the default (0 km/s) or enter the date, time, coordinates, and location for your observation to have the time estimator calculate the observer velocity automatically. Note that if your desired line rest frequency falls close to or in an atmospheric absorption feature, you may still be able to observe the line if you choose the right time of the year as the source is blue- or red-shifted relative to the atmospheric feature.

Return to Table of Contents

6.2.3 On The Fly Technical Details

The three On The Fly (OTF) mapping options are OTF mapping (also referred to as Classic OTF), OTF Array mapping, and OTF Honeycomb mapping. Each OTF Astronomical Observation Template (AOT) can be used with the two instrument configuration of GREAT: LFA H/V and HFA, and 4GREAT and HFA. However, please keep in mind that OTF Array and OTF Honeycomb maps are not designed to be used with the single pixel of 4GREAT. Otherwise, the parameters for OTF observing schemes are flexible and can be easily modified in USPOT depending on the needs of the project. The recommended parameters presented in this section should perform well for most mapping projects.

Any OTF AOT can be executed in Beam Switching (BSW) or Total Power (TP) mode. Some things to consider when deciding between these two modes are:

Efficiency
Maps obtained using BSW modes need an equal amount of integration time on the ON and OFF positions. In contrast, Total Power maps spend less time on the OFF position, and are therefore more efficient.

Baseline Stability
BSW observations generally have better baseline stability. If the source is expected to have faint and/or wide lines, then BSW modes should be preferred. If the source is expected to have bright and/or narrow lines, then the baseline quality is less of an issue.

Reference positions
For a BSW map, there needs to be an emission-free region on the sky that is the same size as the OTF map and within a few arminutes of the map. Finding such a reference position is often a challenge, especially in crowded regions or region with significant extended emission. For Total Power maps, only a single emission-free pointing is needed as a reference position, and it can be significantly farther away from the source (up to 30 arcmin, although baselines will be better for closer reference positions).

Return to Table of Contents

6.2.3.1 Coordinates and Array Geometry

Because upGREAT maps can be rotated relative to standard sky coordinates (e.g., J2000), they have their own coordinate system defined as x and y. With a map rotation of 0 degrees, the +x axis is aligned with the +RA axis, and the +y axis is aligned with the +Dec axis (Fig. 6-2). The map rotation angle increases in the counter-clockwise

direction, and this parameter can be set anywhere between -360° to +360°. For OTF maps, scans in the x-direction are parallel to the x-axis, and scans in the y-direction are parallel to the y-axis.

Figure 6-2.

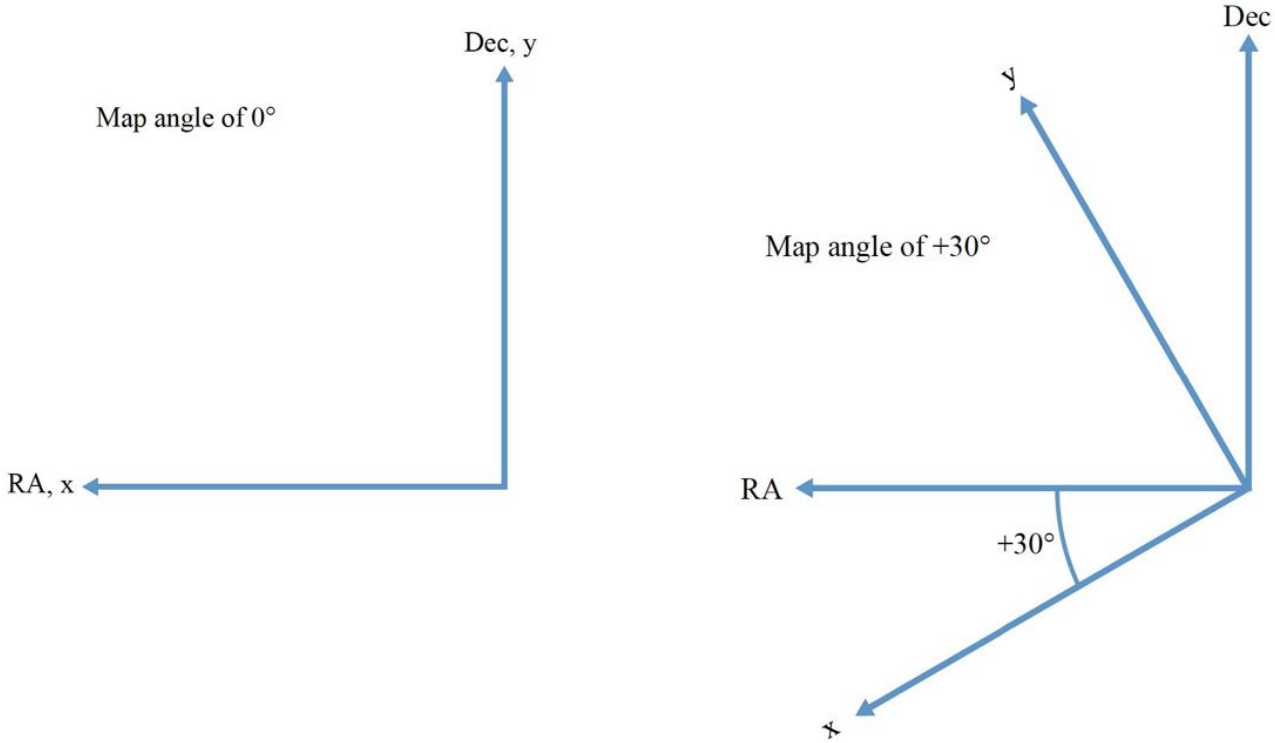

28 Figure 6-2. Left, The x/y map coordinate system is aligned with RA/Dec (J2000) for a map angle of 0°. Right, The x/y coordinate system at a map angle of +30°. The angle is measured in the counter-clockwise direction.

The upGREAT Low Frequency Array (LFA) and High Frequency Array (HFA) are arranged in a hexagonal pattern with a central beam. The spacings between the beams are approximately 2 beam widths (31.7 arcsec for the LFA, 13.8 arcsec for the HFA). For efficient mapping, the array is typically rotated by 19.1 degrees relative to the scan direction, resulting in a projected pixel spacing of 10.4 arcsec for the LFA and 4.6 arecsec for the HFA (see Fig. 6-3). The array can be rotated independently of scanning direction for maximum flexibility during observation planning.

Figure 6-3.

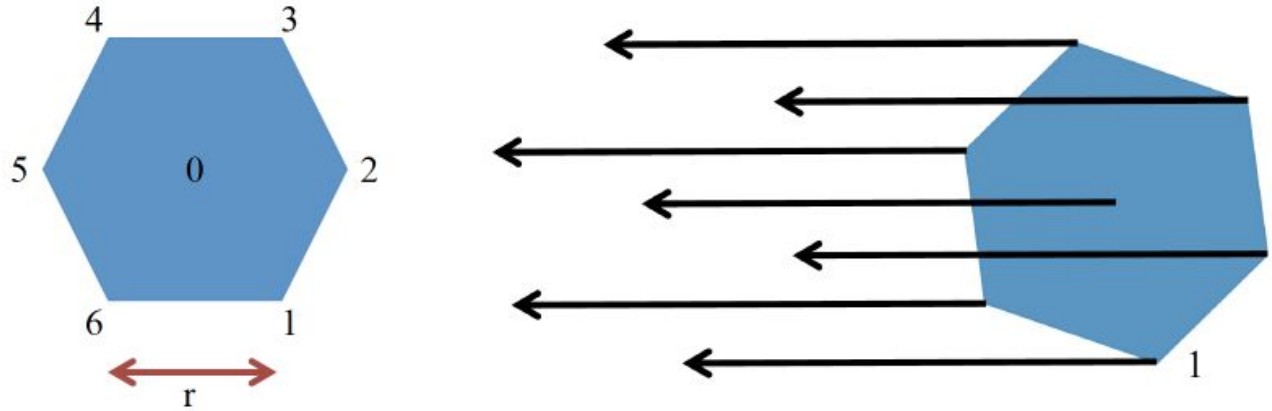

29 Figure 6-3. Left, The configuration of an upGREAT array. The numbers 0-6 mark the pixel numbers of the array, and the separation between the pixels, r, is 31.7 arcsec for the LFA, and 13.8 arcsec for the HFA. Right,

An upGREAT array, rotated by -19.1° (pixel 1 is labeled) with arrows indicating the scan direction. The projected pixel spacing perpendicular to the scan direction is 10.4 arcsec for the LFA, and 4.6 arcsec for the HFA.

When creating a mapping strategy, observers will have to weigh many factors such as the area to be mapped, the required integration time per point, and of course the scientific objectives. Examples given in Section 6.2.3.2, Section 6.2.3.3, and Section 6.2.3.4 aim to provide guidelines

Figure 6-4.

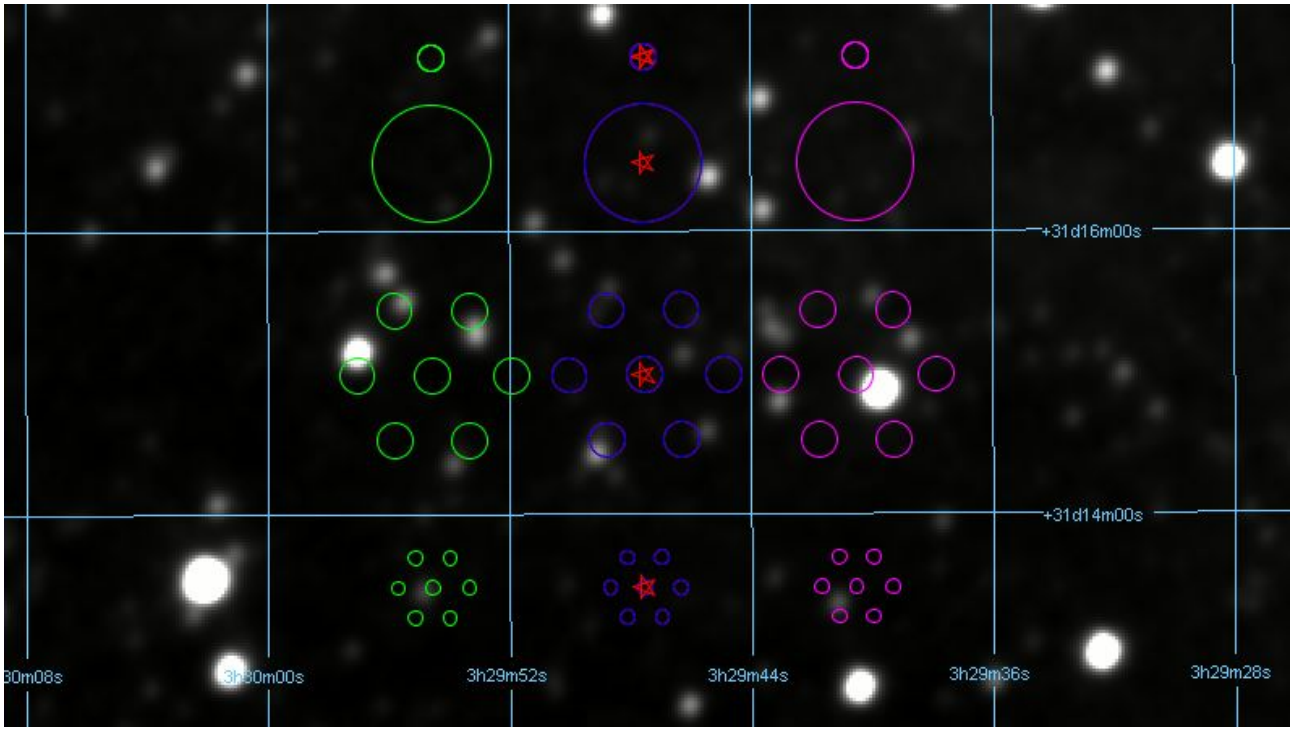

30 Figure 6-4. Comparison of the footprints for each GREAT array. From top to bottom: 4G4, 4G1, LFA, and HFA. This example shows an on-sky visualization of each array using USPOT and Single Point AOTs in Dual Beam Switching mode. The red stars identify the central position for each array, and the blue circles represent their on-source footprints. The green and magenta circles respectively show the two reference positions.

Return to Table of Contents

6.2.3.2 OTF Mapping

The classic OTF mapping can be used effectively with any of the GREAT arrays. For an OTF mapping, each array pixel creates a fully-sampled rectangular map based on the step size along the scan row and the spacing between each row. For the upGREAT arrays (LFA and HFA), the result is seven overlapping rectangular maps (see Section 6.2.3.2a and Section 6.2.3.2b). Classic OTF mapping is currently the only available OTF AOT that can create fully-sampled maps using the single-pixel 4GREAT array.

Return to Table of Contents

6.2.3.2a LFA OTF mapping

In this example, we design an OTF map in Total Power mode to measure [CII] 158 µm line emission in NGC 1333 using the LFA as the primary array. The final map is composed of 14 fully-sampled maps of the central region combining both the LFAH and LFAV polarizations. The step size in the x-direction and the y-direction are set to 6

arcsec. Both the number of steps per row and the number of rows are both set to 60, which provides a 360 arcsec-wide square map (see Fig. 6-5). The array rotation is set to -19.1 degrees.

The on-source exposure time per point is 0.5 s, and so each row scan is completed in 30 s. The time spent on the off-position before each scan is therefore 3.9 s, and so the on+off time for each scan is 33.9 s. For 60 rows, the total integration time for the map is 33.9 minutes, and the total observing time including overheads is approximately 67.8 minutes. For a single coverage of the map, the effective integration time per point for the central region will be T_{on} = 1 x 2 x 7 x 0.5 s = 7 s. Using the GREAT time estimator in SITE, we find a RMS temperature ΔT_R^* of 0.43 K assuming a resolution of 1 km/s, a line width of 10 km/s, an altitude of 41,000 ft, and an elevation of 40 degree.

Figure 6-5.

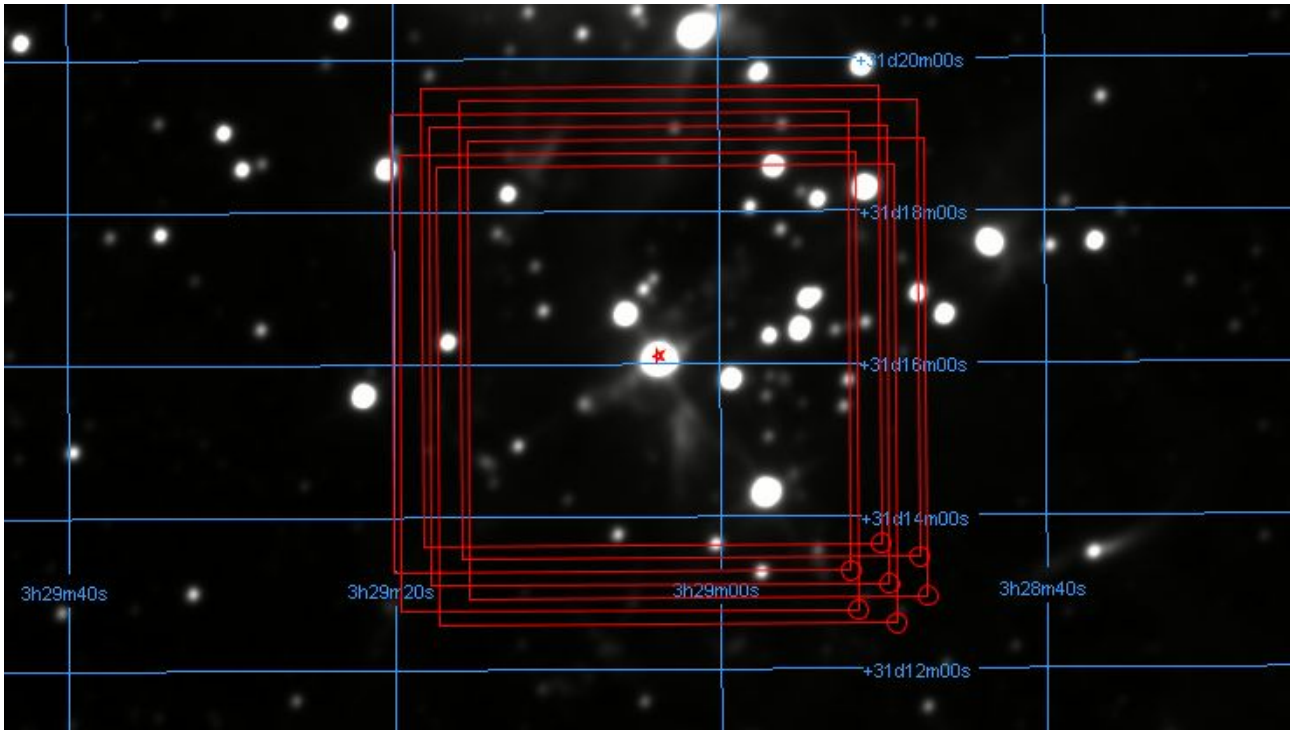

31 Figure 6-5. Overlay of an OTF map designed for the LFA+HFA configuration. The primary array is the LFA. Each red rectangle shows the region mapped by one of the LFA pixels. The footprint of the array is shown by the red circles and marks the starting position of the map. The central region of the map is covered once by each pixel of the array. In this configuration, the HFA will produce a significantly under-sampled map due to the large step size (6 arcsec).

Return to Table of Contents

6.2.3.2b 4GREAT and HFA OTF mapping

In this example, we design an OTF map in Total Power mode of the same region as previously. This time we plan to measure the [OI] 63 µm line with the HFA and the ^{12}CO J=22-21 line with 4G4. All 4GREAT receivers observe simultaneously, but we choose 4G4 for this example because it has the closest beam size (9.9 arcsec) to the HFA (5.2 arcsec). The final results will be 7 fully-sampled [OI] maps of the central region with the HFA and one over-sampled CO map with 4G4. The step size in the x-direction and the y-direction are set to 3 arcsec. Both the number of steps per row and the number of rows are both set to 60, which provides a 180 arcsec-wide square map (see Fig. 6-6). The array rotation is set to -19.1 degrees.

The on-source exposure time per point is 0.3 s, and so each row scan is completed in 18 s. The time spent on the off-position before each scan is therefore 2.3 s, and so the on+off time for each scan is 20.3 s. For 60 rows, the total integration time for the map is 20.3 minutes, and the total observing time including overheads is approximately

40.6 minutes. For a single coverage of the map, the effective integration time per point for the central region will be T_{on} = 1 x 1 x 7 x 0.3 s = 2.1 s for the HFA and T_{on} = 1 x 1 x 1 x 0.3 s for 4G4. Using the GREAT time estimator in SITE with a resolution of 1 km/s, a line width of 10 km/s, an altitude of 41,000 ft, and an elevation of 40 degree, we find a RMS temperature ΔT_R^* = 0.9 K for [OI] 63 µm and ΔT_R^* = 5.4 K for ^{12}CO J=22-21.

Figure 6-6.

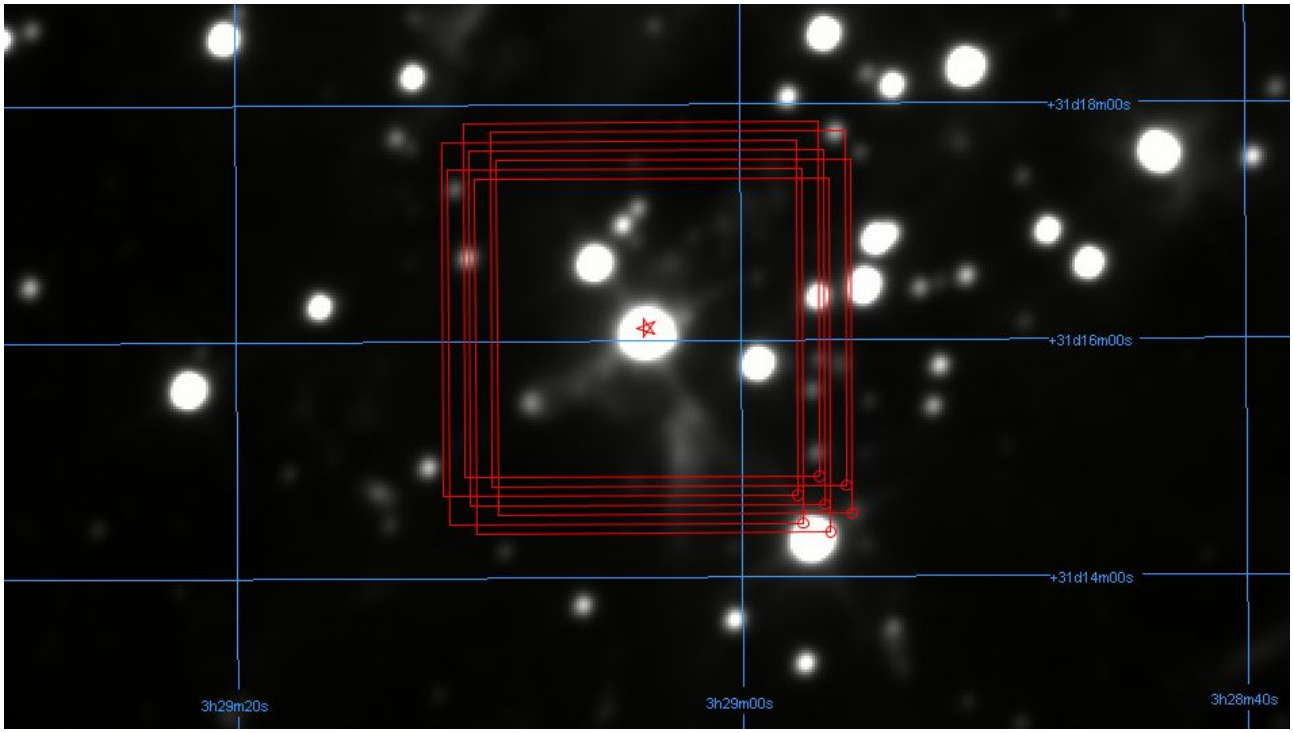

32 Figure 6-6. Overlay of an OTF map designed for the 4G+HFA configuration. The primary array is the HFA. Each red rectangle shows the region mapped by one of the HFA pixels. The footprint of the array is shown by the red circles and marks the starting position of the map. The central region of the map is covered once by each pixel of the HFA, as well as by the single pixel of 4GREAT. In this configuration, the resulting 4GREAT maps will be significantly over-sampled due to the small step size (3 arcsec). USPOT can only show the HFA visualization when using the 4G+HFA instrument configuration.

Return to Table of Contents

6.2.3.3 OTF Array Mapping

The basic unit of the upGREAT array mapping scheme is referred to as a block, which consists of a single or multiple scans of the same length, in the same direction (Fig. 6-7). For both the LFA and the HFA, the projected pixel spacing (after rotating the array by -19.1 degrees) is such that a single scan results in an under-sampled map. To create a fully sampled map, it is necessary to make at least one more scan to fill in the gaps between pixels. The default behavior is to make a second scan, creating a fully sampled map and completing the block. It is possible, however, to scan only a single time (creating an under-sampled map), or more than two times (creating an over-sampled map), depending on the goals of the project.

Figure 6-7.

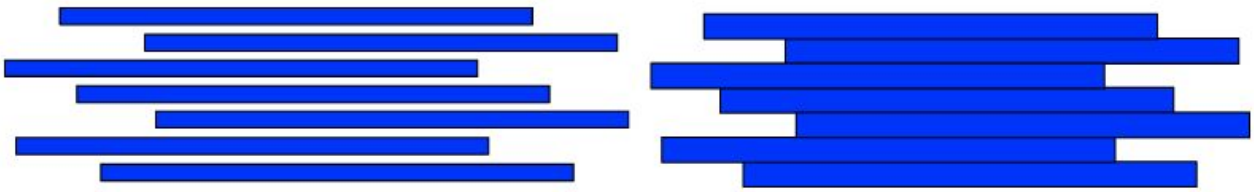

33 Figure 6-7. Left, A block that consists of a single scan of the rotated array. The gaps between the scans indicate an under-sampled map. Right, A block that consists of two scans. This block is fully sampled in the direction perpendicular to the scan direction. The second scan fills in the gaps in the single-scan block.

A single map can consist of any number of blocks, and can scan in the x- or y- direction, or both. The parameters of the x- and y-direction scans are independent, but can be used in concert to create fully-sampled maps of a region in both directions (Fig. 6-8). Scanning in both directions helps to minimize striping effects that can be caused by the different characteristics of individual array pixels.

Figure 6-8.

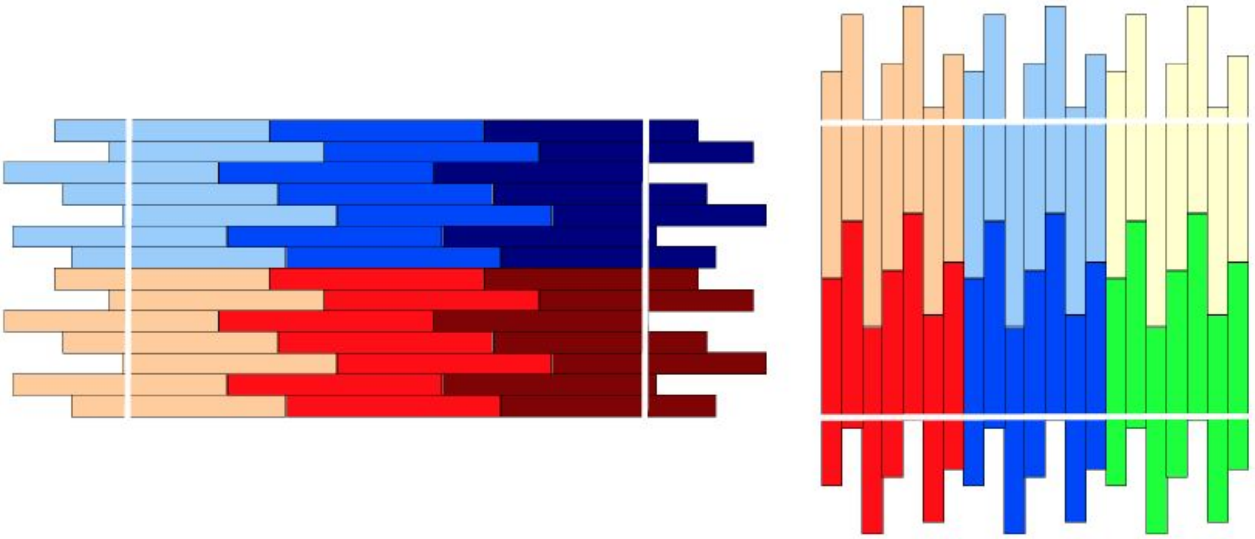

34 Fig. 6-8. Left: A map composed of six blocks scanning in the x-direction. There are three blocks along the scan direction, and two blocks perpendicular to the scan direction. The region within the two vertical white lines shows the inner coverage region. Right: A map composed of six blocks scanning in the y-direction. There are two blocks along the scan direction, and three blocks perpendicular to the scan direction. The region within the two horizontal white lines shows the inner coverage region. Maps scanning in both directions can be set up so that the central regions of each map align.

To calculate the size of the inner coverage region along the scan direction:

inner coverage = [(block length) * (# of blocks in scan direction) – 1] * (array size)

where block length is in units of the array size.

To calculate size of the inner coverage region perpendicular to the scan direction:

inner coverage = (# of blocks perpendicular to scan direction) * (array size)

Because of the flexibility of this mapping scheme, there can be multiple ways to observe the same region. For example, the two setups in Fig. 6-9 fully cover the same area. Some important factors to consider to differentiate thse options are the desired integration time per point, the step size, and the duration of a single scan.

Figure 6-9.

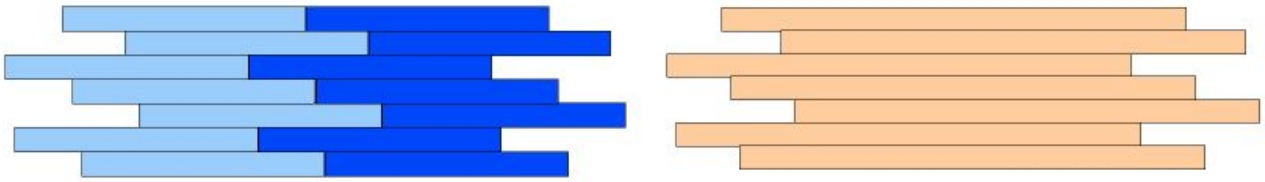

35 Figure 6-9. Left: A map consisting of two blocks, each one 2*(array width) long. Right: A map consisting of a single block that is 4*(array width)-long. The total inner coverage for both maps is the same.

Return to Table of Contents

6.2.3.3a LFA OTF Array mapping

In this example, we design an OTF Array map in Total Power mode to measure [CII] 158 µm line emission in NGC 1333 using the LFA as the primary array. The final map is composed of 2 horizontal and 2 vertical blocks to cover the region of interest (see Fig. 6-10), which are covered by both polarization of the LFA. The parameters in USPOT for this setup are 1 block in the scan direction and 2 blocks perpendicular to the scan direction for both the x and y scans. Each block has a width of 3 arrays, the array is rotated by -19.1 degrees, and the number of lines per block is 2 (which gives a fully-sampled map).

The on-source exposure time per point is 0.5 s, and so each row scan is completed in 21 s. The time spent on the off-position before each scan is therefore 3.2 s, and so the on+off time for each scan is 24.2 s. For each block of two rows, the total integration time for the map is 48.4 s, and the total observing time including overheads is approximately 96.8 s. The total observing time for all four blocks is therefore 6.5 minutes. For a single cycle of the OTF Array map, each position in the central region of the map is going to be covered once in each scan direction. The effective integration time per point for the central region will therefore be T_{on} = 1 x 2 x 2 x 0.5 s = 2 s. Using the GREAT time estimator in SITE, we therefore find a RMS temperature ΔT_R^* of 0.8 K assuming a resolution of 1 km/s, a line width of 10 km/s, an altitude of 41,000 ft, and an elevation of 40 degree.

Figure 6-10.

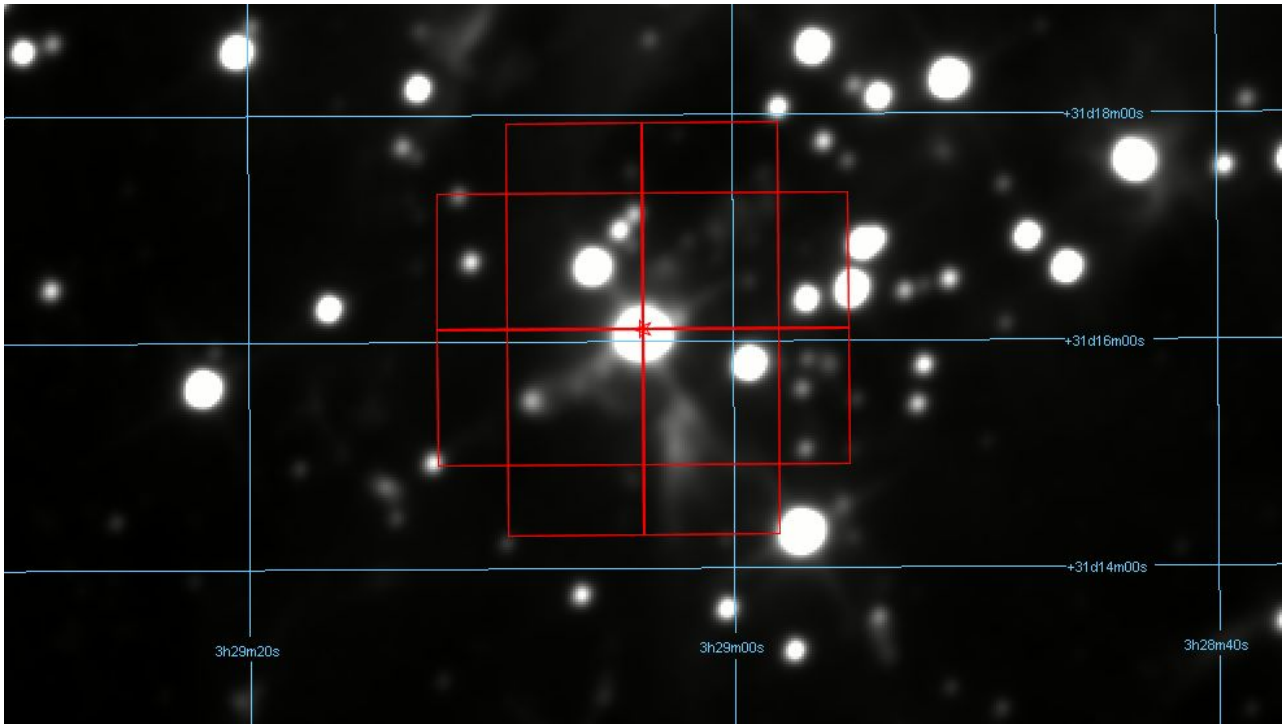

36 Figure 6-10. Overlay of an OTF Array map in the LFA+HFA configuration. The primary array is the LFA. Each red rectangle shows one of the array blocks described in Section 6.2.3.3. In this configuration, the HFA will

produce a significantly under-sampled and inhomogeneous map due to the large step sizes and tiling based on the LFA array size.
Return to Table of Contents

6.2.3.4 OTF Honeycomb Mapping

The OTF Honeycomb mapping AOT can be used to map an area comparable in size to one of the GREAT receiver arrays (HFA or LFA). The resulting map is fully-sampled at the resolution of the respective array. The OTF Honeycomb mappint is optimized for such small maps by avoiding not fully covered edges common to the other two OTF modes.

In this OTF mode, the telescope moves while integrating not in a straight line, but instead by spiraling in a 25-point hexagon pattern filling in the space between the pixels of the array. Figure 6-11 shows this pattern for all pixels, thus illustrating how all pixels combined completely fill the mapping area.

Figure 6-11.

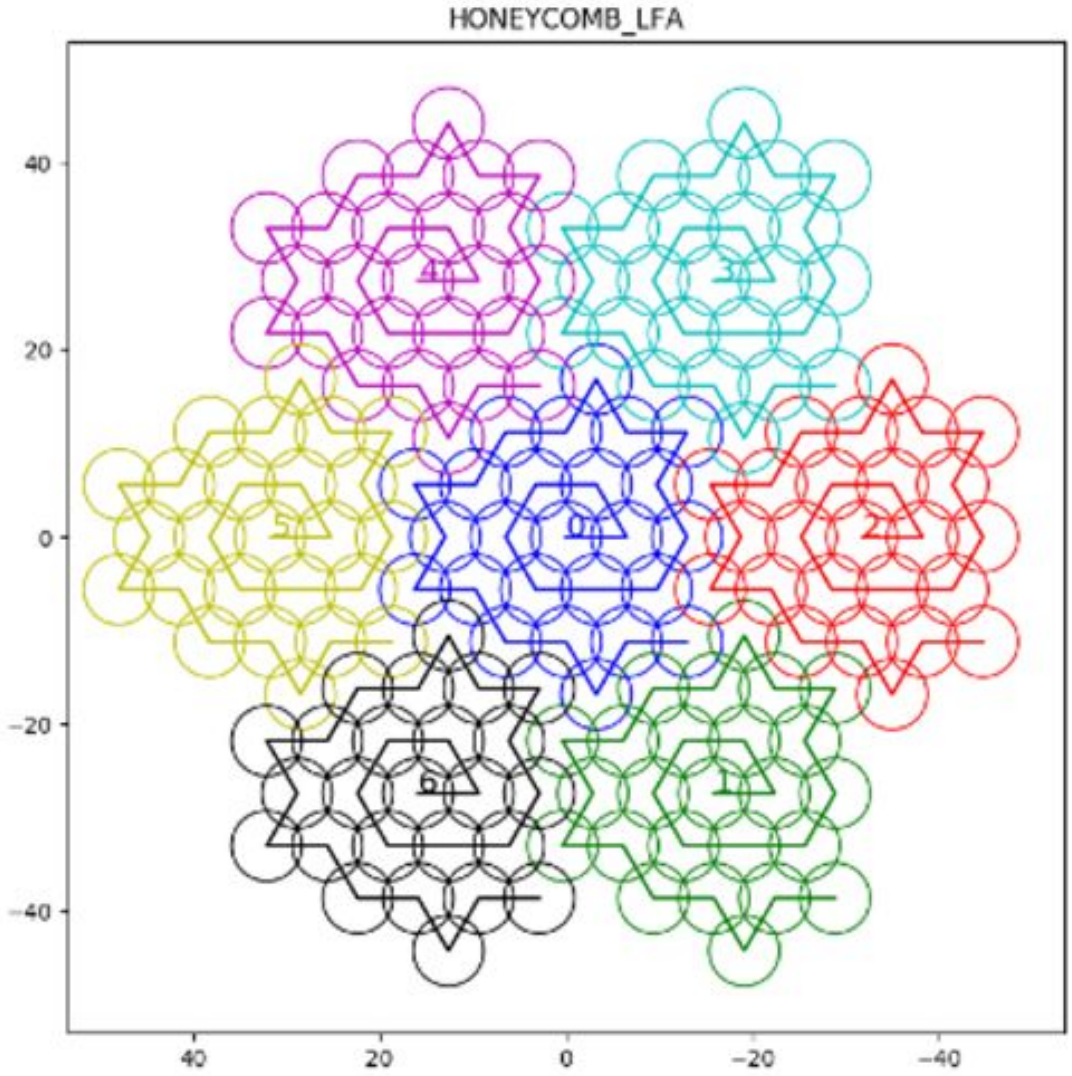

37 Figure 6-11. Honeycomb pattern for the LFA with all pixels showing how the pointings mesh together. The units of the axes are in arcseconds. The patter for the HFA will be a factor of 2.7 smaller since the pattern scales with the array size.

When executing an OTF honeycomb map with the HFA in tha LFA+HFA configuration, the LFA will produce 7 small oversampled maps centered around each LFA pixel locations, with gaps between each of these small maps. Alternatively, when executing an OTF honeycomb map with the LFA, the HFA will produce a sparse map the size of the LFA mapping area.

When planning an OTF honeycomb map, one needs to select the Time Per Point so that one OTF scan, the 25-point pattern, does not take longer than 20 or 30 seconds, for an HFA or LFA map respectively. Each location in the mapping area will be covered only once by one pixel (two for the LFA, if both polarization of the LFA are tuned to the same frequency). Repeat the 25-point pattern (the cycle parameter in USPOT) as often as necessary to reach the integration time per map position estimated with SITE.

The OTF honeycomb pattern can also be tiled, though ideally do not tile more than a few tiles at once; larger maps are covered more efficiently when using the other OTF modes. Each honeycomb tile requires its own AOR, and tiling can be done by offsetting the next tile from the first by moving the AOR center by the following vector (±2.5, ±0.866). The unit of this separation vector is in array sizes, and the angular size is obtained by multiplying it with 31.7 arcsec for the LFA, and 13.8 arcsec for the HFA. Rotate the vector by 60 degrees for adjacent tile positions and/or extend the map in the same way from a new AOR center. Below is an illustration of such a tiling with eight tiles. In practice, please consider the other OTF maps modes for such a large mapping area.

Figure 6-12.

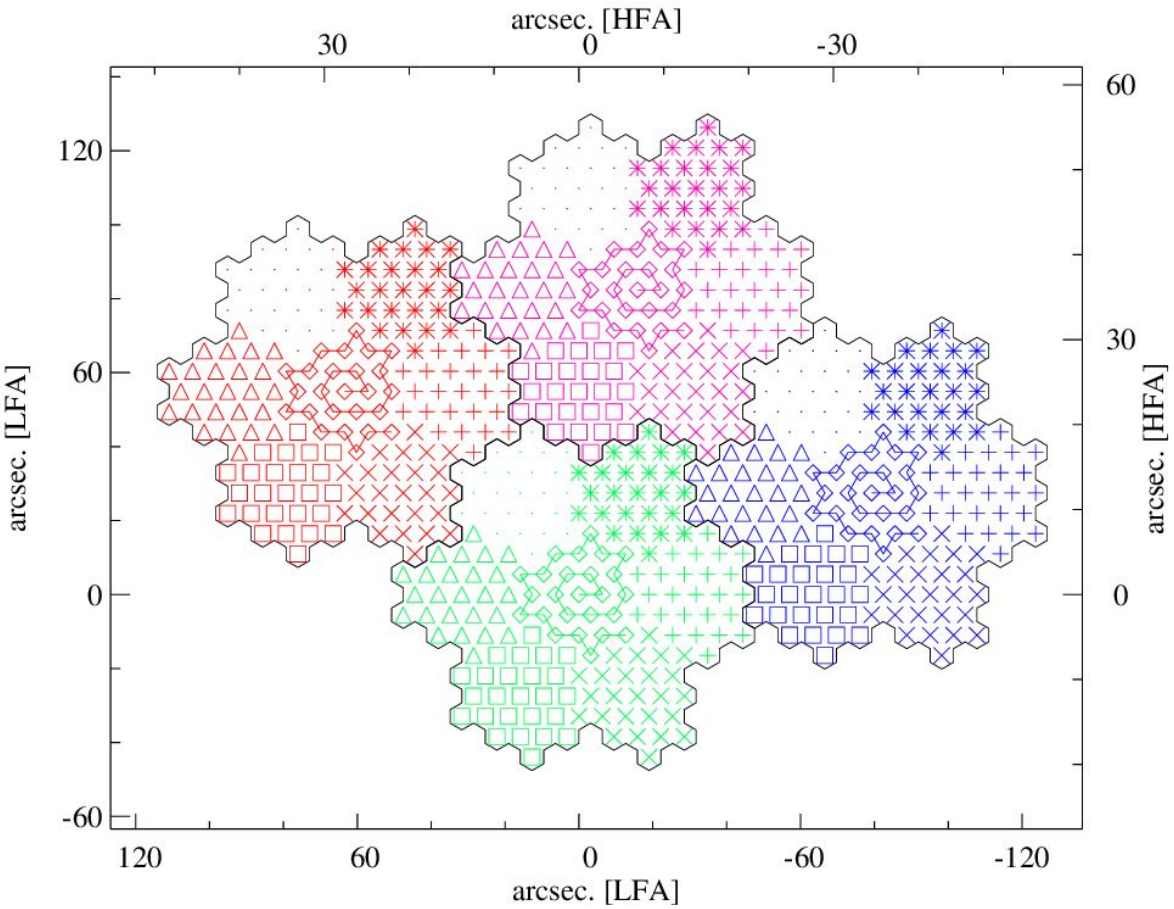

38 Figure 6-12. How a honeycomb map is tiled: Each symbol is a different pixel, each color is a different tile. The snowflake-shaped outline is how each AOR is visualized in USPOT. The left and bottom axes show the size of the tiling for the LFA, and the right and top axes show the size of the tiling for the HFA. The offset of each honeycomb tile is given in Table 6-2.

Table 6-2

Example of Honeycomb Tiling Offsets

	LFA	HFA
Tile 0	(0”,0")	(0”,0")
Tile 1	(-79.25”,+27.45")	(-34.50”,+11.95")

	LFA	HFA
Tile 2	(-15.85”,+82.36”)	(- 6.90”,+35.85”)
Tile 3	(+63.40”,+54.91”)	(+27.60”,+23.90”)

Return to Table of Contents

6.2.3.4a LFA OTF Honeycomb mapping

In this example, we design an OTF Honeycomb map in Total Power mode to measure [CII] 158 µm line emission in NGC 1333 using the LFA as the primary array. The final map is composed of the 4 individual tiles defined in Fig. 6-13 to cover the region of interest (see Fig. 6-13), which are covered by both polarization of the LFA. The parameters in USPOT for each tile are a pattern angle of 0.0 degrees and the Target Offset RA and Target Offset Dec values defined in Table 6-2 for the LFA.

The on-source exposure time per point is 1.0 s, and so each tile is completed in 25 s. The time spent on the off-position before each scan is therefore 5.0 s, and so the on+off time for each scan is 30.0 s. The total observing time including overheads is approximately 120 s. The total observing time for all four tiles is therefore 8 minutes. For a single cycle of the OTF Honeycomb map, each position in the central region of the map is going to be covered once during the scan. The effective integration time per point for the central region will therefore be T_{on} = 1 x 1 x 2 x 1.0 s = 2 s. Using the GREAT time estimator in SITE, and using the Total Power OTF option with a N_{on} of 25, we find a RMS temperature ΔT_R^* of 0.8 K assuming a resolution of 1 km/s, a line width of 10 km/s, an altitude of 41,000 ft, and an elevation of 40 degree.

Figure 6-13.

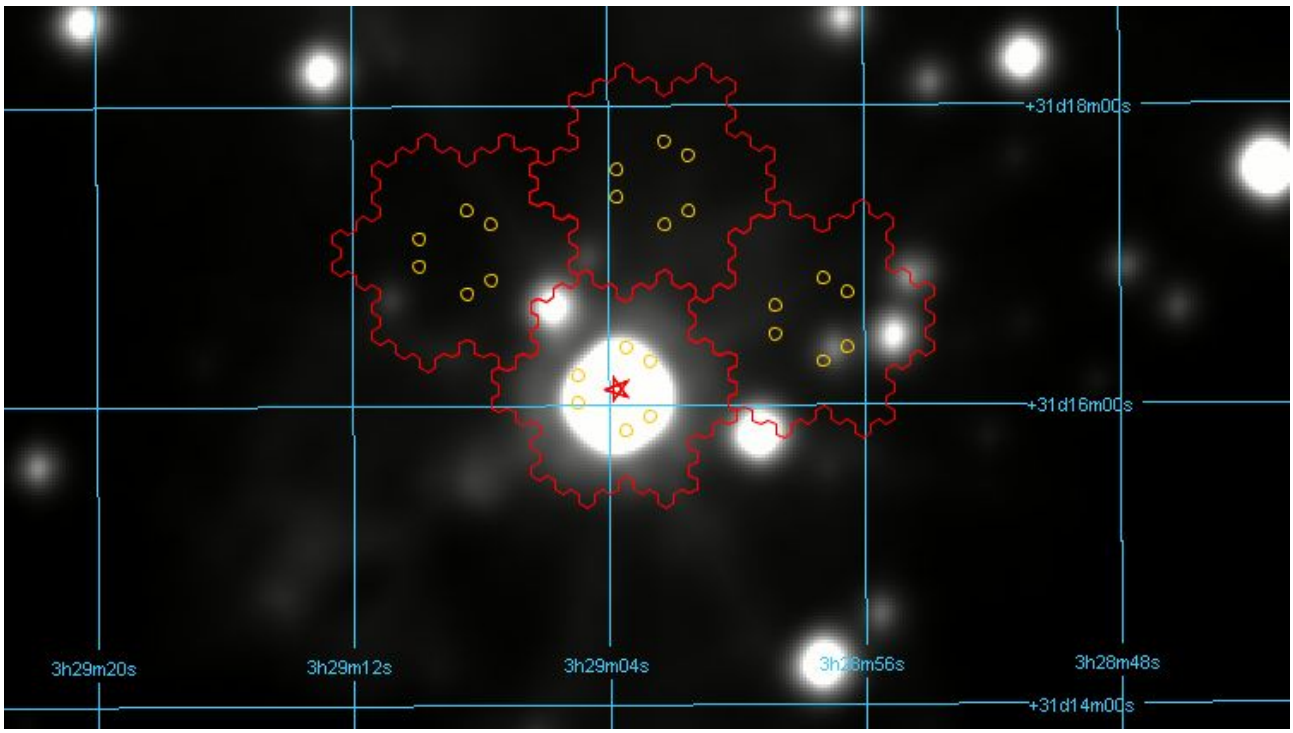

39 Figure 6-13. Overlay of 4 OTF Honeycomb tiles in the LFA+HFA configuration. The primary array is the LFA. Each "hexagon" one of the tiles described in Section 6.2.3.4. The yellow circles represent the corners of the

pattern drawn by the central pixel of the LFA. In this configuration, the HFA will produce an under-sampled and inhomogeneous map due to the large step sizes and tiling based on the LFA array size.
Return to Table of Contents

7. HAWC+

To export the handbook as a PDF, click on the three dots in the upper right, then choose "Export with Scroll PDF Exporter". In the Template drop-down menu, choose "Handbook Template", and then click "Export".

7.1 Specifications

7.1.1 Instrument Overview

The High-resolution Airborne Wideband Camera (HAWC+) is a multi-wavelength far-infrared imager and polarimeter with continuum bandpasses from 50 um to 240 um. HAWC+ Total Intensity Imaging uses a filter wheel and a polarizing grid to split incoming light into two orthogonal components of lineal polarization, the reflected (R) and transmitted (T) rays. For Imaging Polarimetry, a rotating half-wave plate (HWP) is introduced before the filter wheels. The current state of the instrument includes a 64x40 array measuring the R polarization state and a 32x40 array for the T polarization state. HAWC+ observations are diffraction-limited with a spatial resolution of 5 to 20 arcsec and a field of view (FOV) of ~2 to 10 arcmin.

HAWC+ will offer Band B (63 um) during cycle 9 as shared-risk observations for total intensity and polarization observations. Proposals requesting Band B should specify the scientific purpose.

HAWC+ will offer shared-risk observations using the experimental scan-polarimetric (OTFMAP-polarimetry) mode. Although the OTFMAP-polarimetric observations have been successfully applied to calibrators and points sources, this observing mode does not recover diffused faint extended emission from astrophysical objects. This effect may result on compromised data for some scientific goals. Proposal requesting OTFMAP-polarimetric observations should specify the scientific purpose and alternative science output incase this observing mode is not usable for their scientific goals

Return to Table of Contents

7.1.1.1 Design

A schematic of the HAWC+ optical design is shown in Figure 7-1. Prior to entering the HAWC+ cryostat, light from the SOFIA telescope enters the set of warm fore-optics. The light is reflected from a folding mirror to a field mirror, capable of imaging the SOFIA pupil at the cold pupil inside the HAWC+ cryostat. After the fore-optics, light enters the cryostat through a 7.6 cm diameter high-density polyethylene (HDPE) window, then passing through a cold

pupil on a rotatable carousel, a near-infrared blocking filters to define each bandpass and lenses designed to optimize the plate scale. The pupil carousel and the filter wheel are at a temperature of ~10 K. The carousel contains eight aperture positions, four of which contain half wave plates (HWPs) for HAWC+ bands, an open aperture whose diameter is matched to the SOFIA pupil, and three aperture options meant only for instrument alignment tests.

After the pupil carousel, the light passes through a wire grid that reflects one component of linear polarization and transmits the orthogonal component to the detector arrays (R and T arrays, respectively—see Figure 7-2). The polarizing grid is heat-sunk to the HAWC+ 1 Kelvin stage.

To perform polarimetry observations, a HWP matched to the band-pass is rotated (usually through four discrete angles) to modulate the incident light and allow computation of the Stokes parameters. The total intensity can be measured simply by removing the HWPs from the optical path and using the open pupil position, then summing the signal from the R & T arrays.

The 64x40 HAWC+ detector array is composed of two co-mounted 32x40 subarrays from NASA/GSFC and NIST. The detectors are superconducting transition-edge sensor (TES) thermometers on membranes with a wide-band absorber coating. The detector array is indium bump bonded to a matched array of superconducting quantum interference device (SQUID) amplifiers, all cooled to an operating temperature of ~0.2 K in flight.

Figure 7-1.

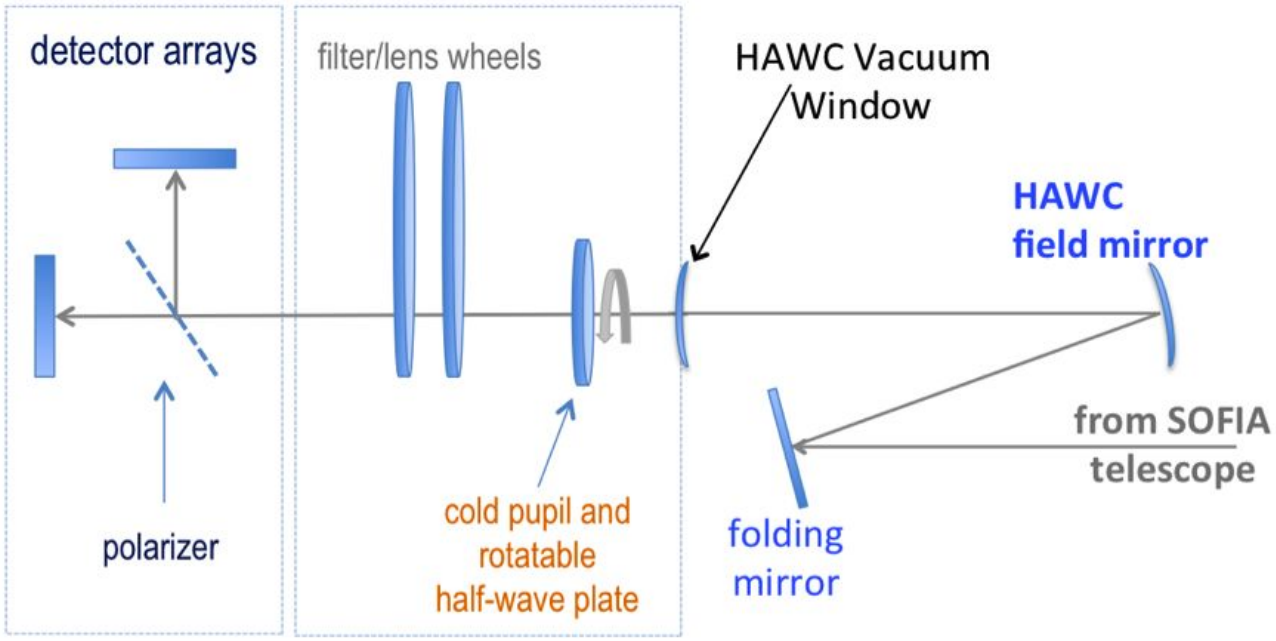

40 Figure 7-1. Schematic of the HAWC+ optics. Light from the SOFIA telescope is incident from the right. The field and folding mirrors are mounted on the HAWC+ cryostat but extend into the SOFIA Nasmyth tube. At the polarizing grid the light is split into two orthogonal components of linear polarization and detected at the two separate arrays.

Figure 7-2.

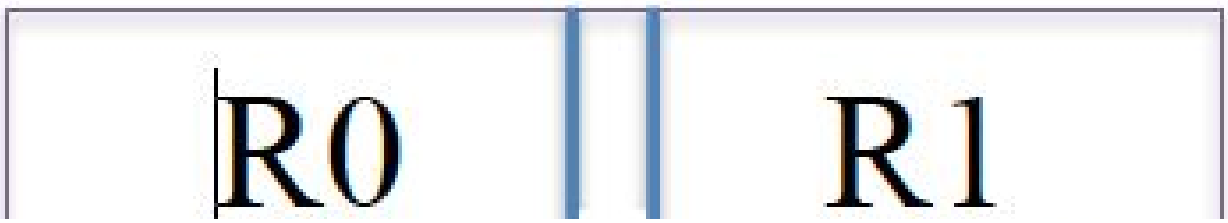

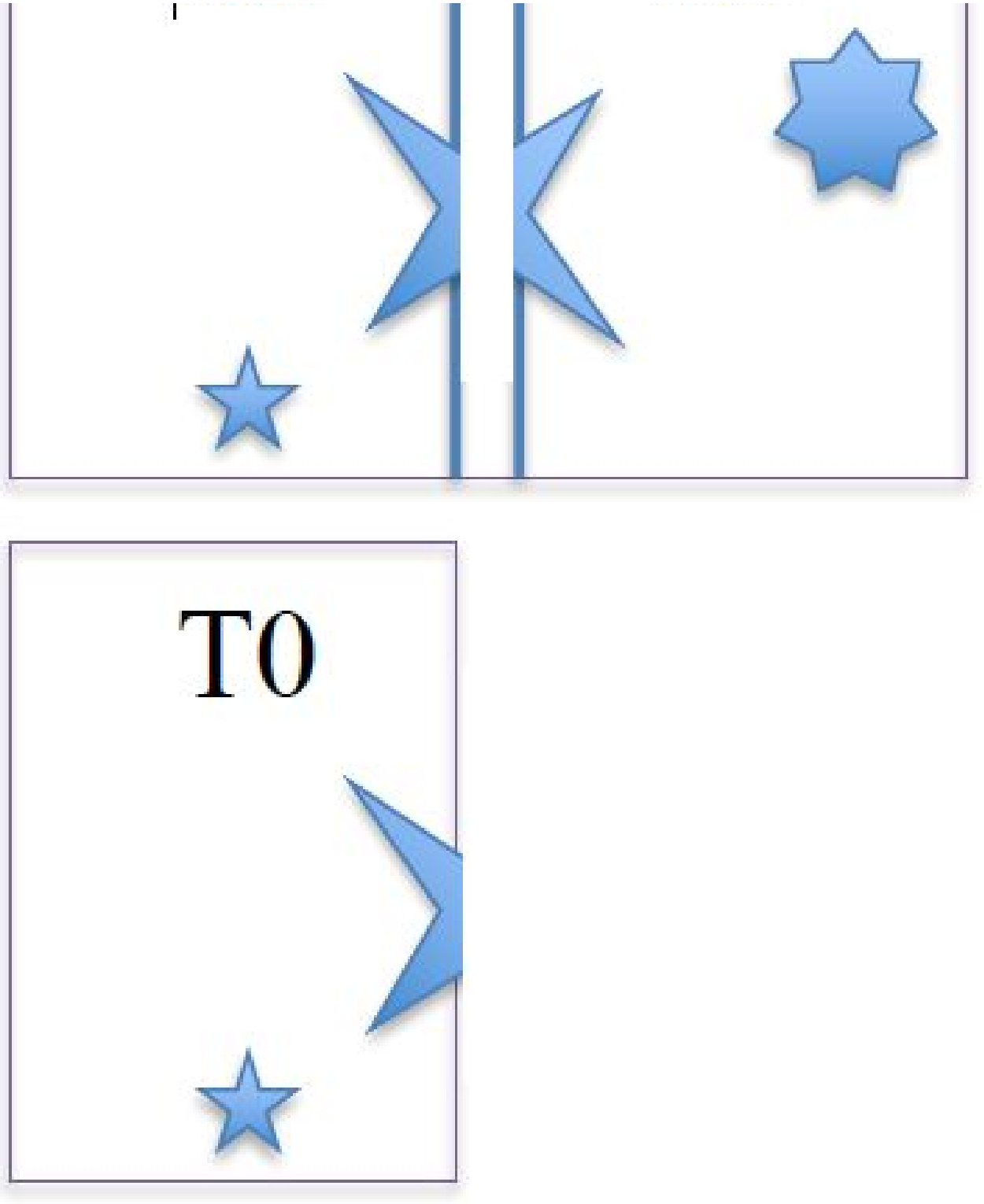

41 Figure 7-2. HAWC+ utilizes two coaligned arrays of TES detectors, each array receiving polarized light from the source either by reflection (the R array) or transmission (the T array). The R array is populated with two 32x40 subarrays separated by 2.0 pixels, referred to as R0 (top left) and R1 (top right). The arrays are coaligned such that R0 and T0 (bottom left) observe the same patch of sky. Polarization observations are only supported using the R0 and T0 subarrays, and therefore observations are limited to the left half of the

nominal field of view, or 32x40 pixels. Total intensity observations are supported using the combined R0 and R1 field of view, or 64x40 pixels with a 2.0 pixel gap between them.
Return to Table of Contents

7.1.2 Performance

The absorbing coatings on the HAWC+ detector arrays were optimized to produce about 50% efficiency across the wide (50–240 μm) range of bandpasses. The TESs were designed to optimize the sensor time constants and background power at which they saturate, with the goal being operation at both laboratory and stratospheric background levels. The final design includes a superconducting transition temperature of ~0.3 K and a detector yield of > 50%. Measurements of detector noise show that their contribution to total measurement uncertainties is negligible such that noise levels are dominated by background photons from the atmosphere.

Measurements of the HAWC+ optical system in the laboratory are consistent with optical models, *and flight data have confirmed that the observations are diffraction limited at all wavelengths.*

Table 7-1 shows the Full Width Half Maxiumum (FWHM) of each bandpass as measured using Gaussian profiles, the finite size of the HAWC+ detectors, and a convolution across the measured filter bandpasses. The Instrumental Polarization (IP) of HAWC+ at each band is shown in terms of the normalized Stokes parameters, q and u, which were estimated using the observations of planets during several observing runs on November 2016 and May 2017. The IP is mainly derived from the tertiary mirror of SOFIA with the position angle of polarization perpendicular to the tertiary mirror direction. The filter transmission curves (text tables) are available as a zip file or individually from Table 7-1.

For polarimetry observations, the current configuration of HAWC+ lacks a second T polarization state array; as such, the field of view is reduced to approximately half in the largest side of the array, providing a 32x40 pixel size rather than 64x40 pixels (the first element of the Field of View in Table 7-1*). Total intensity observations are unaffected and can use the whole field of view via the R polarization state.*

Important: The sensitivities in Table 7-1 account for overheads, including nod slew times, bracketing of internal calibrators, and gyro drift checks. Sensitivities provided by the SOFIA Instrument Time Estimator (SITE) only account for on-source time (i.e. integrating time of the source in the FOV of HAWC+); the total overheads of the observations will be provided through the Unified SOFIA Proposal and Observation Tool (USPOT) after entering the sensitivity values produced by SITE.

Table 7-1: Instrument Characteristics

Parameter	Units	Band A	Band B	Band C	Band D	Band E
Mean Wavelength (λ_0)	μm	53	63	89	154	214
Bandwidth ($\Delta\lambda$)	-	8.70	8.90	17.00	34.00	44.00
Filter Width ($\Delta\lambda/(\lambda)$	-	0.171	0.15	0.194	0.219	0.204
Beam Size (FWHM)	arcsec	4.85	10.5	7.8	13.6	18.2

Parameter	Units	Band A	Band B	Band C	Band D	Band E
Pixel Size[a]	arcsec	2.55	4	4.02	6.90	9.37
Total Intensity FOV	arcmin	2.8x1.7	4.2x2.7	4.2x2.7	7.4x4.6	8.4x6.2
Polarimetry FOV	arcmin	1.4x1.7	2.1x2.7	2.1x2.7	3.7x4.6	4.2x6.2
NESB[b] (photo)	MJy sr^{-1} $h^{1/2}$	18.8	11.4	6.3	1.6	0.8
MDCF[c]	mJy	250	400	300	260	230
Mapping Speed[d]	See footnote [d]	0.0027	0.0290	0.029	1.10	7.0
MDCPF[e]	Jy	80	150.0	50	50	50
IP[f]	q	-0.0154	See footnote[f]	-0.0151	0.0028	-0.0129
	u	-0.0030	See footnote[f]	0.0090	0.0191	0.0111
MIfP[g]	MJy sr^{-1} $h^{1/2}$	28,000	17,000	6,000	2,000	1,300
Response Curve		png file txt file	png file txt file	png file txt file	png file txt file	png file txt file

[a] The center-to-center spacing of the pixels; pixel sizes (the space taken up by the photon sensitive area) are smaller by 0.21 arcsec at 53 µm and 0.75 arcsec at 215 µm.

[b] Noise Equivalent Surface Brightness for S/N = 1 into a single HAWC+ beam (FWHM given here).

[c] Minimum Detectable Continuum Flux for a point source with S/N = 4 in a 900 second integration.

[d] Real scan rate required to achieve a given an NESB. Units: $arcmin^2$ h^{-1} $(MJy\ sr^{-1})^{-2}$

[e] Minimum Total Continuum Flux for a point source required to measure the polarization fraction to an uncertainty level of $\sigma p < 0.3\%$ with a SNR (in the polarization fraction)≥4 in 900s.

[f] Instrumental Polarization estimated using the observations of planets during several observing runs. The uncertainty of the instrumental polarization is smaller than 0.003 in both Stokes q and u. IP for Band B is still TBD.

[g]Minimum total Intensity required to measure Polarization (MIfP) to an uncertainty level $\sigma_p \leq 0.3\%$. All chop/nod and polarization overhead values have been applied to this value.

HAWC+ point source sensitivities were updated on June 2, 2017 and the values given here are based on the in-flight performance of the instrument. Note that values used in previous SOFIA observing cycles (Cycles 4 & 5) were estimates that contained an overestimated point source sensitivity by approximately a factor of two, so proposals should be updated accordingly for Cycle 8 before submission.

Band B (63 μm) will be under commissioning during Cycle 7 and is offered as shared-risk observations during Cycle 8 and 9. (Instrumental Polarization (IP) for Band B will be estimated during Cycle 8.) Historically, this band has suffered of oversaturation effects that render it unusable but a cold aperture has been installed to minimize the saturation effects. Proposals requesting Band B should specify the scientific purpose and alternative science output in case this band is not usable.

Return to Table of Contents

7.1.2.1 Filters

HAWC+ can produce images using continuum bandpasses in either Total Intensity Imaging or Imaging Polarimetry configurations. In Imaging Polarimetry, the dual-beam nature of HAWC+ allows for the simultaneous measurement of both orthogonal lineal polarization components and obtain the Stokes parameters I, Q, and U. In Total Intensity Imaging, the sum of the R and T arrays provides the total intensity, Stokes I. As the HWP are used in Imaging Polarimetry, there is a slight loss of sensitivity as the HWP transmission is < 100% and additional overhead is required to account for rotating the HWP.

Both observing modes can utilize any one of the five available filters (including Band B offered as shared-risk during Cycle 9). Figure 7-3 shows transmission profiles including all filters for all bandpasses. The effective wavelengths and bandwidths averaged over the total filter transmission are given in Table 7-1.

Figure 7-3.

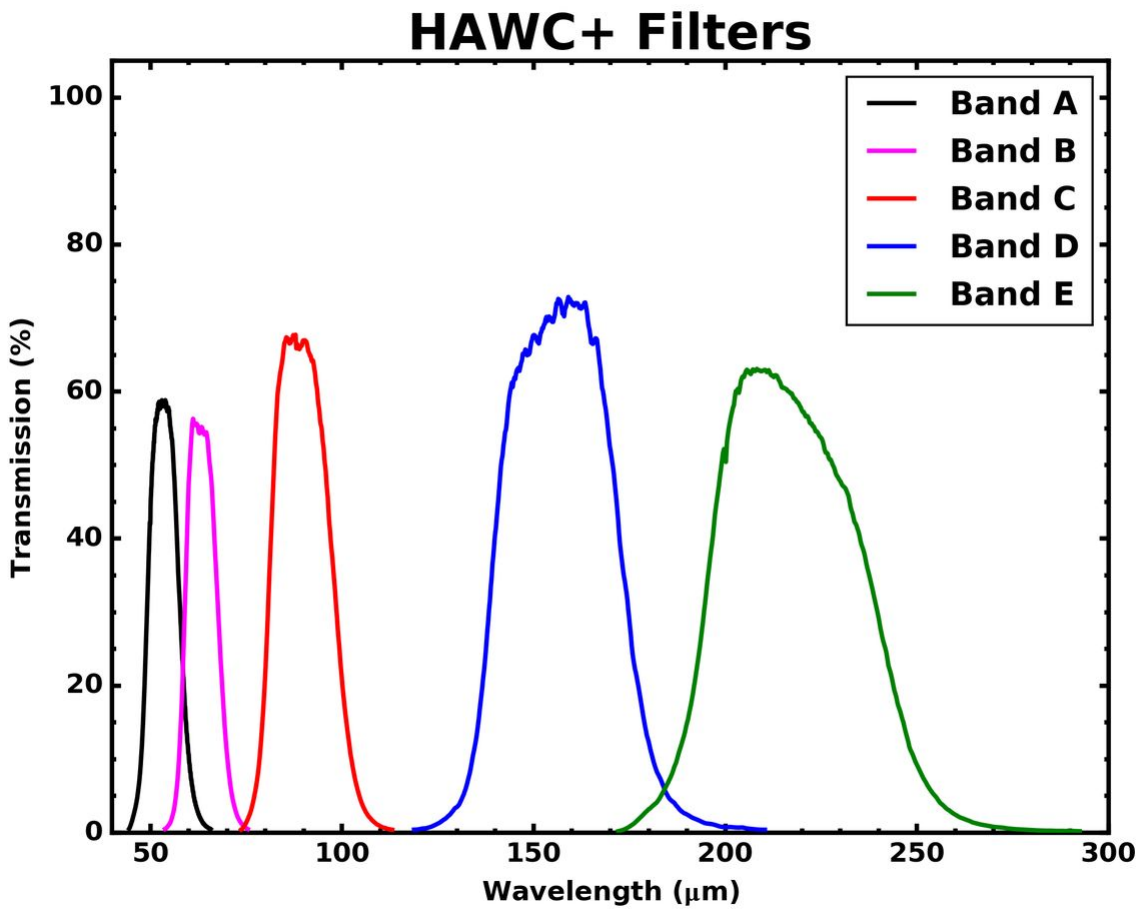

42 Figure 7-3.
Return to Table of Contents

7.1.2.2 Total Intensity Imaging Sensitivities

The equations provided below are included for informational purposes only, and should *not* be entered into USPOT. Integration times calculated using the equations below include overheads, and USPOT already adds the telescope overheads into the exposure times entered. For USPOT entries use SITE, which only takes into account on-source time.

Observations with HAWC+ for measurements of Total Intensity can be performed using either on-the-fly scanning (OTFMAP, where the telescope moves continuously at rates of ~10–200 arcsec/second without chopping of the secondary mirror) or using rapid modulation (chopping ~ 5–10 Hz) of the secondary accompanied by slow nodding of the telescope. The chopping option consists of a two-position chop, parallel to the nod direction where the chop amplitude matches the nod amplitude (NMC). However, we strongly encourage using OTFMAP mode for total intensity observations, which provides better sensitivity and lower overheads for an overall superior observing efficiency.

Table 7-1 presents HAWC+ imaging sensitivities for point sources, surface brightness, and mapping speed through each bandpass. Surface brightness is measured in units of MJy/sr and is the intensity required for a S/N = 1 observation in a one-hour integration time averaged over a single HAWC+ beam. The Minimum Detectable Continuum Flux into a HAWC+ beam is that needed to obtain a S/N = 4 in 900 seconds of on-source integration time.

HAWC+ time estimates should be made using the on-line exposure time calculator, SITE. Note that integration times scale as shown in Equation 7-1 and Equation 7-2 from the values in Table 7-1:

(Eq. 7-1)

(1)

$$t = \left(\frac{\mathrm{NESB}}{\sigma} \right)^2$$

(Eq. 7-2)

(2)

$$t = (900\ \mathrm{s}) \left(\frac{\mathrm{NESB}}{\sigma} \right)^2$$

where t is the integration time and σ is the desired sensitivity for S/N = 1, each in the appropriate units. For OTFMAP, a useful sensitivity value is the mapping speed given in Equation 7-3:

(Eq. 7-3)

(3)

$$M = \frac{d\Omega}{\mathrm{dt}} = \frac{\gamma \Omega_{\mathrm{array}}}{s^2}$$

where γ is related to the filling factor, Ω_{array} is the solid angle of the HAWC+ detector array, and *s* is some measure of the instrument sensitivity (e.g., MDCF or NESB). The values in Table 7-1 are given for S/N = 1 in a one-hour integration time assuming γ = 1, while SITE and Figure 7-3 use a more realistic value γ = 0.75. The time to map an area Ω (≥ Ω_{array}) to a sensitivity level σ is given by Equation 7-4:

(Eq. 7-4)

(4)

$$t = \frac{\Omega}{M \sigma^2}$$

Note that this scaling only applies to map areas larger than the array field of view.

Atmospheric transmission will affect sensitivity, depending on water vapor overburden as will telescope zenith angle and telescope emissivity. For the estimates in Table 7-1 and Figure 7-3 we use a precipitable water vapor of 7.3 µm, a 50° zenith angle, and a telescope emissivity of 15%.

Return to Table of Contents

7.1.2.3 Imaging Polarimetry Sensitivities

The equations provided below are included for informational purposes only, and should *not* be entered into USPOT. Integration times calculated using the equations below include overheads, and USPOT already adds the telescope overheads into the exposure times entered. For USPOT entries use SITE, which only takes into account on-source time.

HAWC+ contains four monochromatic HWPs. For Bands C, D, and E, the HWP thicknesses are matched to the bandpass filters. The thickness of the Band A HWP is matched to a wavelength between those of Bands A (53 µm) and B (63 µm), approximately 58 µm. However, this slight mismatch should not introduce significant systematics into the system. For the pre-flight HAWC+ sensitivity estimate here, the total system polarization efficiency (HWP + polarizing grid + all other optics) is assumed to be 90% for all five passbands.

The polarization sensitivity σ_p follows from the imaging sensitivity σ_I so that Equation 7-5 is true:

(Eq. 7-5)

(5)

$$\sigma_P = \frac{\sigma_I \sqrt{2}}{\eta_p I}$$

where *I* is the source intensity, η_p is the system polarization efficiency, and σ_p is measured in units of percent (%). The Minimum Detectable Continuum Polarized Flux (MDCPF) reported in Table 7-1 is the value σ_p x *I* above, and follows from the total intensity MDCF. USPOT will add overhead values appropriate to NMC mode for polarimetry.

For Imaging Polarimetry, another useful quantity is the Minimum total Intensity required in order to measure polarization (MIfP) to a given depth in a given time interval. Choosing σ_p = 0.3% allows a polarization S/N = 3 for a source polarization of 1%, a value not atypical of bright Galactic clouds and a likely lower limit for HAWC+ systematic uncertainties. Table 7-1 lists these values for a one-hour integration time in units of surface brightness for an extended source where, unlike other values in Table 7-1, all appropriate overhead values have been added.

HAWC+ time estimates should be made using the online exposure time calculator, SITE. Note that integration times scale as shown in Equation 7-6 and Equation 7-7 from the values in Table 7-1:

(Eq. 7-6)

(6)

$$t = (1\ \mathrm{h})\left(\frac{\mathrm{MIfP}}{I}\right)^2 \left(\frac{0.3\%}{\sigma_p}\right)^2$$

(Eq. 7-7)

(7)

$$t = (900\ \mathrm{s})\left(\frac{\mathrm{MDCPF}}{4\sigma_p I}\right)^2$$

where t is the integration time and σ_p is the desired sensitivity for S/N = 1, each in the appropriate units.

A simple estimate for the polarization angle uncertainty is given by Equation 7-8:

(Eq. 7-8)

(8)

$$\sigma_\phi = \frac{180}{\pi}\frac{\sigma_p}{2p}[\mathrm{degrees}]$$

Current best estimates for systematic uncertainties are 0.8% in percent polarization and 10° in polarization position angle.

Return to Table of Contents

7.2 Planning Observations

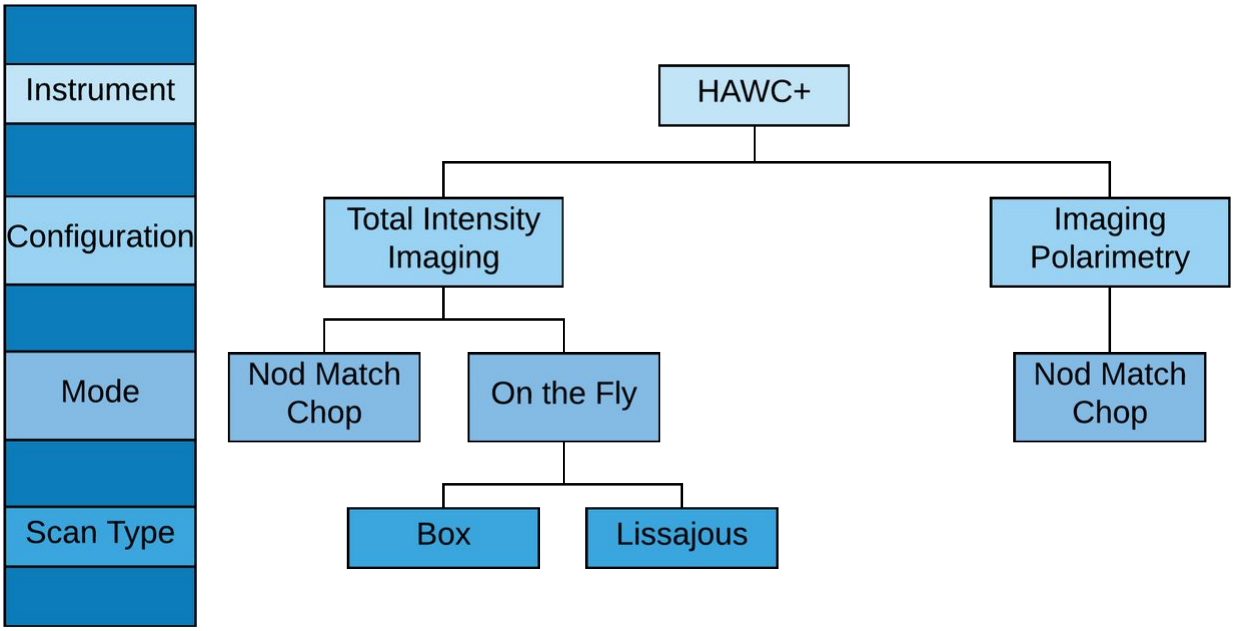

The HAWC instrument has two main observing configurations: Total Intensity Imaging and Imaging Polarization. The instrument also has two standard observing modes for imaging: the Nod Match Chop (NMC) mode combines traditional chopping with nodding and On the Fly Mapping (OTFMAP) mode keeps the secondary mirror fixed as the telescope primary is scanned across the source. For polarization observations, the NMC observing mode is mostly used; this mode includes chopping and nodding cycles in multiple half wave plate (HWP) positions.

The standard NMC mode is a subset of the standard two-position chopping with nodding mode (C2N). NMC consists of several steps, listed below and illustrated in Figure 7-5.

1. *Chop*, where the secondary mirror of the telescope is moved at some frequency and angle.
2. *Nod*, where the telescope nods back and forth, each chopper beam being placed on the desired source.
3. *Dither*, which is a set of Nods at small offsets on the sky (nominally four positions), with each position having a Chop/Nod observation taken.

Figure 7-5.

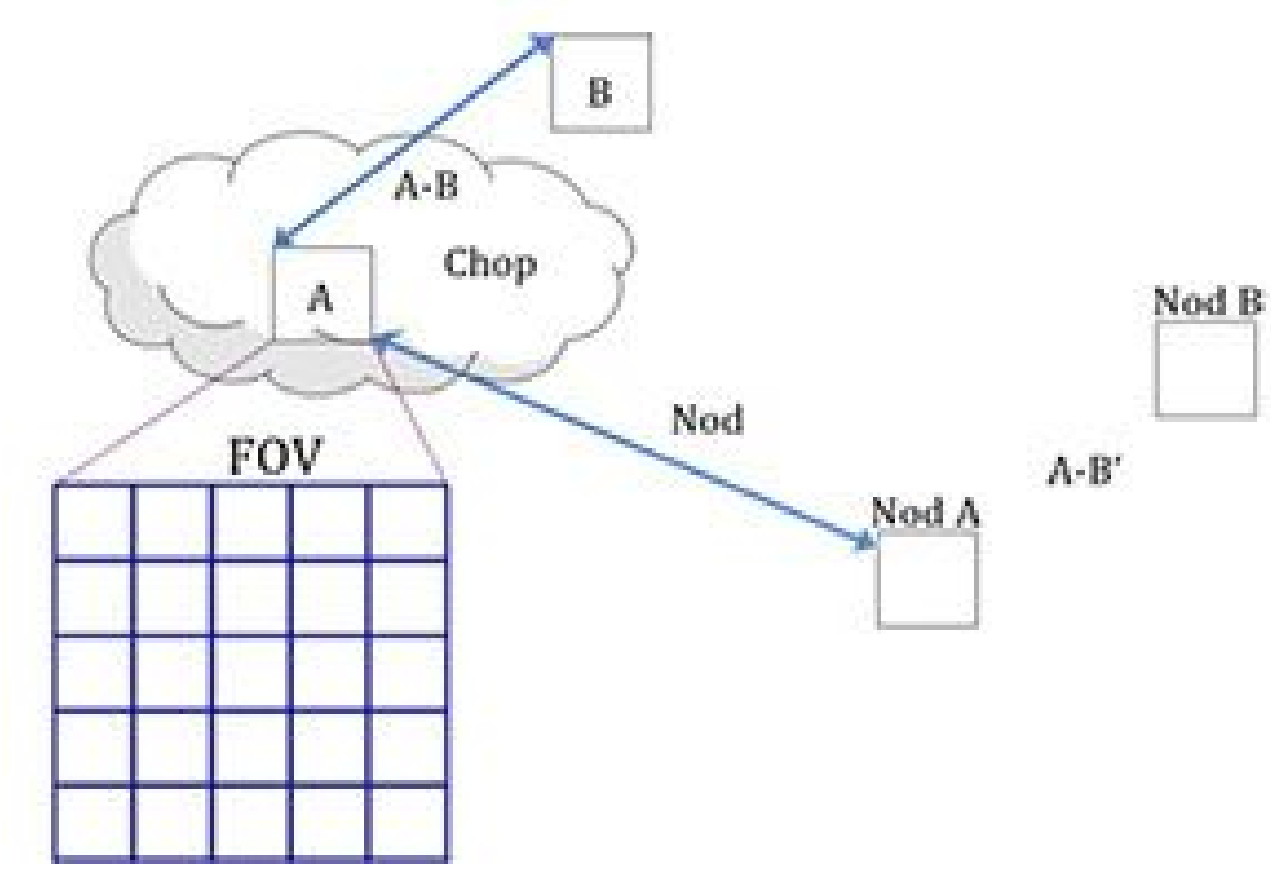

43 Figure 7-5. The standard ABBA nod sequence of NMC mode.

Total Intensity observations with OTFMAP mode produce a continuous telescope motion with a two choices of pattern shape, the sizes of which are selected by the proposer. The first pattern (Box) is a series of linear scans used to map some rectangular region on the sky. The second pattern (Lissajous) is a curvilinear shape meant to cover a small region whose size is less than the array field of view.

Return to Table of Contents

7.2.1 Total Intensity Observations

7.2.1.1 On the Fly Mapping

In OTF mode, the secondary mirror remains stationary on the optical axis of the telescope while the telescope assembly itself slowly moves with respect to the sky. This scan motion modulates the celestial source with respect to the atmosphere in a manner similar to chopping the secondary mirror. Scan rates must reach (~2 Hz) x (HAWC+ beam width) in order to remove the source from the atmospheric background. This implies rates ~10–80 arcseconds per second depending on the bandpass.

In order to ensure absolute flux calibration in this mode, observers must carefully plan observations so that some of the mapped region contains no extended emission from the science target. Otherwise, one can only measure a differential flux with respect to the lowest measured intensity level. Further removal of residual atmospheric signal is performed by removing common-mode noise observed in all HAWC+ detectors. This averaging amounts to a spatial filter with size equal to the HAWC+ FOV. Therefore, while large maps may be necessary to reach a true zero-intensity level, users should be aware that one cannot also recover all spatial scales in a given region. The OTFMAP in total intensity can be used to map large areas also with a potential loss of extended structures larger than 1-2FOV at a given band'

HAWC+ offers two scan types for OTFMAP scan patterns: Lissajous and Box. Lissajous scans are recommended for sources smaller than the HAWC+ field of view (FOV) at a given bandpass, while Box scans (analogous to traditional raster scanning methods) are more efficient at mapping large areas several times the FOV. The patterns in Figure 7-6 show the two-dimensional location of the array center during the progression of a scan, with Lissajous scans depicted in the two top images and Box scans shown in the two bottom images. Two-dimensional scans are necessary in order to reconstruct all spatial scales in a map. The Lissajous scans are two-dimensional by definition; however Box scans require multiple scans, even in the case where a source fits completely in the HAWC+ FOV. The secondary (or cross) scan direction of a Box scan should by rotated with respect to the initial scan (orthogonal scans are best, although not absolutely necessary).

Figure 7-6.

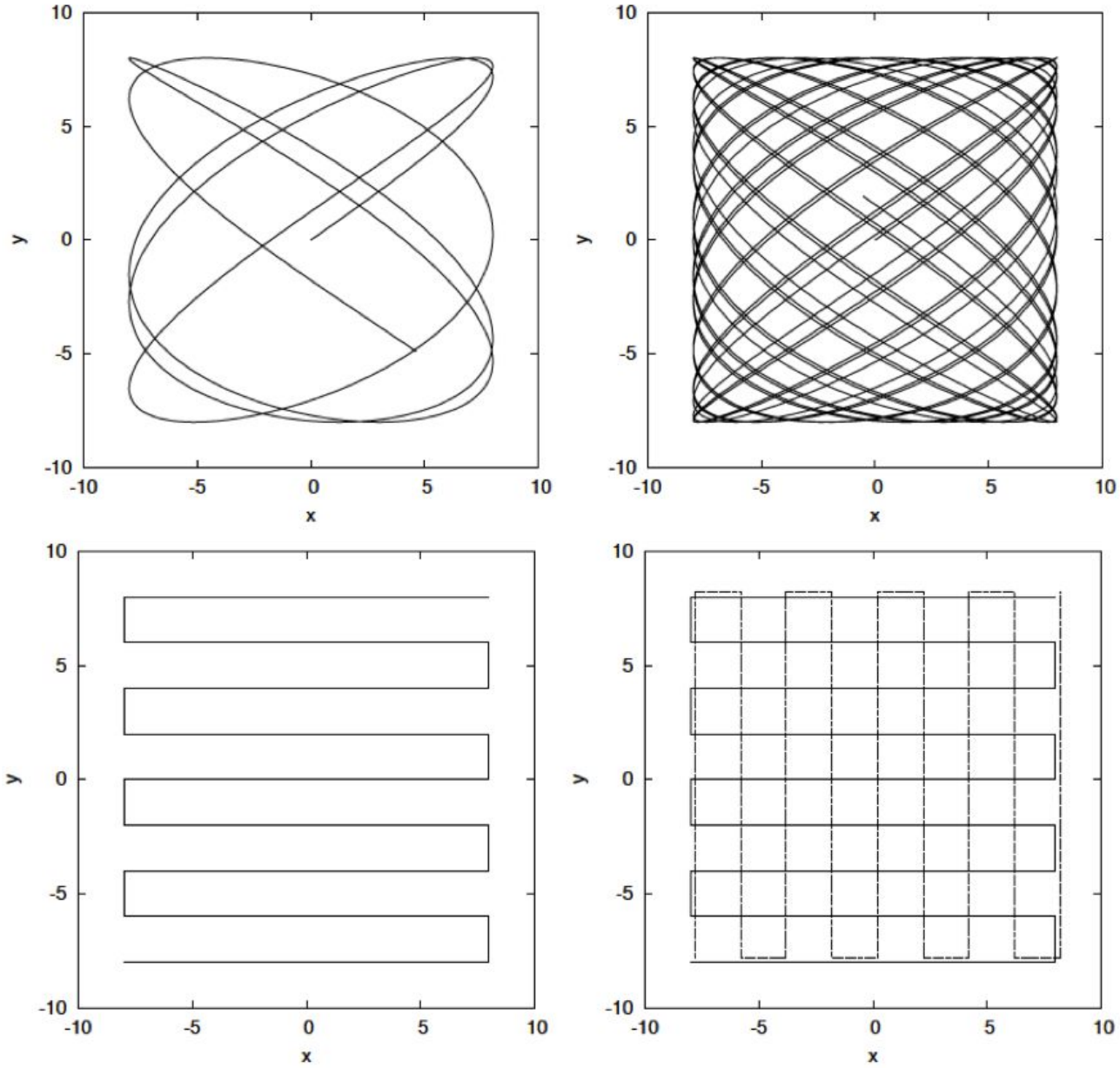

44 Figure 7-6. Example scan patterns for HAWC+ OTFMAP mode. These patterns show the location of the central array pixel, which moves along the paths at a user-defined rate. The upper panels are Lissajous patterns. The top-left panel is shortly after starting an integration, while the top-right panel is after a longer time period. The lower-left panel shows a series of linear scans used to cover a larger region. The lower-right panel also shows the required cross-scan in the case of linearly scanned areas. Plots taken from Kovács (2008).

While proposers must request an area for scan mapping, they do not need to specify any specific pattern in Phase I proposals. Successful proposers will work with a SOFIA Support Scientist to choose an optimal scan pattern and strategy for their observations. For the purposes of the proposal, scan map time estimates should be made using the sensitivity estimates in Table 7-1. For sources smaller than the HAWC+ FOV, use the MDCF or NESB. For larger maps one may use the Mapping Speed.

Scan durations shorter than 10 min are recommended to ensure the stability of continuous OTFMAP observations for large periods of time. If a given map area and sensitivity cannot be achieved in that time, then multiple pointing positions should be used.

Return to Table of Contents

7.2.1.1a Lissajous

In Lissajous observations, the telescope is driven to follow a parametric curve at a non-repeating period; as the scan progresses longer in time, more and more of the area defined by a scan amplitude will be covered.

Figure 7-7 demonstrates the actual scan modes used in flight. The white box shows the Total Intensity FOV, the orange line shows the actual path as taken by the telescope, and the background images are the resulting image after the scan data is reduced.

Figure 7-7.

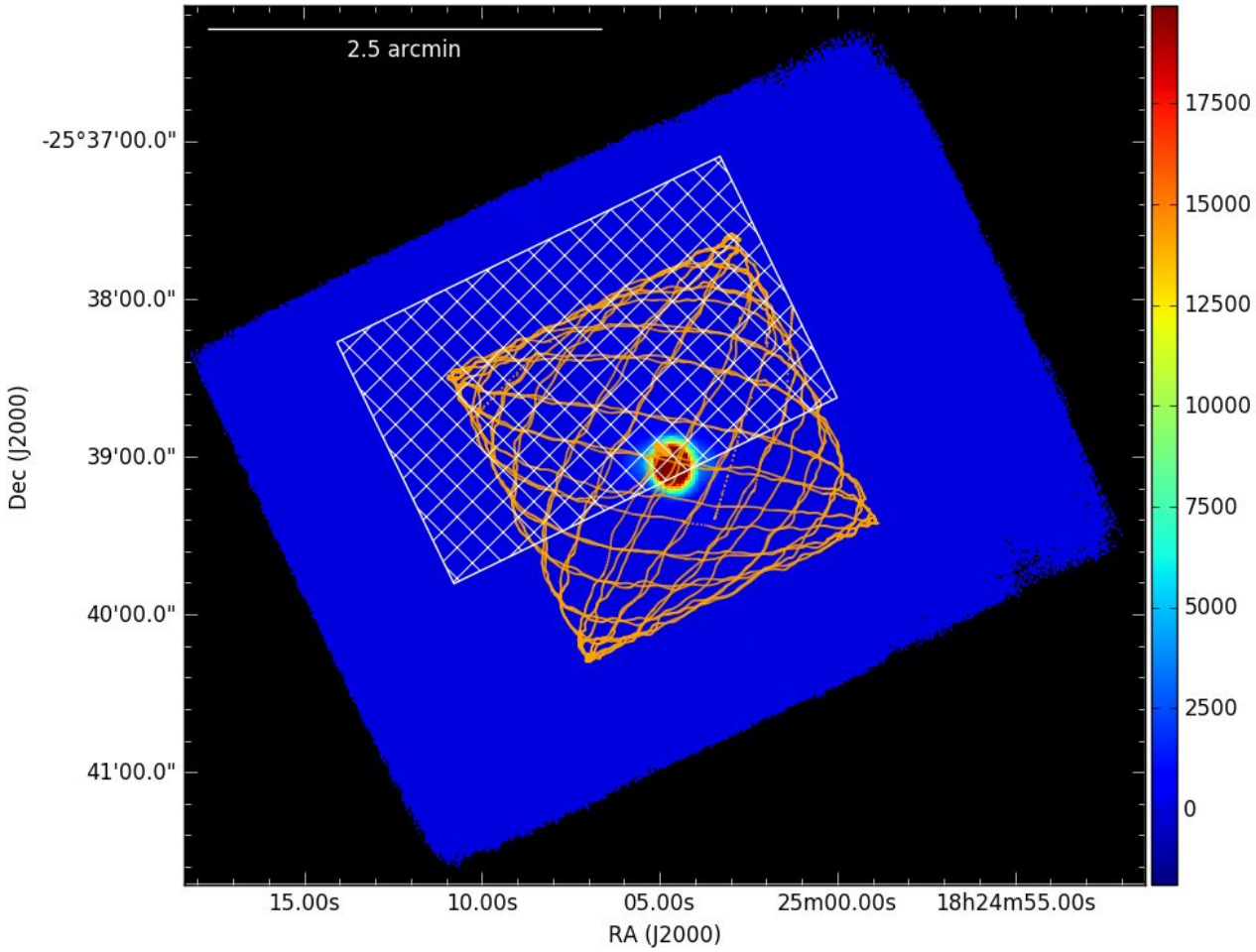

45 Figure 7-7.

Return to Table of Contents

7.2.1.1b Box

In Box scans, the telescope is driven in a linear fashion at the specified rate in one direction for the given length and then moved perpendicularly before scanning in the reverse direction—similar to how one would mow a very large lawn. This is continued until the desired area is covered, after which the process repeats in the perpendicular direction to cross the same areas in the perpendicular direction. For optimal reduction and coverage, three scans are performed, each at a slightly different starting angle to improve coverage and provide reduction robustness against systematic effects.

Figures 7-8, 7-9, and 7-10 demonstrate the actual scan modes used in flight. The white box shows the Total Intensity field of view, the orange line shows the actual path as taken by the telescope, and the background images are the resulting image after the scan data is reduced.

Figure 7-8.

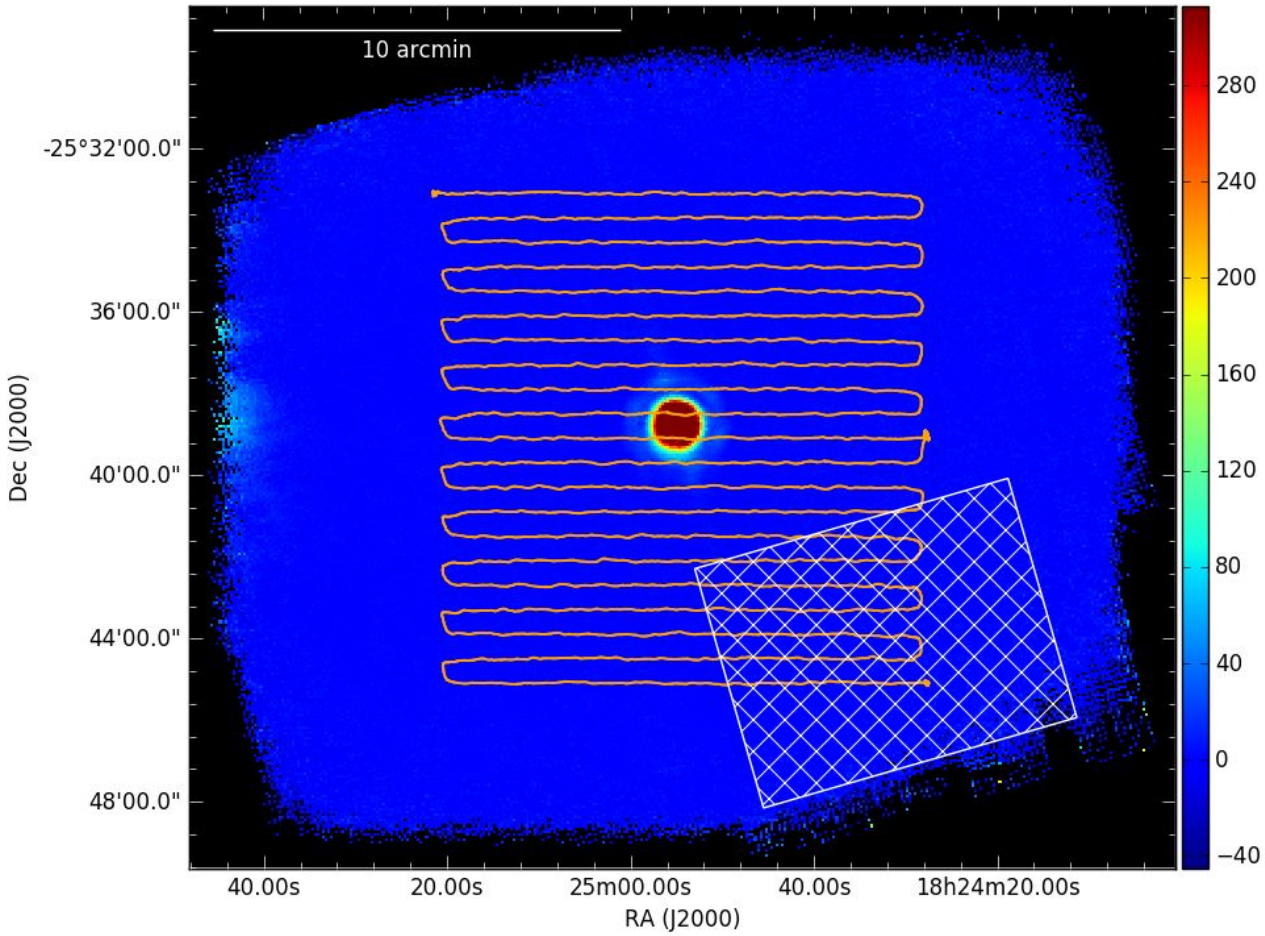

46 Figure 7-8. The scan starts at the bottom right, pauses midway through to obtain an estimate of tracking performance (the orange dot on the middle right) and then proceeds until the end.
Figure 7-9.

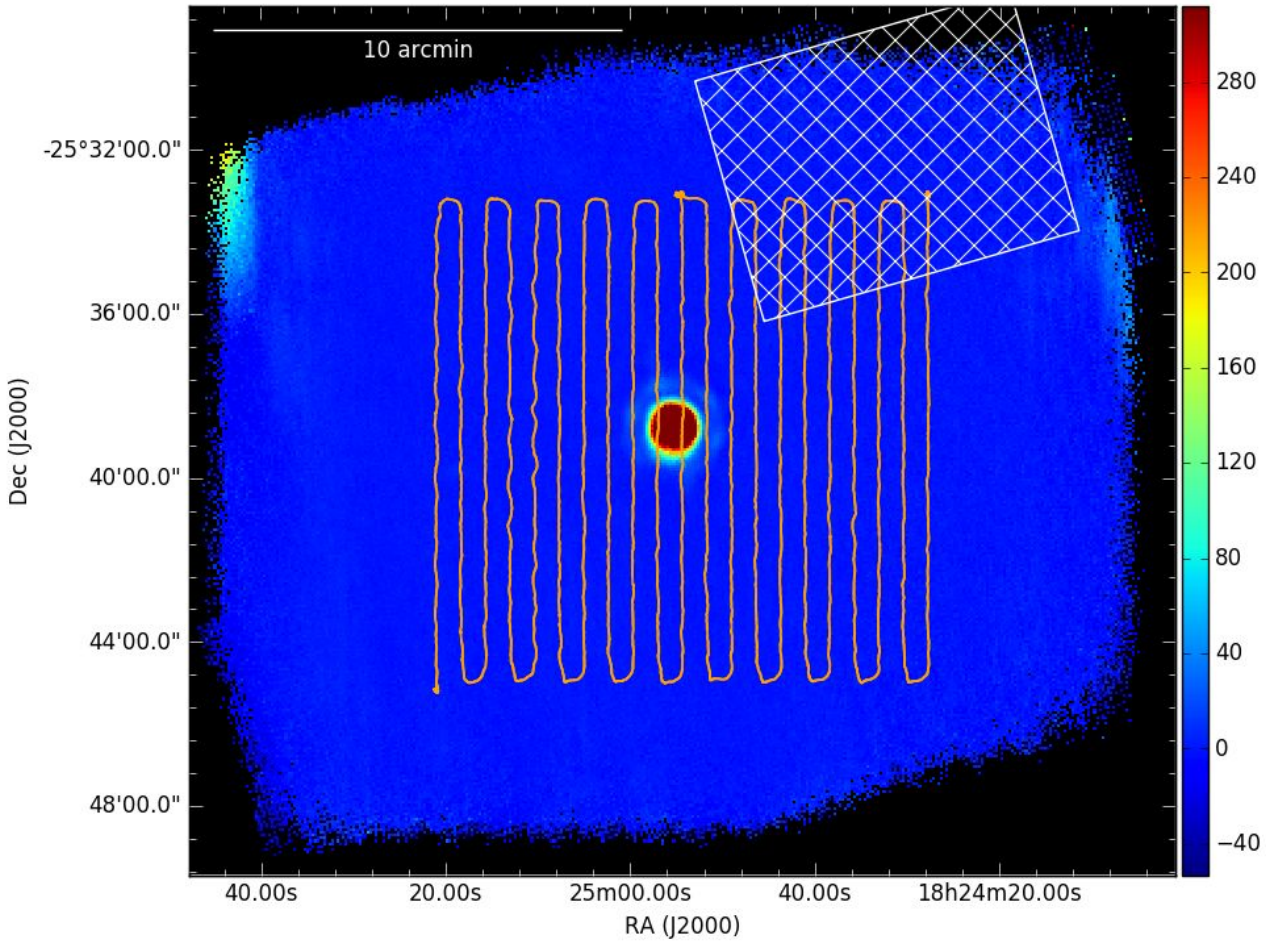

47 Figure 7-9. The scan starts at the upper right, pauses midway through to obtain an estimate of tracking performance (the orange dot on the middle of the top) and then proceeds until the end. The two directions are then combined to obtain the image below.
Figure 7-10.

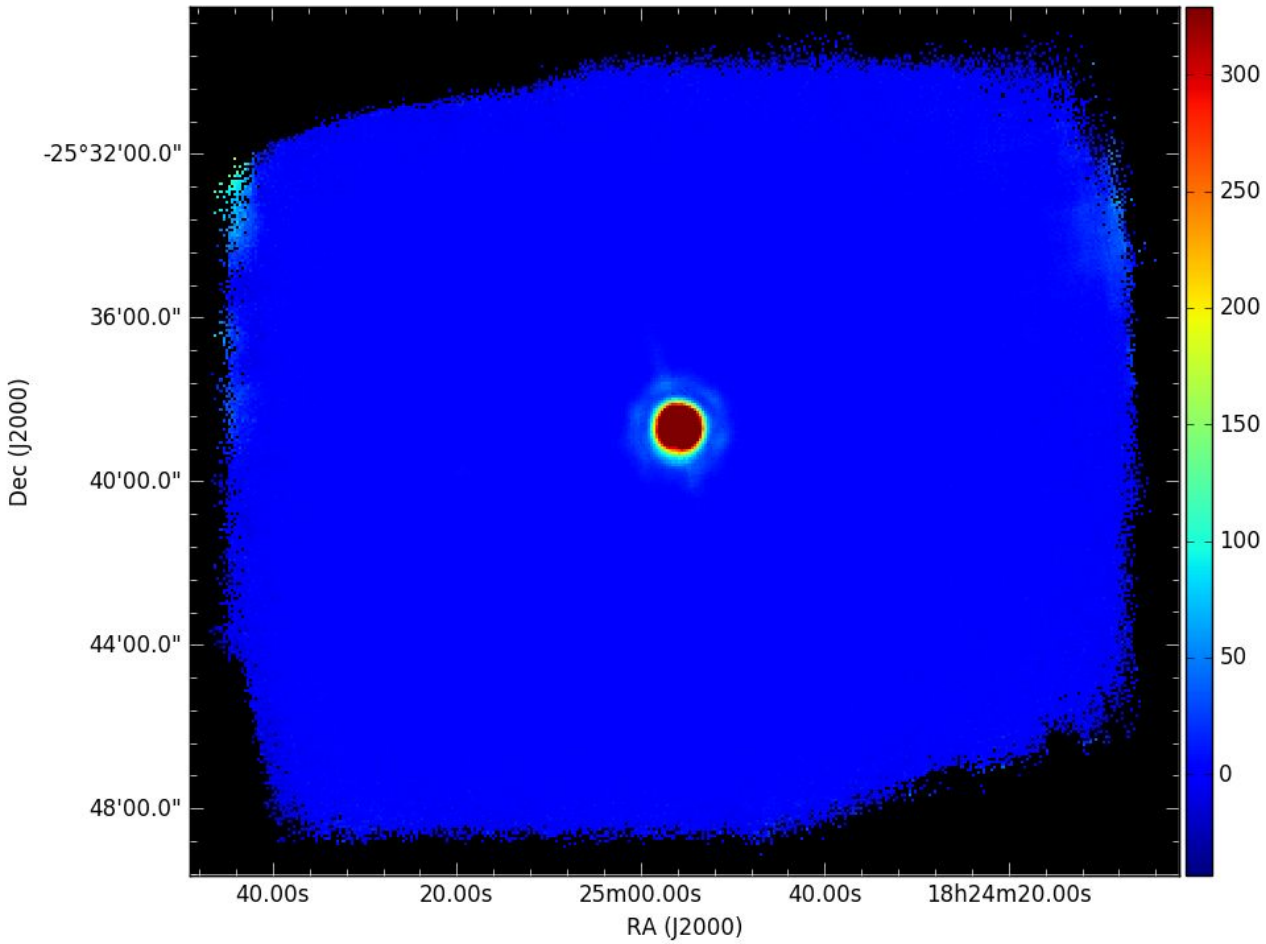

48 Figure 7-10. The two directions from Fig.7-7 are then combined to obtain this image.
Return to Table of Contents

7.2.1.2 Nod Match Chop

In NMC mode, four dither points are created symmetrically about the central object coordinates; an example is given in Figure 7-11. At each dither position, chopping is started at the given throw and angle and the telescope is nodded between two symmetrically located points 180 degrees separated from each other (positions A and B).

NMC mode observations, are very time intensive and are subject to large observational overheads waiting for the telescope and/or secondary mirror assembly to complete chop/nod/dither movements. For total intensity observations, OTFMAP is strongly encouraged. This mode provides better sensitivity and lower overheads, which provides better overall observing efficiency.

If the source has an angular extent larger than the HAWC+ FOV in NMC mode, or larger than can be accommodated in a 10 minute OTFMAP, the central position of each HAWC+ field must be specified, with due consideration of the desired overlap of the individual frames. For mosaic observations, proposers should ensure that they request the total integration time required for all fields.

Figure 7-11.

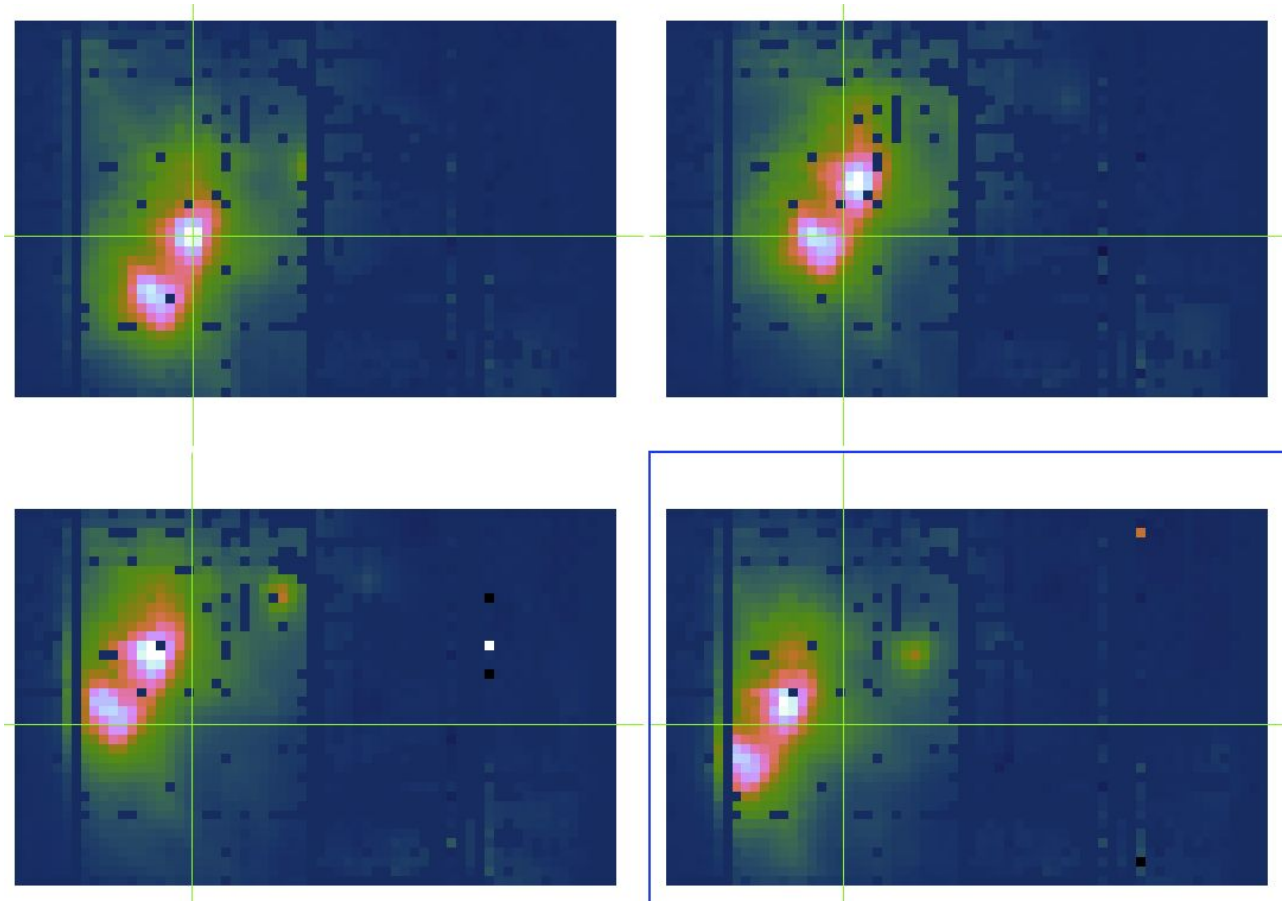

49 Figure 7-11. Example of a source being dithered between four positions. The green crosshairs give the position of one of the sources and is at the same physical location for each image, showing the image movement.

Return to Table of Contents

7.2.2 Polarimetry Observations

For Cycle 9, HAWC+ polarization observations are recommended to be performed using the NMC observing mode. OTFMAP polarization mode is still in shared-risk but previous observations from cycle 7 and 8 have shown that extended diffuse emission can be recovered to an extend of ~1FOV. However, heavy data reduction algorithms are used which introduce noise penalties as a function the length of the extended emission. Polarization may be highly affected by these data reduction schemes and an exhaustive data reduction procedure requires to be performed by the GO. Those proposals requesting large maps these should provide specific scientific purposes and alternative scientific outputs if this mode does not provide the expected scientific results.

As in the case of NMC observations, chopping into regions of bright, extended flux must be carefully avoided. Additionally, the polarization state of that reference flux must be considered in both percent polarization and angle. Typically, neither of these values will be known for HAWC+ observations (although proposers may want to consult the latest Planck data release). This polarized reference beam will produce additional systematic uncertainties in the data. In the case where the source and reference beam have the same polarization level, the systematic polarization uncertainty is linearly proportional to the reference-to-source intensity ratio. For further discussion, see Schleuning et al. (1997) and Novak et al. (1997).

If the source has an angular extent larger than the HAWC+ FOV in NMC mode, the central position of each HAWC+ field must be specified, with due consideration of the desired overlap of the individual frames. For mosaic observations, proposers should ensure that they request the total integration time required for all fields.

Return to Table of Contents

7.2.2.1 Nod Match Chop

In NMC mode, a nominal four dither points (with a maximum of 9-point dither points) with a three detector pixels offset are created symmetrically about the central object coordinates. At each dither position, chopping is started at the given throw and angle and the telescope is nodded between two symmetrically located points 180 degrees separated from each other (positions A and B). Observations are performed in sequence at position A, then B, then B again, and back to position A. After one of these ABBA nod sequences, the HWP is rotated to the next angle; this continues until the HWP has gone through four angles, after which the telescope moves to the next dither position and repeats.

Figure 7-12 below shows both the change in source RA (illustrating the nodding of the source) and the half-wave plate angle for a single dither position of a polarization sequence. The dashed lines denote the completion of a half-wave plate observing sequence. This same sequence (four half-wave plate angles) is repeated for each dither position to move the source appreciably and assist in the correction of bad/missing pixels. The source is being chopped during this entire sequence (and accounts for the thickness of the blue source RA line) but is not specifically highlighted here. The standard ABBA nod sequence and the half-wave-plate angles are highlighted.

Figure 7-12.

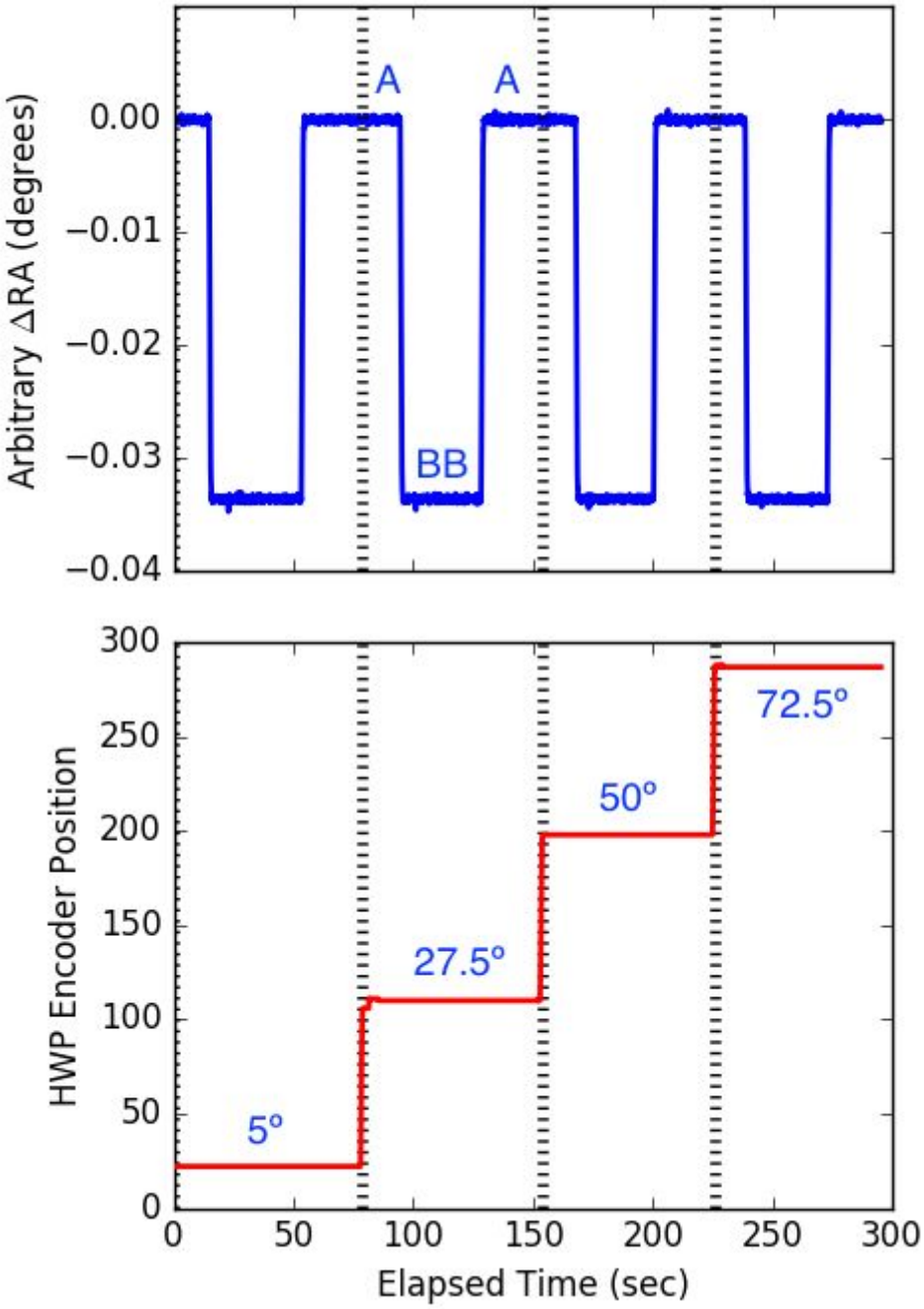

50 Figure 7-12.
NMC mode observations, are very time intensive and are subject to large observational overheads waiting for the telescope and/or secondary mirror assembly to complete chop/nod/dither movements. These overhead factors are included in USPOT after the on-source time estimation in SITE.

Note: OTFMAP in polarimetry mode will be offered as shared-risk during Cycle 9. This observing mode is under commissioning during Cycle 8.

Return to Table of Contents

8. The Data Cycle System

To export the handbook as a PDF, click on the three dots in the upper right, then choose "Export with Scroll PDF Exporter". In the Template drop-down menu, choose "Handbook Template", and then click "Export".

8. The Data Cycle System

SOFIA proposals and astronomical observation requests (AORs) are managed by the SOFIA Data Cycle System (DCS). The DCS is designed primarily to support Science and Mission Operations activities associated with observing programs.

A proposal are submitted to the SOFIA Science Mission Operations (SMO) through the USPOT tool, which is an interface to the DCS. Once approved, the proposal becomes an observing plan that the proposer uses to create and update astronomical observation requests (AORs) that are used in both flight planning and on-aircraft execution. After execution of the observations in-flight, the resulting raw data are processed to produce the final data products. Those products are then served back to the original proposer via the SOFIA Archive at IRSA. The data products are made available to the astronomical community for archival research purposes after an appropriate proprietary period.

The goal of the SOFIA DCS is to maximize the scientific productivity and efficiency of the observatory by providing a suite of easy-to-use tools and infrastructure that are integrated with each other as well as other applications (e.g. Flight Management Infrastructure) at each step in the data cycle.

In order to make use of most of the features of the DCS website, users must register by clicking on the Register with DCS link on the DCS home page. After the registration form has been submitted, the user will be notified by e-mail when the account has been created. (Users should verify that mail from "sofia.usra.edu" is not blocked by any spam filters.) After logging in, a registered user can change his/her profile and password at any time using the View Profile link displayed next to the login name at the top of the DCS pages.

The DCS includes a suite of software tools to assist in the preparation and submission of proposals, including USPOT, SITE, ATRAN, and VT (see Section 8.2.1). USPOT installation instructions for all supported platforms are provided on the USPOT download webpage. The USPOT Manual contains instrument-specific instructions for submitting proposals. Additional help files are included with the USPOT application distribution.

In addition, the DCS provides users with a variety of search options for proposals and observing plans.

Proposal Search
SOFIA proposals are created and modified using the Unified SOFIA Proposal Tool (USPOT) and are stored in the DCS observation planning database. Users can retrieve summary data for available proposals by using the Proposal Search page and entering the relevant search criteria for the proposal(s) of interest. Summary information will be displayed for each proposal (appropriate to the permissions of the user).

Observing Plans Search
Once a proposal is approved, it becomes an observing plan, which can be accessed and modified as needed to support science and mission requirements by the proposer and selected SMO staff members. Observing plans can be accessed from the planning database using the Search Observing Plans link on the DCS web page. Summary information will be displayed for each observing plan along with links to the Observing Plan Details page. The

Observing Plan Details page provides all the information available for a plan and corresponding links to the editor functions to make changes (for users with appropriate permissions).

Return to Table of Contents

8.1 Data Rights and Availability

The SOFIA Science Center provides raw and calibrated data for all instruments via the SOFIA Archive at IRSA. All data will be archived as Level 1 data (raw). Where appropriate, Level 2 data (corrected for instrumental and atmospheric effects), Level 3 data (flux calibrated), and Level 4 data (a combination of Level 3 files to produce maps, mosaics, etc) will also be archived. Data that are still proprietary are available only to those on the associated observing plan. These data will be accessible to the general community after a proprietary period of twelve months, starting at the ingestion of the calibrated data into the archive. For tips on SOFIA specific archive searches and taking advantage of IRSA visualization features, video tutorials are available here.

Return to Table of Contents

8.2 Resources for Using SOFIA Data

8.2.1. Data Documents & Tools

Data Documents

The Data Documents webpage contains helpful documentation for using SOFIA data. The Data Handbooks describe the data products, processing steps, calibration procedures, and known issues. In addition, the Cookbook Recipes provide guided examples of common data analysis objectives using SOFIA processed data. They are generally written for a graduate student audience and are intended to be used with the Data Handbooks.

Data Tools

Data Cycle System (DCS)
SOFIA proposals and observation data are managed by the SOFIA Data Cycle System (DCS). The DCS is designed primarily to support Science and Mission Operations activities associated with Guest Observer (GO) programs for the observatory.

SOFIA Instrument Time Estimator (SITE)
SITE is an instrument-specific exposure time calculator that provides the total integration time or S/N for a given instrument, filter(s), source type (point, extended, emission line), and water vapor overburden.

Atmospheric Transmission (ATRAN)
The atmospheric transmission as a function of wavelength may be obtained using the on-line Atmospheric Transmission tool (ATRAN), developed and provided to the SOFIA program by Steve Lord. The use of ATRAN is necessary for planning SOFIA high-resolution spectroscopic observations. For a specified observing altitude and wavelength range, ATRAN will generate a downloadable output file and plot of the atmospheric transmission as a function of wavelength.

Target Visibility Tool
The downloadable Target Visibility Tool (VT)—which is also now an integrated feature of USPOT—provides the capability to estimate what date, time, and aircraft heading are required to observe an astronomical target. A target is visible to SOFIA if the elevation is in the range 20° to 60°. For flights that take off from and return to Palmdale, the southernmost allowed declination is -36°. Southern targets will be scheduled for observation during the Southern Hemisphere Deployment that will take place during the southern winter of 2019. Proposers may use VT to check the periods of visibility for their targets, however, the use of VT is not a requirement because detailed flight planning is done by the SMO staff.

SOSPEX
The SOSPEX tool, written by Dario Fadda and Ed Chambers, allows users to explore the final data cubes produced by the data reduction pipeline. An overview of its use can be found on the AAS poster. (See also "SOSPEX, an interactive tool to explore SOFIA spectral cubes")

FLUXER
The FLUXER tool, written by Christof Iserlohe, allows users to fit the continuum and estimate line strengths in the final FIFI-LS data cubes.

8.2.2. Citations for Publications using SOFIA Data

When writing publications, the Information for Authors webpage provides instructions for acknowledgements and citations. Additional references may be found on the SOFIA Refereed Papers webpage.

Return to Table of Contents